





NEURODEGENERATIVE EFFECTS OF RADIOFREQUENCY FIELDS

AMELIE GAVARD

Somerville College
Department of Pharmacology
University of Oxford

Supervisors: Dr Daniel Anthony & Dr Kerry Broom

Abstract:

This thesis studied the cognitive and structural effects of radiofrequency fields exposure on Alzheimer's disease (AD) and ageing. Two mice models were chosen, the J20 transgenic mice as a model of AD, and the senescence-accelerated mouse model SAMP8 for ageing. Mice underwent a chronic exposure and behavioural assessments either immediately post-exposure or after a latency period. At the end of the study, histological analysis was performed. Results were analysed with Minitab® and showed a possible transient effect of EMF exposure on activity and motivation in the J20 mouse model of AD.

General introduction

There has been a continuous growth in mobile phone use in all countries of the world over the past decade. While mobile communications have provided opportunities and benefits to society, at the same time, a number of concerns have been raised about the safety of radiofrequency (RF) fields used by mobile phones and wireless technologies for the individual, and the possibility remains that repeated exposure to low intensity RF fields could have adverse effects on health. Concerns include an increased risk of brain tumours associated with long-term mobile phone use (IARC, 2013), detrimental effects on cognitive function in elderly and other vulnerable people, and increased prevalence of Alzheimer's disease (AD). In 2010, approximately 35.6 million people suffered from dementia (WHO 2012, 2015), mainly linked to Alzheimer's disease (Wimo and Prince, 2010), and that this number is expected to roughly double every 20 years. Considering that the life expectancy after appearance of the symptoms is, on average, 8.5 years, and that, during this period, the loss of autonomy according to the decline of mental faculties involves dependence and frequent hospitalizations, this represents a massive cost for societies. For example, in the UK, dementia costs £23 billion a year, more than cancer, heart disease or stroke, and the costs are expected to soar. The purpose of my study was to investigate the impact of radiofrequency on cognitive function in mice that exhibit premature aging or animals that have been engineered to exhibit AD-like pathology.

Table des matières

ABSTRACT: **2**

GENERAL INTRODUCTION **3**

1. ELECTROMAGNETIC FIELDS **7**

1.1. DEFINITION AND PHYSICAL CHARACTERISTICS **7**
1.2. RADIOFREQUENCY FIELDS **8**
1.2.1. SOURCES OF RF AND EXPOSURE LEVELS OF RF FIELDS 8
1.2.2. INTERACTION WITH BIOLOGICAL TISSUES 10
1.2.2.1. Penetration in body 10
1.2.2.2. Dosimetry 11
1.2.3. BIOLOGICAL AND HEALTH EFFECTS 11
1.2.3.1. Epidemiological studies 11
1.2.3.2. In vivo studies 12
1.2.3.2.1. Effects of RF fields on AD 12
1.2.3.2.2. Effects of RF on ageing 13

2. ALZHEIMER'S DISEASE **14**

2.1. DEFINITION **14**
2.2. COGNITIVE SYMPTOMS **14**
2.3. NEUROPATHOLOGY **15**
2.3.1. Aβ PATHOLOGY 15
2.3.2. TAU PATHWAYS 18
2.3.3. INFLAMMATION 18
2.4. ANIMAL MODELS OF AD **20**
2.5. CURRENT TREATMENTS **22**

3. AGEING **24**

3.1. COGNITIVE DEFICITS **24**
3.2. NEUROPATHOLOGY **24**
3.2.1. NEURONAL LOSS 24
3.2.2. INFLAMMATION 25
3.2.3. AXONS AND SYNAPTIC DENSITY 25
3.3. MODELS OF AGEING: SENESCENCE ACCELERATED MOUSE **26**

4. MATERIALS AND METHODS **28**

4.1. ANIMAL WORK **28**
4.1.1. MODELS 28
4.1.1.1. Alzheimer's disease mouse model 28
4.1.1.2. Senescence-accelerated mouse model 29
4.1.2. BEHAVIOURAL TESTING 30
4.1.2.1. Morris Water Maze 30

4.1.2.2. Elevated O-Maze 32
4.1.2.3. Rotarod 33
4.1.2.4. Termination 33
4.1.3. EXPOSURES 34
4.2. IMMUNOHISTOCHEMISTRY 35
4.2.1. TISSUE PREPARATION FOR IMMUNOHISTOCHEMISTRY 35
4.2.1.1. Formalin fixing 35
4.2.1.2. Processing 35
4.2.1.3. Sectioning 36
4.2.2. STAINING 36
4.2.2.1. Antigen retrieval 36
..... 37
4.2.2.2. Immunohistochemistry on the Autostainer 38
4.2.2.3. Counterstaining 38
4.3. IMMUNOHISTOCHEMISTRY ANALYSIS 39
4.3.1. SYNAPTOPHYSIN DENSITY 39
4.3.2. QUANTIFICATION OF ASTROGLIA WITH GFAP POSITIVE ASTROCYTES 39
4.3.3. QUANTIFICATION OF IBA1 POSITIVE MICROGLIA 40
4.3.4. QUANTIFICATION OF B-AMYLOID 41
4.3.5. QUANTIFICATION OF NEUN POSITIVE NUCLEI 41
..... 42
4.4. STATISTICS 42

5. THE EFFECT OF EMF EXPOSURE ON A MOUSE MODEL OF ALZHEIMER DISEASE 43

5.1. GENERAL BACKGROUND 43
5.1.1. EXPERIMENTAL APPROACH 43
5.1.2. MOUSE MODEL 43
5.2. EXPERIMENTAL PROTOCOL 44
5.3. RESULTS 44
5.3.1. BEHAVIOURAL ENDPOINTS 44
5.3.1.1. Rotarod 44
5.3.1.2. O-Maze 45
5.3.1.2.1. Frequency of exits ..... **Erreur ! Signet non défini.**
5.3.1.2.2. Latency to exit compartments 47
5.3.1.3. Morris Water Maze 49
5.3.1.3.1. Acquisition 49
5.3.1.3.2. Memory 53
5.3.1.3.2.2. Probe-trial 56
5.3.2. HISTOLOGICAL ENDPOINTS 60
5.3.2.1. Synaptophysin 60
5.3.2.1.1. CA1 60
5.3.2.1.2. CA3 61
5.3.2.1.3. Dentate Gyrus 63
5.3.2.2. Iba1 64
5.3.2.3. β-amyloid 65
5.4. DISCUSSION 66
5.4.1. BEHAVIOURAL ENDPOINTS 66
5.4.2. HISTOLOGICAL ENDPOINTS 70
5.4.3. CONCLUSION ON THE EFFECT OF EXPOSURE ON J20 MODEL 72

6. SAM MODEL 74

6.1. GENERAL BACKGROUND 74
6.1.1. EXPERIMENTAL APPROACH 74
6.1.2. MOUSE MODEL 74
6.2. EXPERIMENTAL PROTOCOL 75
6.3. RESULTS 75
6.3.1. BEHAVIOURAL ENDPOINTS 75
6.3.1.1. ROTAROD 75
6.3.1.2. WATERMAZE 76
6.3.1.2.1. Memory 76
6.3.1.2.1.1. Pre-trial 76
6.3.1.2.1.2. Probe-trial 78
6.3.1.2.2. Acquisition 82
6.3.1.2.2.1. Trials 2 82
6.3.1.2.2.2. Trials 3 85
6.3.2. HISTOLOGY 86
6.3.2.1. GFAP 86
6.3.2.1.1. CA1 86
6.3.2.1.2. CA3 87
6.3.2.1.3. Dentate Gyrus 88
6.3.2.2. SYP 89
6.3.2.2.1. CA1 89
6.3.2.2.2. CA3 89
6.3.2.2.3. Dentate Gyrus 90
6.3.2.3. IbA1 91
6.3.2.4. NeuN 91
6.3.2.4.1. CA1 91
6.3.2.4.2. CA3 92
6.3.2.4.3. Dentate Gyrus 93
6.3.2.5. β-amyloid 93
6.4. DISCUSSION 94
6.4.1. GENERAL CONSIDERATIONS 94
6.4.2. DISCUSSION 94

7. CONCLUSION 97

BIBLIOGRAPHY 101

1. Electromagnetic fields

1.1. Definition and physical characteristics

Electromagnetic fields (EMFs) are composed of electric and magnetic fields, coupled to form oscillating electric waves.

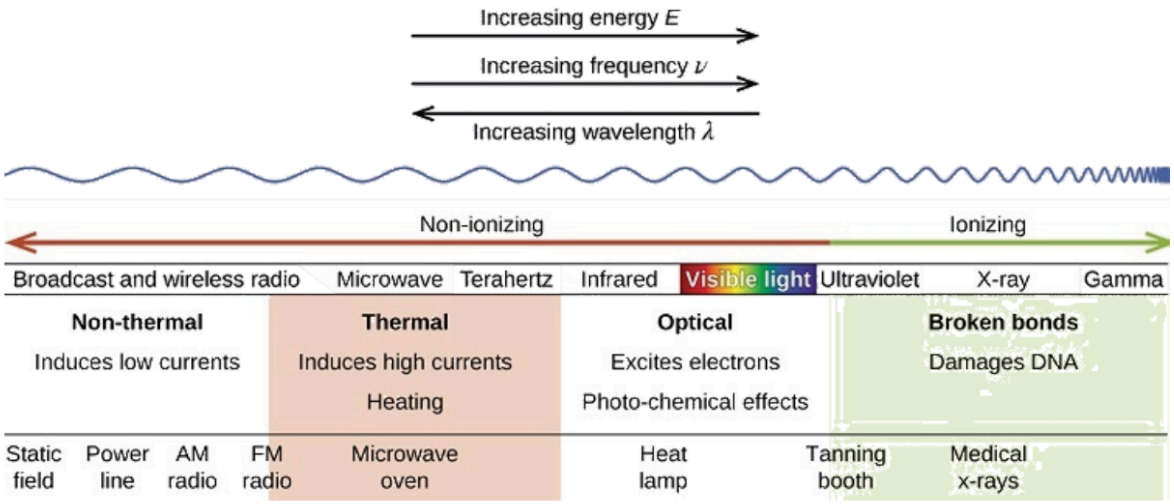


Figure 2: Classification of electromagnetic radiations according to their properties and characteristics, with the practical applications associated to different wavelengths.

The spectrum of electromagnetic radiation, described in Fig. 2, is usually divided into ionizing (gamma-rays and x-rays) and non-ionizing radiation. The non-ionizing radiation spectrum is composed of static electric and magnetic fields, extremely low frequency fields (ELF), intermediate frequency fields, radiofrequency (RF) fields (microwaves are considered to be a part of the radiofrequency range), infrared radiation, visible light and ultraviolet radiation. The speed of oscillations determines their frequency, which can be used (along with their wavelength) to classify them into different bands (for example, very high frequency, or ultra-high frequency). The frequency (f) and wavelength (λ) of electromagnetic waves are inversely proportional to each other according to the equation $c = f\lambda$, where c is the speed of light. Photon

energy increases with increasing frequency (or decreasing wavelength) according to the equation E = hf, where h is the Planck constant.

There are three different types of EMF, with different applications and effects: Extremely Low Frequencies (ELF), with wavelengths below 300 Hz, Intermediate Frequencies (IF), for wavelength of 300 Hz to 10 MHz and Radio Frequencies, which include wavelengths between 100MHz and 300GHz (WHO, 1993). ELF is found in power chargers, such as laptop chargers, IF are associated with household appliances, such as induction hobs, and finally RF is associated with communication (e.g., mobile phones, WiFi), with frequencies between about 400 MHz and 2200 MHz.

1.2. Radiofrequency fields

1.2.1. Sources of RF and exposure levels of RF fields

The possible effects on human health of exposure to radio frequency and microwave radiations remain of public concern, and given the proximity of hand-held mobile phone (transmitters) to the head, understanding the impact of non-ionizing radiation on brain function and structure is of the utmost importance. When exposed to radiofrequency fields, the body absorbs energy over time, and the rate at which this energy is absorbed is known as the Specific Absorption Rate (SAR), which varies throughout the body. For handheld mobile phones, the exposure is largely confined to part of the head nearest to the phone's antenna. GSM phones transmitting at 900 MHz, which is an important frequency for mobile communication, have a maximum time-averaged power of 250 mW. Key sources of RF fields include mobile phones, cordless phones, local wireless networks and radio transmission towers, as shown in Fig. 3, but exposure from these sources is usually lower than from mobile

phones. Mobile phones are tested by assuming worst-case conditions: the rate at which energy is transmitted by a mobile phone operating at maximum power. In practice, the power transmitted during a mobile phone conversation is generally hundreds or thousands of times lower than the maximum power possible. In accordance with European regulations, the power is averaged over six minutes as GSM phones transmit radio signals in bursts of information rather than continuously. On average, during a six-minute conversation under worst-case conditions – a mobile phone held to the head and operating at maximum power – the 10 grams of body tissue that absorb most energy would typically absorb between 200 and 1500 mW per kilogram depending on the type of phone.

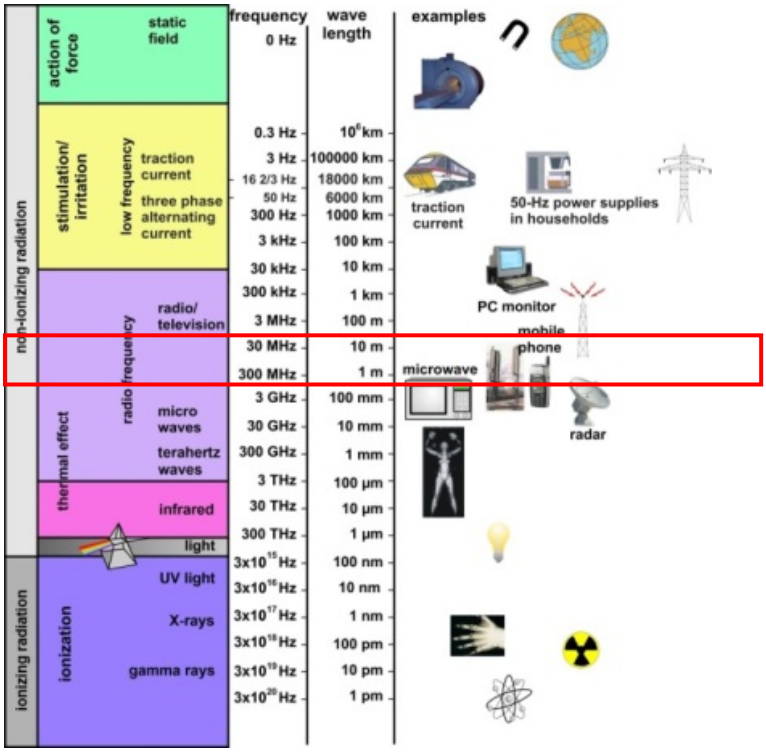


Figure 3: Examples of devices with associated range of frequencies. *Mobiles phones frequencies are included between 900 and 1800MHz, which are included in the non-ionizing domain.*

Modern devices often generate electromagnetic fields of radio frequency (RF) ranging from 100 kHz to 300 GHz.

1.2.2. Interaction with biological tissues

When biological tissues are exposed to RF fields, the main effect is an increase in tissue temperature due to the vibration of water and other polar molecules induced by charge oscillation - these rapid movements result in heating. The International Commission on Non-Ionizing Radiation Protection (ICNIRP) has guidelines for restricting human exposure based on the known heating effects as a result of acute exposure to RF fields (ICNIRP, 1998), but effects in the apparent absence of heating (called non thermal effects) have sometimes been reported in both epidemiological and experimental studies (see reviews by AGNIR, 2012; IARC, 2013; SCENIHR, 2015) (Health Protection Agency, 2012; IARC, 2013; SCENIHR, 2015), but none of these possibilities are considered to be sufficiently well-established at present to be used as the basis for limiting exposure. Nevertheless, current guidelines limit whole-body exposure for the general public to 0.08 W/kg.

1.2.2.1. Penetration in body

Energy from radio frequency can be absorbed by the body. To determine how much radio frequency energy any given individual absorbs on a daily basis is not an easy calculation as the exposure depends on many factors, especially distance from the various sources. Field strength falls off rapidly with distance (according to the inverse square law decay of $1/r^2$), meaning a person may absorb more energy from a device used at close quarters – a handheld mobile phone for example – than from a more powerful source, like a radio transmission tower, that is further away.

1.2.2.2. Dosimetry

While it is possible to measure the electric field next to an antenna, such measurements are not useful for biology. A more relevant dosimetric measurement is obtained by considering the rate at which energy is absorbed by living tissues. This is usually expressed as the specific energy absorption rate (SAR) and is calculated according to the electrical conductivity, the induced electric field and the density of the tissues involved. SAR is measured in W/kg. To know what exposure an individual has received, the use of methods such as dosimeters, devices carried by individuals to measure their exposure to electromagnetic energy over time, is the best way, but this is not possible with as mouse or a rat.

1.2.3. Biological and health effects

1.2.3.1. Epidemiological studies

Thus far, most of the studies on the health effects of RF on the brain were focused on cancer and the International Agency for Research on Cancer has classified exposure by mobile phone as "possibly carcinogenic". But in 2011, a study concluded "In this update of a large nationwide cohort study of mobile phone use, there were no increased risks of tumours of the central nervous system, providing little evidence for a causal association" (Mohler et al., 2012). However, the link between RF and AD specifically has not been widely studied, and there are only few epidemiologic studies on an effect of RF exposure from mobile phone use on cognition, learning and memory. In contrast to the fears of increased carcinogenicity risk, a Singaporean study (Ng et al., 2012) showed that elderly patients performed better in the Mini Mental State Evaluation (MMSE) test with increasing phone use. A Danish study associated mobile phone use with slightly reduced risk of developing AD (Schüz et al., 2009). However,

one could easily argue that individuals who are developing a neurodegenerative disease might be less social compared to those that are still in the prodromal state.

1.2.3.2. In vivo studies

While epidemiological studies provide compelling, human-based evidence concerning the health risks of RF, there is an uncertainty due to the difficulty to quantify RF exposure resulting from use of mobile phones. Therefore, data that can be derived from animals has the potential to provide insights in the effects of exposure in a more controlled manner than is possible in the human population.

1.2.3.2.1. Effects of RF fields on AD

1.2.3.2.1.1. Cognition

The first observable signs of AD are during the second phase and are characterized by the progressive appearance of cognitive and behavioural disorders - usually a marked loss of memory. However, as many factors can interfere with cognitive studies in humans, in vivo studies have been conducted to investigate the influence of RF on animals. Effects from the studies have been surprising. In vivo studies have reported a negative effect on memory in rats (Wang et al., 2014), and in mice (Sharma et al., 2014) after short-term exposure. However, in studies in a mouse transgenic model of AD, it has been reported that long-term exposure to RF protected the young transgenic mice from cognitive impairment later in life (Arendash et al., 2010)and RF exposure was able reverse the cognitive impairment and AD-like pathology in old transgenic mice (Arendash et al., 2012). In another study by Banaceur et al. (2013) employing a triple mutant mouse model of AD, the team were able to show no differences in cognition between exposed and sham transgenic mice, but they did report a reduction of anxiety in the AD mice.

1.2.3.2.1.2. Neuropathology

Structural changes to the brain following RF exposure have been reported. An *in vivo* study in male rats (Lecomte et al., 2010) reported an increase in GFAP expression after RF exposure, which suggests that astrocytes, which provide metabolic support to the synapse, are responding to altered signalling. In this study, male rats were exposed to 900MHz EMF at a SAR of 1.5 W/kg for 45 minutes per day or at a SAR of 6 W/kg for 15 per day, five days per week for 8 weeks and reactive astrocytosis was investigated three- and ten-days post-exposure. While they were able to show an increase in GFAP levels, no gross structural changes were observed.

1.2.3.2.2. Effects of RF on ageing

Overall, the majority of studies have concluded that exposure to RF does not have any deleterious effect on brain structure, activity or neurodegeneration, and could even have a protective effect. However, most of the studies lack of full dosimetry and differences in the exposure protocols are confounding. While most animal studies have explored the effects of acute RF exposure, with doses far above the exposure levels recommended by ICNIRP for human exposures, few describe the long-term effects of repeated low level exposure on cognitive function (AGNIR, 2012) and thus, before the studies described herein were performed, there was a clear need to understand more fully have RF affects the aging brain and a brain that is beginning to exhibit AD-like pathology. The aim of my work was to assess whether short-term or long-term exposure to radiofrequency signals have a long-term impact on learning and memory in the senescence accelerated mouse model (SAMP) and the J20 mouse-model of AD.

.

2. Alzheimer's disease

2.1. Definition

Alzheimer's disease (AD) is considered to be the most frequent neurodegenerative disease and is defined as a neurodegenerative condition of the central nervous system, leading to the progressive and irreversible loss of neuronal cells, thus involving a loss of the mental functions and usually starting by a memory loss. According to the DMS-IV-TR "*Alzheimer's disease dementia is defined by the association of an irrational syndrome with the histological examination of the brain, by the existence of Aβ plaques, neurofibrillary tangles and neuronal loss. The syndrome corresponds to the following medical definition: disorders of the cognitive functions (memory, language, praxies, gnosies, executive functions, etc) important enough to impact on the daily life and which have lasted for at least 6 months*." It is worth noting that, as of yet, there is no surrogate biomarker for the diagnosis of AD and post-mortem confirmation of the presence of the characteristic pathology remains the only way to confirm a diagnosis.

2.2. Cognitive symptoms

The disease can be divided in three consecutive phases:

- The first one is silent and can start 15 to 30 years before the appearance of any clinical signs. It corresponds to the appearance of cerebral lesions.
- The second is characterized by a progressive appearance of cognitive and behavioural disorders, usually a sudden memory loss. This, however, is not sufficient to make a diagnosis.
- In the third phase, clinical symptoms appear, bringing the diagnosis of dementia, and AD. The memory loss observed in phase two is aggravated and followed by deficits of

the motor, gnostic (such as multisensory integration, allowing for body image, self-location and first-person perspective) functions.

2.3. Neuropathology

AD initially affects memory structures such as the hippocampus and the entorhinal cortex. The first assumptions on the physiopathology of the disease were thus directly related to the observations made at the time of autopsies by a histological examination of the postmortem patient brains. Three major characteristics of the disease were noted:

- The presence of extracellular Aβ plaques in the brain;
- The presence of neurofibrillary tangles, i.e. intracellular inclusions in the cellular body of the neurons and dendrites;
- And significant neuronal loss.

2.3.1. Aβ pathology

Pathologically, AD presents with deposits of amyloid beta (Aβ) protein in senile plaques, and hyper-phosphorylated Tau protein in neurofibrillary tangles (NFTs)(Price and Morris, 1999; Mudher and Lovestone, 2002), which begins in the trans-entorhinal area, spreading to entorhinal and then hippocampal cortices, then finally spreading to other subcortical structures (such as the amygdala and nucleus basalis of Meynert) and the neocortex, with primary visual and motor areas only affected in the very late stages of the disease (Arnold et al., 1991; Braak and Braak, 1991; Geula et al., 2002). Other features of the disease include cell loss, microglial activation and proliferation, gross cerebral atrophy and synaptic loss. The Aβ peptide, in its physiological form, is the result of a section of a transmembrane protein, the APP (Amyloid Protein Precursor) (Selkoe et al., 1988). This protein has a role in cellular

adhesion when it is located on the cellular membrane, as well as having a role in intracellular neuronal behaviour - particularly in memory processing (Zhou et al., 2011). The hypothesis, known as “the Aβ cascade”, places a greater importance to the Aβ plaques and postulates that the accumulation of Aβ plaques in the brain is an essential event in AD (Selkoe, 2001; Pavlov et al., 2009; Musiek and Holtzman, 2015).

The hypothesis that amyloid has a central role in AD is supported by observations in that have been made in the experimental mutant mouse models that have been engineered to over-express the human mutant genes responsible for the genetic forms of the disease. These models all develop deposits of Aβ-peptides in the brain, similar to the senile plaques in humans and show behavioural disorders particularly in training and memory abilities (Mucke et al., 2000). It is worth noting that neuronal cell death is not normally observed in these pathologies. However, the 2-year-long life span of a mouse cannot properly mimic a pathology that develops over decades. Indeed, it is now thought that neuronal loss and morphological change is likely to be a later aspect of the disease, with synaptic loss being an early feature of the disease, even present before amyloid deposition, and is probably most associated with clinical progression (Terry et al., 1991). Under physiological conditions, APP is a transmembrane protein with several isoforms, found everywhere, but particularly in axons and astrocytes. Its physiological role is not completely established, but it would seem that it plays a part in the cellular adhesion and the transduction of the signals. From the precursor, two pathways are possible:

- APP is cut by an α-secretase, then by a γ-secretase and does not lead to the secretion of an Aβ peptide,
- APP is cleaved by a β-secretase (BACE: β-site precursory Amyloid protein Cleaving Enzyme), then by a γ-secretase, which generates the Aβ fragment.

Aβ peptides can be recognized by antibodies, but they remain soluble or may be aggregated in plaques. Soluble forms can be difficult to be detected with microscopy, but monoclonal antibodies are useful to detect plaques.

Although the production of Aβ42 is part of normal physiology, the ratio of Aβ 42/40 seems more important in AD (Kumar-Singh et al., 2006). If this ratio leans towards Aβ42, the peptides aggregate into oligomers that will then become fibrils. Aβ plaques can be found in the central nervous system. Some regions of the brain, such as in the hippocampus, are particularly prone to plaque development. As the hippocampus is recognised as an important structure for the processing of memories from short-term to long-term, damage in this area of the brain is likely to be the cause of the principal symptoms of AD. The exact role of Aβ-plaques in the pathogenesis of AD is not well understood. For some time now there has been a debate regarding the relative importance of senile plaques and NFTs in the progression of AD, but it is now mostly thought that AD is primarily a due to a disorder in amyloid metabolism (Hardy and Selkoe, 2002), and for this reason most animal models have focused on one or more of the three genes which have a direct role in metabolism of amyloid precursor protein (APP), mutations of which are associated with familial AD (FAD). These genes are the APP gene itself, and the presenilins (PSEN1 and PSEN2), which are part of the γ-secretase complex that is involved in metabolism of β-APP (McGowan et al., 2006). The more common, sporadic type of Alzheimer's disease has a typical age of onset greater than 65 years of age, with a mean age of onset of 80 years, but mutations in one of these three genes leads to a disease that typically affects individuals at a much younger age (60-65), although FAD is fairly rare, accounting for only around 1% for all AD cases.

2.3.2. Tau pathways

Neurofibrillary tangles are another histopathological hallmark characteristic of AD. They involve the twisting of Tau protein threads in neurites. (Kowall and Kosik, 1987).

Tau is a protein involved in the stabilization of the cytoskeleton by association to the microtubules. It also plays a significant role in cell division. Tau's association with the microtubules is controlled by its phosphorylation state: in the phosphorylated form, it is detached from the microtubules, thus decreasing their stability (Henríquez et al., 1995). In AD cognitive decline correlates with the advancement of tau deposition, the main component of NFTs (Wilcock and Esiri, 1982). During pathology, tau becomes abnormally hyperphosphorylated, leading to decreased microtubule affinity. Soluble hyperphosphorylated tau may then form aggregates known as neurofibrillary tangles (NFTs), a pathological marker of AD in dystrophic APP-containing neurites (Barron et al., 2017). A study of approximately 900 staged AD brains aged 25 to 95 demonstrated that approximately fifty years elapse from the first appearance of NFTs to end stage AD (Braak and Braak, 1995). During this period, cognitive decline reflects the severity of tau pathology with greater precision than amyloid beta (Aβ) (Schöll et al., 2016). As a result, end stage AD is associated with the invasion of NFTs into all subdivisions of the cerebral cortex seemingly along neuroanatomically connected pathways, accompanied by severe destruction of the neocortical association areas (Braak and Braak, 1995).

2.3.3. Inflammation

Inflammation appears to be an important component of AD (Akiyama et al., 2000). Inflammatory changes can be observed in the brain as early as in the Mild Cognitive Impairment phase (Morris and Price, 2001). Aβ peptides trigger an acute early phase immunological

response, which leads to chronic inflammation. During this progression, a decrease in the efficiency of the immune response can be observed, leading to accumulation of Aβ plaques.

Early in the progression of the disease, the evidence that inflammation is present and contributing to AD pathology is supported by the presence of activated microglia, which is driven by the accumulation of Aβ protein aggregates. Microglia were named by Pío del Río-Hortega, who divided the term 'neuroglia' or Santiago y Cajal's 'third element' of the CNS into microglia and oligodendrocytes (Tremblay et al., 2015). Microglia are yolk-sac-derived resident macrophages of the brain (Ginhoux et al., 2010). Microglia play many roles in normal brain function and maintenance, where they interact with neurons, astrocytes and oligodendrocytes, and are quick to respond to changes by modulating their behaviour and by adopting different activation states. Microglial activation and/or dysfunction can be observed in almost all CNS diseases and injuries (Aguzzi et al., 2013).They can become activated by inflammatory challenges or damage. When they do so, they retract their processes and turn into cells with an 'amoeboid' morphology, characterised by a larger, rounder cell body. Depending on the type of challenge, microglia will become more phagocytic, markedly change their transcriptome, and secrete context-dependent cytokines, chemokines, and trophic factors (Li and Barres, 2018).

Astrocytes also seem to play a significant role in AD pathogenesis and are activated by Aβ (Söllvander et al., 2016) to a reactive inflammatory state called astrogliosis. Astrocytes have many roles in the CNS, including regulation of synapse formation and plasticity. They are involved in the detoxification and elimination of Aβ (Gomez-Arboledas et al., 2018), but this process can lead to potential neuronal toxicity. The mechanisms of the Aβ-induced toxicity are unclear, but hypotheses include disruption of calcium homeostasis (Kuchibhotla et al., 2009)

or a metabolic dysfunction (Allaman et al., 2010). It has also been hypothesised that the astrocytes secrete Aβ , adding to the Aβ burden in AD (Perez-Nievas and Serrano-Pozo, 2018).

2.4. Animal models of AD

AD is behaviourally identified by progressive memory impairment and pathologically characterized by the triad of β-amyloid plaques, neurofibrillary tangles, and neurodegeneration, but is rarely found in nature in other species, leading to the development of genetically modified animals to study the disease.

The first models were based on the expression in mice of the human genes responsible for the genetic forms of AD. These mice develop deposits of Aβ-peptides in the brain similar to humans' senile plaques and show behavioural disorders, particularly in training and memory abilities, similar to those of AD patients.

Other genetic mutations and risk factors, that can be either causal or modify AD progression, have been identified. These genetic and pathological features served as basis for the creation and validation of mouse models of AD. Efforts made in the past quarter-century have produced over 100 genetically engineered mouse lines that recapitulate some aspects of AD clinicopathology (Jankowsky and Zheng, 2017). Mouse models have been made that express one or more mutated human gene (APP, PSEN1 or PSEN2) (Hsiao et al., 1996; Holcomb et al., 1998). All of these models show excessive amyloid load and senile plaques, which are not found in wild-type mice (Wengenack et al., 2000a, 2000b) with the amyloid load and rate of aggregation differing between strains. The three most commonly used mouse models in the literature are: i) overexpression model of mutated human APP (Games et al., 1995; Hsiao

et al., 1996; Sturchler-Pierrat et al., 1997; Chishti et al., 2001) ii) Co-expression of human mutated PSEN1 and APP proteins (APP-PS1) (Duff et al., 1996; Holcomb et al., 1998); and iii) overexpression of human mutant PSEN2 and APP (PS2APP) (Richards et al., 2003). As could be predicted, the single APP transgenic takes the longest time to develop mature aggregates of Aβ, developing plaques primarily in the neocortex and hippocampus by 10 months of age. By contrast the double APP-PS1 animals develop plaques at around 3 months, with the number and size of Aβ-positive plaques increasing rapidly after this time, whilst the PS2APP mice develop amyloid aggregates more slowly (starting around 8 months), but with a wider expression, in the neocortex and limbic areas (including the hippocampus and amygdala) as well as thalamic and pontine nuclei. However, even though these mouse models seem to model the amyloidogenic features of AD fairly well (even if with varied time courses) they do not model tangle pathology, as in most cases this is limited to enhanced phospho-Tau around the senile plaques, but no actual NFTs formed (Takeuchi et al., 2000). Also, none of the amyloidogenic mouse models are associated with any significant neuronal loss (Irizarry et al., 1997a, 1997b). Interestingly, mouse models have also been developed based on the Tau protein, by introducing mutations in the gene for this protein, MAPT, which models the other side of the disease, presenting with tangle pathology (but are not amyloidogenic) associated with phosphorylated Tau (Lewis et al., 2001), as well as neuronal loss in affected regions (Lewis et al., 2000; Allen, 2002; Santacruz et al., 2005). Thus, there remains no ideal mouse model with which to study AD pathology.

The J20 mouse model of AD is a transgenic over-expresser of human APP with familial AD mutations (the ‘Swedish’ and ‘Indiana’ mutations) and has been extensively utilised in preclinical studies (Kitazawa et al., 2015). Starting from 5 to 7 months of age, J20 mice show diffuse Aß plaque deposits in the hippocampus that progresses to the accumulation of

widespread plaques by 8 to 10 months. The J20 animals do not normally exhibit neurofibrillary tangles or significant neuronal loss. The pathology is dependent on brain region. For example, in the CA1 region of the hippocampus plaques appear at 3 months compared to age-matched wild-type animals (Wright et al., 2013). At five months, a significant increase in the number of reactive GFAP-positive astrocytes and in microglia can be observed in the hippocampus of J20 mice when compared to age-matched wild-type controls (Wright et al., 2013). J20 mice also show age-dependent synaptic loss in the hippocampus at 3 months (Hong et al., 2016). Behaviourally, the J20 model shows deficits in spatial memory and learning from 4 months, as measured by Morris water maze (Cheng et al., 2007), making it a useful model for the studies presented here.

2.5. Current treatments

AD is regarded as progressive and irreversible disease as no satisfactory intervention exists to halt its progression. However, some treatments are proposed to combat the effects or provide relief to patients. Some approaches can help by delaying the appearance of the symptoms of the disease.

AD principally involves the loss of cholinergic neurons (Davies and Maloney, 1976) in the brain. Inhibiters of cholinesterase are used to counteract this loss as these drugs block the degradation of acetylcholine to avoid deficit of transmission by neurotransmitters. Efficacy appears to be similar for the subjects with light or moderated forms of Alzheimer's disease. Antagonists of NMDA receptors are also employed to slow AD progression; memantine for example. The excessive stimulation of glutaminergic receptors (AMPA or NMDA for example) is known to results in neuronal death, but the acute elevation of glutamate in the synapse is unlikely to be a feature of AD as it is after a stroke. The Kynurenine Pathway (KP) is a

tryptophan metabolism pathway that results in the generation of nicotinamide adenine dinucleotide (NAD+). Approximately 95% of tryptophan found in the body is metabolised by the KP (Vécsei et al., 2013). The KP is expressed in cells of the brain and of the periphery and is activated in times of stress and by an inflammatory immune response, resulting in the production of neuroactive metabolites (O'Farrell and Harkin, 2017). The first step of the pathway is the oxidative cleavage of tryptophan into N-Formyl-L-Kynurenine by one of two rate-limiting enzymes, indoleamine 2,3-dioxygenase (IDO) or tryptophan 2,3-dioxygenase (TDO). N-Formyl-L-Kynurenine is then hydrolysed by the enzyme formamidase to produce kynurenine (KYN), which is further metabolised by enzymes of the pathway to form neuroactive metabolites (Campbell et al., 2014). The KP is divided into two arms, the neurotoxic arm which produces the NMDA receptor agonist quinolinic acid (QUIN) and the neuroprotective arm, which results in the synthesis of kynurenic acid (KYNA) which is an NMDAR and AMPAR antagonist (O'Farrell and Harkin, 2017). Excessive levels of QUIN can lead to over activation of the NMDAR, resulting in excitotoxicity and neuronal damage (Zwilling et al., 2011) and this may be the metabolite that is responsible for some -sensitive cell death in AD. Studies have detected elevated IDO-1 in dystrophic pyramidal neurons and in glial cells and it has also been found to be highly accumulated in NFT and amyloid deposits (Guillemin et al., 2005; Bonda et al., 2010). Furthermore, Rahman et al. (2009) reported QUIN to be co-localised within NFT and in dystrophic neurons. QUIN was also found to increase the hyperphosphorylation and accumulation of tau in primary human neuronal cultures. The NMDAR antagonists MK-801 and memantine reduced this QUIN induced hyperphosphorylation. Thus, the endogenous NMDAR antagonist KYNA may have similar protective effects (Rahman et al., 2009).

3. Ageing

3.1. Cognitive deficits

Compared to young adults, healthy aged people show a decrease in acquisition and cognitive efficiency and spatial orientation associated with a decrease in the prefrontal cortex volume. There is also a decrease in real-time information processing and the formation of new memories, while long-term memories, semantic knowledge and analysis stay constant throughout life (Erickson and Barnes, 2003; Hedden and Gabrieli, 2004). Thus far, most of the functional neurobiological studies have been conducted in the aged rat. The link between rodent and human work could be made much stronger by combining neurophysiological and behavioural investigation of normal aging in non-human primate (Erickson and Barnes, 2003). However, ethical dilemmas and the expense of such experiments require that rodent alternatives are sought.

3.2. Neuropathology

3.2.1. Neuronal loss

It has been hypothesized that the cognitive deficits associated with ageing are linked to neuronal death, but studies on humans (West, 1993) and mice (Calhoun et al., 1998) show that, oddly, there is no correlation between neuronal loss and cognitive deficits. In the ageing brain, less than 10% of neurons are lost in very specific areas (neocortex and hippocampus) (Morrison and Hof, 1997), suggesting that the changes probably make a significant contribution to the behavioural impairment and cognitive decline that often accompany normal aging and were more due to a functional and physiological remodelling than cellular death (Burke and Barnes, 2006; Pannese, 2011).

3.2.2. Inflammation

Microglia and astroglia appear to decrease in number during human ageing (Unger 2008; Lynch 2010), the current theory being an exhaustion of the immune response to Aß peptides that progressively overwhelm the system (Franceschi 2007). Studies, however, show an increase in microglial cell numbers in rodents, but also morphological atrophy of the cells (Tremblay 2012; Streit Xue 2013; Sheit 2009).

3.2.3. Axons and synaptic density

In humans, once axons develop, they are considered to maintain their structure throughout adulthood (hardwired), but they do remain plastic in respect of their terminal and dendritic arborisation (De Paola 2006), which appears to be a significant contributor to memory formation (Hooltmat 2009). New memories are facilitated by the formation of new connections between neurons and the strengthening of others at a synaptic level (Millecamp Julien 2013; Gillet 2012). This phenomenon has been shown in both human and rodents, with changes observed in mouse hippocampus that are similar to humans (Samuel 2011; Gray Barnes 2015). The loss of upstream and downstream connectivity can lead to the death of neurons. For example, the transection of an axon will often lead to neuronal death, but the extent of cell death does not correlate with the numbers predicted by axonal loss as collateral connections still provide trophic support (Smith 2000; Geinsman 2004; Nicholson 2004). In older rats and mice, it has been shown that the number of synapses decreases, but the remaining synapses are strengthened and increase in size (Barnes McNaughton 1980). This may lead to a decrease in plasticity (Morrison and Hof, 1997) and it is unclear how many synapses are required in the dendritic arborisation to keep a neuron alive.

3.3. Models of ageing: Senescence Accelerated Mouse

Theoretically, for a model of ageing one only needs to wait. However, waiting for mice to come to the end of their natural life results in expensive and long-lasting experiments. To overcome this, the Senescence Accelerated Mouse (SAM) presents itself as an interesting model. Originally, the SAM mouse arose from the AKR/J strain, in which some litters were observed to show loss of activity, alopecia and shortened lifespan. Those litters were selected for inbreeding, which lead to the development of several of senescence-prone and senescence-resistant strains of mice (Takeda et al., 1981). The lineage of the SAM is drawn in Figure 1.
The genetic differences between the SAM lines are not known, as it has not yet proved possible to identify the gene (or genes) responsible for the ageing phenotype. Nevertheless genetic studies of the different lines has allowed it to be demonstrated that each strain was a "genetically distinct entity", though related, and the existence of outbreeding in the AKR/J line before the start of inbreeding (Kitado et al., 1994). The different lines of the SAM and their relations to each other are shown in Figure 1. The control SAM mice used in our studies are labelled as SAMR1 in the figure.

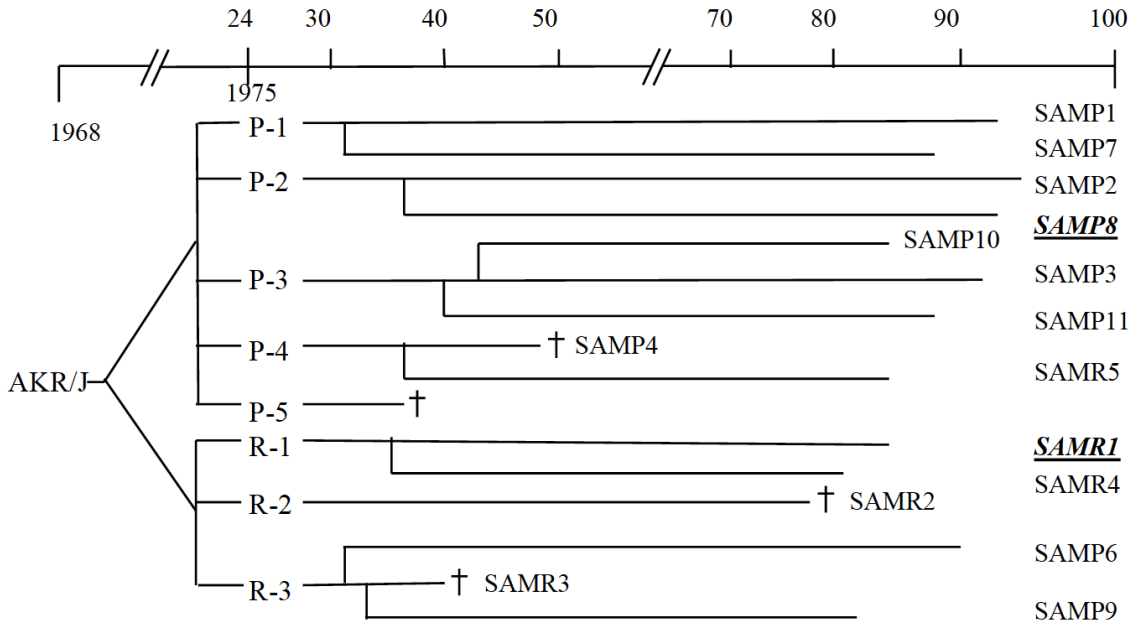


Figure 1: Drawing of the genetic evolution to create different branches of the senescence-accelerated mouse model from the background strain AKR/J to the current models available. *In bold and underlined are the two strains used for this work. (From Takeda, 1997)*

The different strains show different phenotypes, especially regarding cognitive effects. The commonly used model in studies of brain ageing is the SAMP8 model.

Various studies on SAMP8 show that the SAMP8 mice have age-related deficits in memory (Miyamoto et al., 1986; Flood and Morley, 1993), and, particularly, in learning. The mice show an early increase in general activity (Yagi et al., 1988) before an age-related decline in locomotor performance (Markowska et al., 1998a). When compared to the SAMR1 senescence-resistant strain, SAMP8 mice show reduced anxiety-like behaviours (Miyamoto, 1994), which mimics a phenomenon observed in AD patterns. The concomitant occurrence of both general ageing and AD-like symptoms suggested that this would be an interesting and relevant model for use in our studies.

4. Materials and Methods

4.1. Animal Work

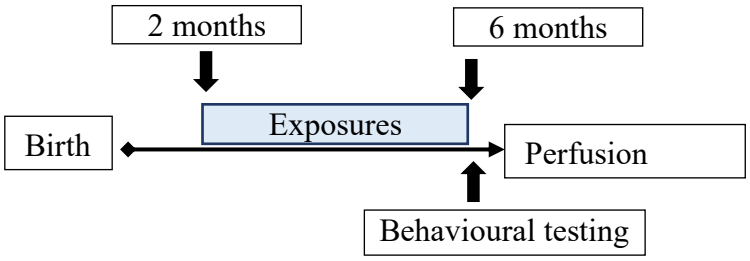
All procedures were carried out in accordance with the UK Animals (Scientific Procedures) Act 1986 and approved by the local Animal Welfare Ethical Review Body at Chilton. All animals were bred within the facilities in Chilton and housed under a 12-hour light/ dark cycle and given free access to standard laboratory diet and water. The ambient conditions in the holding room and the behavioural laboratory were kept between 21 and 23°C and 45 to 60% relative humidity. All animals were randomly assigned to an exposure level and given an identification number to be used throughout the experiments. Due to the availability of limited technical support, it was not possible to conduct the study in a fully blinded fashion, but the use of identification numbers helped to anonymise the exposure status of the animals.

4.1.1. Models

4.1.1.1. Alzheimer's disease mouse model

Two breeding pairs of B6.Cg-Tg(PDGF-APPSwInd)20Lms/2Mmjax (J20 model) were purchased from Jackson (Laboratories) and bred in the facilities at Chilton. The mating scheme was a heterozygous male with a wild-type C57B/L6 female. All progeny was genotyped at weaning for their transgenic status. All genotyping was outsourced to Transnetyx (Cordoba, USA). To increase animal numbers, an additional colony was set up under the same conditions at the University of Oxford, and the animals were transferred to Chilton at six weeks of age. At least two weeks were given for the animals to recover from any stress associated with the transfer before any experiment was carried out. Mice were exposed during four months from two months old until 6 months old, before being tested at either 6 or 12 months of age, as shown in Fig. 4.

- For the 6-month-old J20 cohort:



- For the 12-month-old J20 cohort:

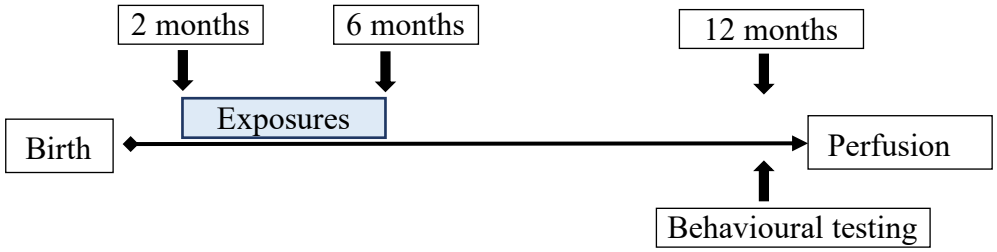


Figure 4: Timeline of experimentations for the J20 AD mouse model and its WT control, for the 12 months and the 6 months cohort.

4.1.1.2. Senescence-accelerated mouse model

Two breeding pairs of senescence-accelerated mouse (SAM) model SAMP8 mice and SAMR1 mice were purchased from Harlan (Harlan UK Ltd, Bicester, UK) An inbred colony was established at Chilton by breeding brothers and sisters from the same litter. The animals were housed together in litters until the start of their RF exposure, at 8 weeks of age, when they were then individually housed. They were subject to the behavioural tests at baseline before exposure to 0, 0.3, or 3 W/kg SAR exposure for 30 minutes per day, for 5 days per week for 8 weeks, before being tested at 30 weeks old. The outline of the experiment can be seen in figure 5.

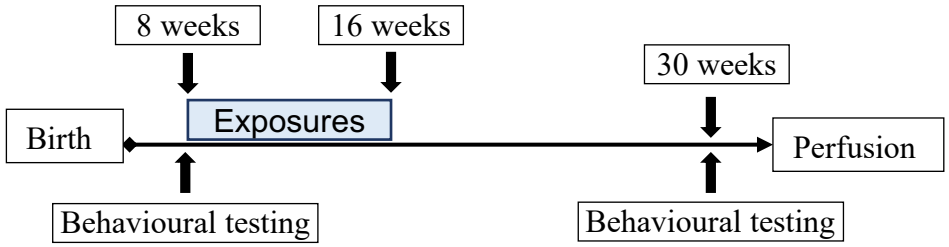


Figure 5: Timeline of experimentations for the senescence accelerated-mouse model SAMP8 and its control SAMR1.

4.1.2. Behavioural testing

Mice were brought to the experimental room at least 30 minutes prior to any testing to minimize stress. Light levels were kept at 5 lux and the animals were provided with floor-level lighting to reduce reflection during testing. Mouse behaviour was recorded using a video camera fixed to the ceiling and connected to a personal computer. The behaviour was analysed using Ethovision software v11.1 (Noldus Information Technology, Wageningen, The Netherlands).

4.1.2.1. Morris Water Maze

To assess spatial learning and memory, a version of the Morris Water Maze (MWM) task (Morris, 1984), adapted for mice, was used.

Each mouse was placed in a pool of water (106 cm diameter and 33 cm deep) maintained at 19°C +/- 1°C and filled with water up to 17cm deep as shown by Fig 6.

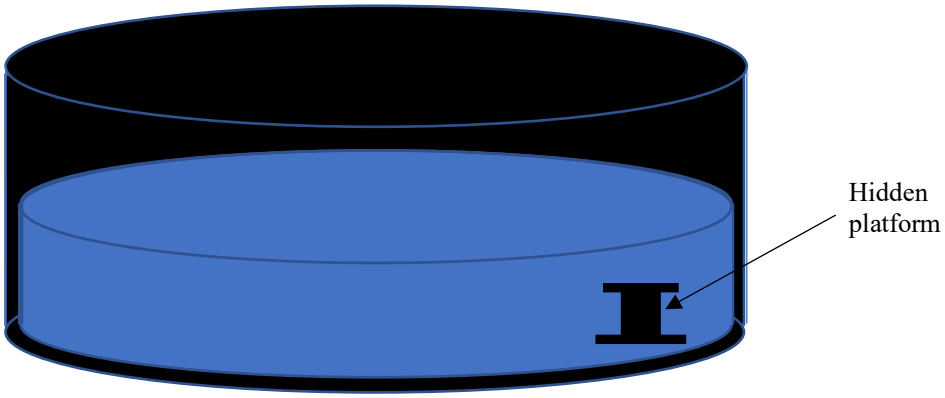


Figure 6: Drawing of the Morris Water Maze test apparatus. *The black plastic pool was lit from below and contained a hidden platform below the surface, and visual cues (1, 2, 3) were fixed on the walls. A camera was fixed to the ceiling and recorded the trial.*

The pool contained an escape platform (8 cm diameter, height 16.5 cm) located 0.5 cm from the surface in a consistent location. Several three-dimensional, fixed visual cues were installed around the pool. The water was made opaque by the addition of a standardised amount of paint and, depending on the mouse model being tested, either black paint (for the SAMP8 and SAMR1 model with a white coat colour) or white paint (for the J20 model, with a brown coat colour) to allow good contrast for video tracking. An example of tracks is shown in Fig 7.

For the first swim in the pool (the pre-trial), the platform was not placed in the pool, and the mice were allowed to swim freely for one minute. They were removed from the pool and dried and allowed to rest. Two hours later, the platform was installed, and the mice were placed in the pool again and allowed to find the platform. If, after one minute, a mouse had not found the platform, they were gently guided onto it by hand. The release locations around the cardinal points of the pool (identified as North, West, South and East) were randomly alternated, and the results of the four consecutive trials were averaged. The distance travelled before reaching the escape platform, the time to escape and the swimming speed were determined.

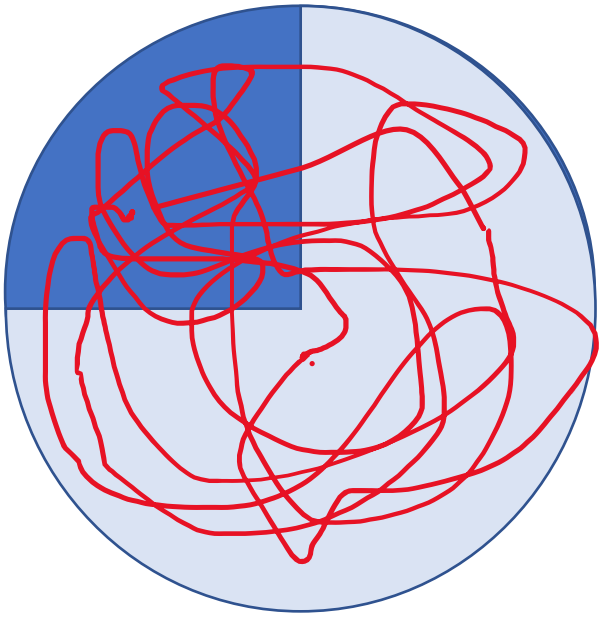


Figure 7: Example of tracking of MWM trial. The quadrant in darker colour is the one containing the platform, the red line materialises the path of the mouse.

After seven acquisition trials, a probe-trial was performed without the platform. The mice had to swim for one minute again. The behaviour of the animals was again recorded and to assess performance in the task, the number of platform crossings, the swimming speed and the distance travelled were determined.

4.1.2.2. Elevated O-Maze

To assess anxiety-like behaviour, the mice underwent an elevated O-maze test. The maze (Technosmart, Rome, Italy) consisted of a circular path, made of black polyvinylchloride covered in white electrical tape to allow good contrast for video tracking, with a runway width of 5.5 cm and a diameter of 46 cm. It was placed 20 cm above the floor, with two opposing compartments protected by walls of black polyvinylchloride (height 10 cm). The floor level lighting was kept constant at 5 lx. The recorded behaviour was analysed using Ethovision software v11.1.

Mice were introduced to one of the closed compartments of the apparatus, and their behaviour was recorded and assessed for five minutes, before being removed and the apparatus cleared of debris or faeces. The latency to the first exit from these compartments and the total time spent inside the compartments were scored as a measure of anxiety (Kulkarni et al., 2007).

4.1.2.3. Rotarod

The animals were placed on an accelerating Rota-rod (Ugo Basile, Gemonio, Italy), following an Accelerated Rotation Rate (ARR) protocol. After ten seconds of acclimatization at 4 rpm, the speed of the rotating rod was steadily increased, up to 20 rpm/min. Each animal was tested three times on the same day, with a 15-minute rest period between tests.

The time to fall off the rotating rod onto the platform underneath was measured automatically. If an animal clung to the rod and completed a full passive rotation, this occurrence was treated as a failure in performance, and the timer was stopped manually for this animal. If an animal fell before the start of the acceleration (i.e., within the first ten seconds), this was not considered a failure and the animal was replaced on the rod. Any faeces were removed, and the apparatus wiped down with a solution of 70% ethanol between each group of animals.

4.1.2.4. Termination

The animals were terminally anesthetised with an intra-peritoneal injection of 0.3ml of sodium pentobarbitone and transcardially perfused with 15 ml of 0.9% heparinized saline (5U/ml, H4784, Sigma Aldrich, St Louis, MO, USA), followed by 20 ml of 10% formalin (HT

501640, Sigma Aldrich, St Louis, MO, USA). The brains were then excised and stored in 10% formalin prior to processing.

4.1.3. Exposures

Animals were exposed to a whole-body exposure 1800 MHz pulsed fields of 3W/kg, 0.3W/kg or sham exposure using reverberation chambers. These were designed and manufactured by IT'IS Foundation for Research on Information (Zurich, Switzerland).

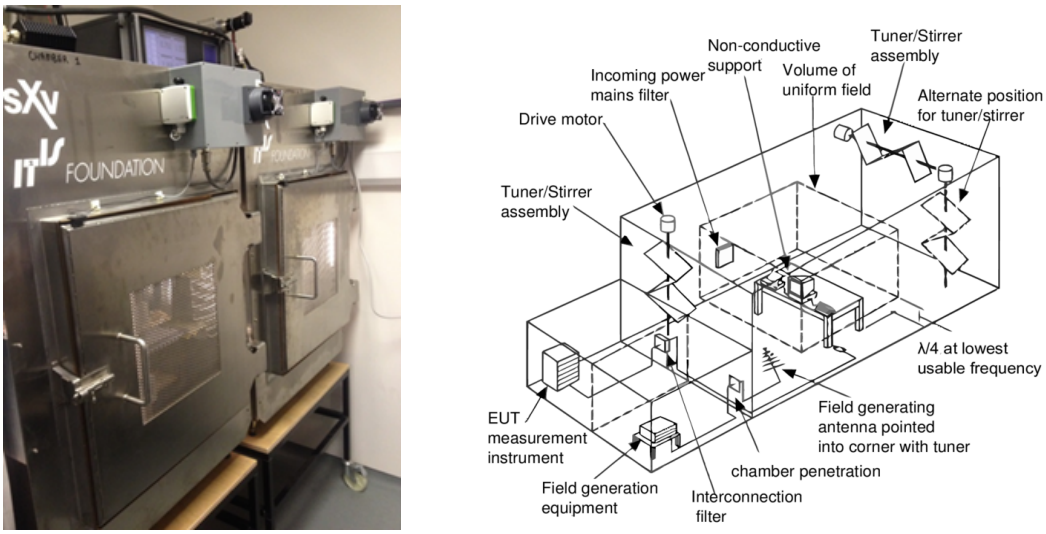


Figure 8: Two of the three reverberation chambers used. Access to the chambers was provided at the front by the doors and the animals could be observed through the aperture in each door.

The apparatus provided an electromagnetic field exposure, according to the average weight of the animals that were introduced in each exposure group. It produced a uniform and homogenous exposure field for unrestrained animals, using a system of orthogonal mechanical stirrers installed in the ceiling and rear walls of each chambers. The signal used Global System for Mobile Communication (GSM) modulation, as used by mobile phones. The system was composed of a signal generator, a signal amplifier, a control unit and a computer.

Dimensions of each chamber were 70cm wide, 65cm deep, 1m high and each chamber could hold six individually housed mice, with each cage 100mm away from walls or stirrers. Exposure was controlled by software and all exposures and environmental parameters recorded by data acquisition unit EASY 4 (Exposure Acquisition SYstem 4). Exposures only lasted 30 min, it was not considered necessary to provide either food or water during the exposure; also the addition of water would have affected the dosimetry. The mice were returned to their home cages immediately after the end of exposure, where food and water were provided *ad libitum*.

The dosimetry was performed by IT'is Zurich using FDTD simulation platform SEMACAD X as described in Capstick et al. (2014). The field homogeneity inside the exposure region was 0.61 dB +/- 2.0dB, with a field isotropy of 0.88dB where was the energy going, distribution of energy into specific organs especially the brain.

4.2. Immunohistochemistry

4.2.1. Tissue preparation for immunohistochemistry

4.2.1.1. Formalin fixing

After dissection, the brains were post-fixed for 24 h in 10% formalin, then dehydrated in 70% ethanol) over three days before being stored in 70% ethanol (E/0650DF/17, Fisher Chemicals, Loughborough, UK) prior to processing.

4.2.1.2. Processing

The brains were processed using a Tissue-Tek® VIP® Vacuum infiltration processor (Sakura, Torrance, CA, USA), using the following program: 70% Ethanol 4 hours, followed by

80%, 90%, 95% and 100%, each for two hours, 50/50 Ethanol /Histochoice one hour, 25/75 Ethanol /Histochoice one hour, 100% Histochoice two hours x 2, one-hour paraffin x 4. After processing, the brains were embedded using a tissue embedding centre (EG1150H, Leica Microsystems, Milton Keynes, UK).

4.2.1.3. Sectioning

7 µm-thick sagittal sections, starting 2.35 mm lateral to the bregma line were obtained using a microtome (LRM2255, Leica) before being transferred on to slides (Flex, IHC microscope slides reference K8020, Dako, Burlington, USA) by the free-floating method. Sections were left to fully adhere and dry for two hours at 58°C, then left at room temperature for at least 30 minutes before immunohistochemistry.

4.2.2. Staining

All staining was performed using an automated slide staining workstation (Autostainer Link48, Dako, USA). After staining slides were transferred into distilled water, before being dehydrated in 70% Ethanol (Fisher Chemicals, UK) 90% Ethanol, two successive solutions of absolute alcohol and three solutions of xylene (X/0200/17, Fisher Chemicals, UK), where they were kept until they were coverslipped using DPX-mountant (36029, BDH, UK)

4.2.2.1. Antigen retrieval

Prior to immunohistochemistry, antigen retrieval was performed. Depending on the antibody investigated, a low pH, high pH or a formic acid pre-treatment was given (see Table 1). Low and high pH pre-treatments were carried out in the PT link (REFERENCE XXX) and included rehydration. For the low pH treatments, a Tris/EDTA solution (pH 6.1) was used

(EnVision FLEX Target Retrieval Solution, Low pH (50x), K8005, Dako), and for the high pH pre-treatments, a citrate solution (pH 9) (EnVision FLEX Target Retrieval Solution, High pH (50x), K8004, Dako) was used. A formic acid pre-treatment was used for the Beta-Amyloid Antibody (4G8), where slides were rehydrated through a succession of xylene, absolute ethanol, 90% ethanol and 70% ethanol before being placed in 10% formic acid solution, pH= 1.6 (F/1900/PB08, Fisher Chemicals, UK) for 30 minutes at room temperature. Slides were then rinsed 2x2 minutes in 0.1% PBS Tween 20 (P4417, Sigma Aldrich, USA).

Antibody	Pre-treatment	Staining		Counterstaining
		Target	Dilution	
GFAP **Polyclonal rabbit** **anti-GFAP** **(Z0334, Dako)**	High pH, 20min, 97°C	Astroglia	1:2000	NO
Synaptophysin **SY38** **Mouse monoclonal** **(ab8049, Abcam)**	Low pH, 30min, 65°C	Presynaptic vesicles	1:600	NO
NeuN **Mouse Ms X** **(ab178846, Abcam)**	Low pH, 20min, 97°C	Neurons	1:9000	NO
IbA1 **Rabbit monoclonal** **(ab178846, Abcam)**	High pH, 20min, 97°C	Microglia	1:9000	Mayer's Haematoxylin
4G8 **Mouse monoclonal** **(800701, Biolegend)**	10% formic acid, 30 min, room temperature	ß-amyloid	1:5000	Cresyl Violet

Table 1: Timeline of experiment for the senescence accelerated-mouse model SAMP8 and its control SAMR1.

4.2.2.2. *Immunohistochemistry on the Autostainer*

First, endogenous peroxidase was blocked by peroxidase-blocking agent (reference). After washing with wash buffer, the primary antibody (see table 1) diluted in antibody diluent (EnVision FLEX+ antibody diluent, K800621, Dako) was added to the slides for 30 minutes. After washing, the slides were incubated with the secondary antibody (coupled to HRP peroxidase by a dextran backbone). After washing, hydrogen peroxide and diaminobenzidine was added.

The Flex + protocol was used when signal amplification was required (for synaptophysin and Beta amyloid. Slides were then placed in distilled water, to be either counterstained and dehydrated, or directly dehydrated.

4.2.2.3. *Counterstaining*

Counterstaining was required for IbA1 and ß-amyloid immunohistochemistry, as tissues structures were not easily visible for analysis.

For the IbA1 the slides were briefly dipped in Mayer's haematoxylin (MHS16, Sigma Aldrich, USA) solution, before being left for seven minutes under running warm tap water, then in Scott's tap water, before being dehydrated and coverslipped.

For ß-amyloid, slides were immersed for five minutes in 0.5 % Cresyl violet solution (Cresyl Fast Violet (C5042, Sigma Aldrich, USA), distilled water, Acetic Acid) before being rinsed in distilled water for one minute, dehydrated and coverslipped.

4.3. Immunohistochemistry Analysis

Digital microphotographs were taken on a microscope (Leica DC 2000, Leica Microsystems, Milton Keynes, UK) coupled to a digital camera (Leica DFC 450 C) and using Leica Qwin standard software, v3.5.1. All image analysis was performed on Image J (v1.47, NIH). Two sections per brain were analysed and averaged.

4.3.1. Synaptophysin density

Grayscale images of the whole hippocampus were recorded at 5 x magnification, and regional synaptophysin density was taken in the CA1, CA3 and in DG regions, as shown in figure 9.

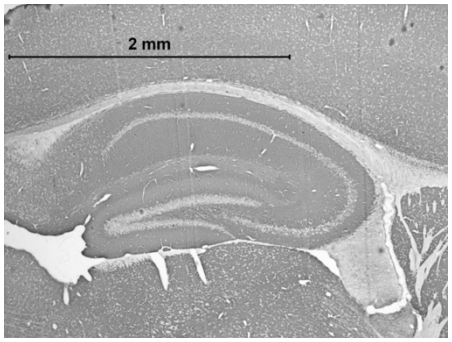


Figure 9: Synaptophysin staining of a SAMP8 hippocampus, magnification 5X.

4.3.2. Quantification of astroglia with GFAP positive astrocytes

Grayscale images of CA1, CA3 and DG were recorded at a 20 times magnification. The background was digitally removed, and the images were thresholded to enable quantification with Image J software as shown in figures 10 and 11.

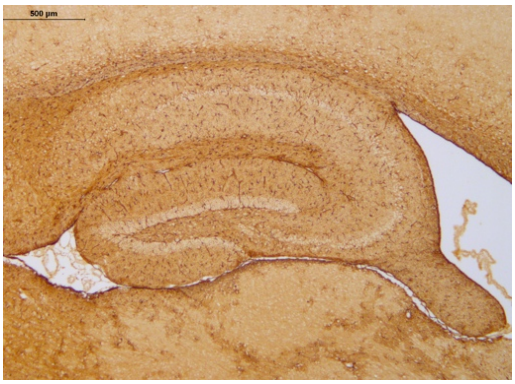
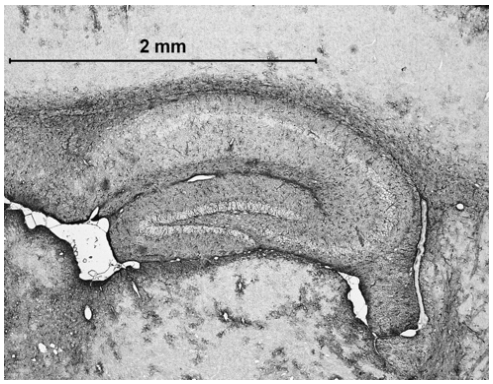
a)  b) 

Figure 10: GFAP staining in SAMP8 hippocampus, magnification 5x.

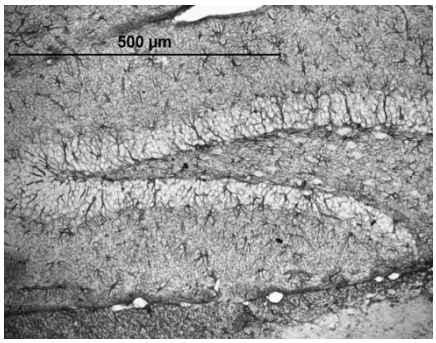


Figure 11: Magnification 40x of GFAP in SAMP8 DG.

4.3.3. Quantification of Iba1 positive microglia

Colour images of the whole hippocampus were taken at a 5 times magnification as shown in figure 12. The background was digitally removed, and the images were thresholded to enable quantification with Image J software.

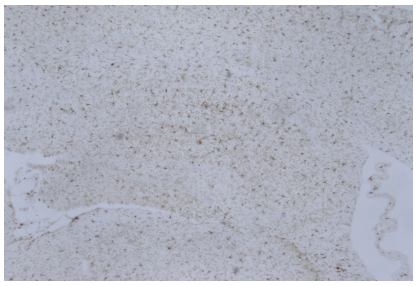


Figure 12: IbA1 staining, J20 hippocampus, magnification 5X.

4.3.4. Quantification of β-amyloid

Colour images of the whole hippocampus were taken at a 20 times magnification as shown in figure 13. Figure 14 shows a 40X magnification of an Aβ deposit. After a region of interest including the entire hippocampus was defined, the Aβ plaques area measured by Image J.

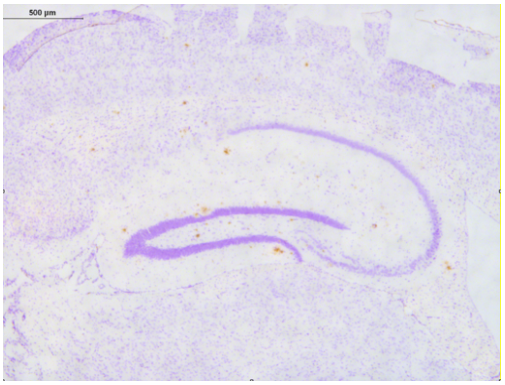
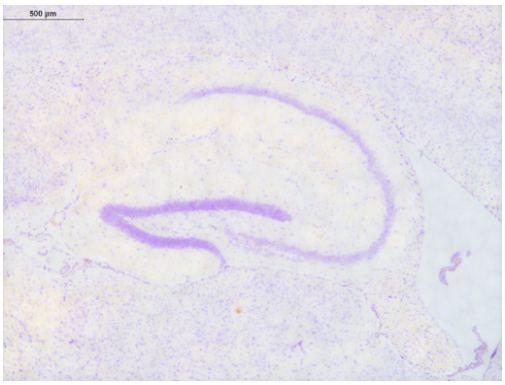
a)  b) 

Figure 13: Aβ staining in J20 and WT hippocampus. a) *Image of a J20 hippocampus after Aβ-staining;* ***b)*** *Image of a J20 hippocampus after Aβ-staining.*

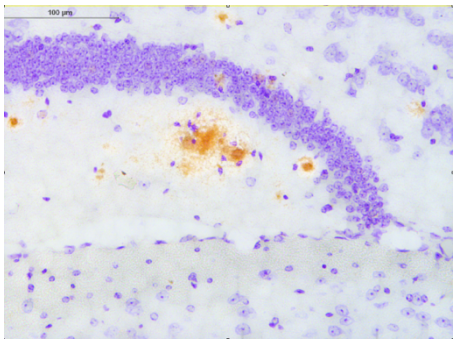


Figure 14: Magnification 40x of an AB deposit.

4.3.5. Quantification of NeuN positive Nuclei

Colour images of the whole hippocampus were taken at a 40 times magnification, as shown in figures 15 and 16. After definition of regions of interest in the CA1, CA3 and DG areas, the

number of NeuN positive nuclei within each region were manually counted by using the cell counting tool within ImageJ.

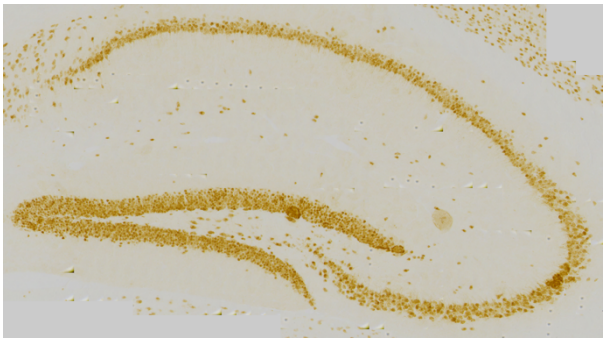


Figure 15: NeuN staining, magnification 40x, in SAMR1 hippocampus.

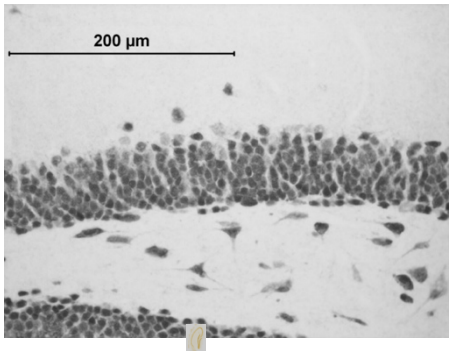


Figure 16: Magnification 40x of NeuN staining in the DG area.

4.4. Statistics

The number of animals per group was determined by the MWM experiment, following Charan (2013) (Charan and Kantharia, 2013)using the G Power software (Faul et al., 2007), on the basis of a two-tailed test, with $\alpha = 0.05$. The power was set to 80%. The effect size was set to 0.5 (medium effect), according to Reed (Reed et al., 2010). Data analysis was performed using Minitab® v17. Statistical significance was set at $p<0.05$. Group means of all tests were compared by a two-way ANOVA test, followed by a post-hoc Tukey t-test if the ANOVA was significant. Errors bars on the graphs were set using a 95% confidence interval.

5. The effect of EMF exposure on a mouse model of Alzheimer disease

5.1. General background

5.1.1. Experimental approach

To assess whether RF exposure had a long-term impact on learning and memory in Alzheimer disease following an early exposure, an Alzheimer's disease mouse model (J20) and its wild type control (C57Bl/6) were subjected to long-term, chronic exposure of 1800 MHz pulsed fields, which are the maximum wavelength for mobile phones. The whole-body SARs were chosen to reflect the values currently in use in international guidelines for limiting the exposure of workers and the general population (ICNIRP, 1998). These values are well below the exposures required for whole body heating, as an investigation of overt thermal effects was not the subject of this work.

5.1.2. Mouse model

Starting at 5 to 7 months of age, the J20 mice exhibit diffuse Aß plaque deposits in the hippocampus that will progress to widespread plaques by 8 to 10 months. They show no neurofibrillary tangles, and any neuronal loss varies depending on brain region, for example in the CA1 region of the hippocampus the pathology is first observable at 3 months compared to age-matched wild-type animals (Wright et al., 2013). From five months, a significant increase in the number of reactive GFAP-positive astrocytes and in microglia was observed in the hippocampi of J20 mice when compared to age-matched wild-type controls (Wright et al., 2013). J20 mice also show age-dependent synaptic loss in the hippocampus by 3 months (Hong et al., 2016).

Behaviourally, the J20 model shows deficits in spatial memory and learning by 4 months, as measured by Morris water maze (Cheng et al., 2007), making it an ideal model for our study.

5.2. Experimental protocol

J20 and C57 mice were randomly distributed into three groups and were then exposed to 1800 MHz pulsed fields, at three different SARs: 3 W/kg, 0.3 W/kg and 0 W/kg (sham-exposed controls). To assess the effect of early exposures to RF in aged adults, mice were exposed at two months old until 6 months, before being tested at either 6 or 12-month of age.

5.3. Results

5.3.1. Behavioural endpoints

5.3.1.1. Rotarod

At 6 months, there was a significant difference (ANOVA, p= 0.015) between J20 and WT mice, with J20 mice managing to stay for longer on the rod than their WT counterparts. There was no significant difference between exposure levels (ANOVA, p= 0.431), and there was no interaction between the strain and the exposure (ANOVA, p= 0.808), as shown in figure 16a.

At 12 months, there were no significant differences (ANOVA, p= 0.439) in the time to fall off the Rotarod between the J20 and WT mice. There was no significant difference between exposure levels (ANOVA, p= 0.721). There was an interaction between the strain and the exposure (ANOVA, p= 0.034), though the Tuckey post hoc test did not highlight differences between groups, as shown in figure 16b.

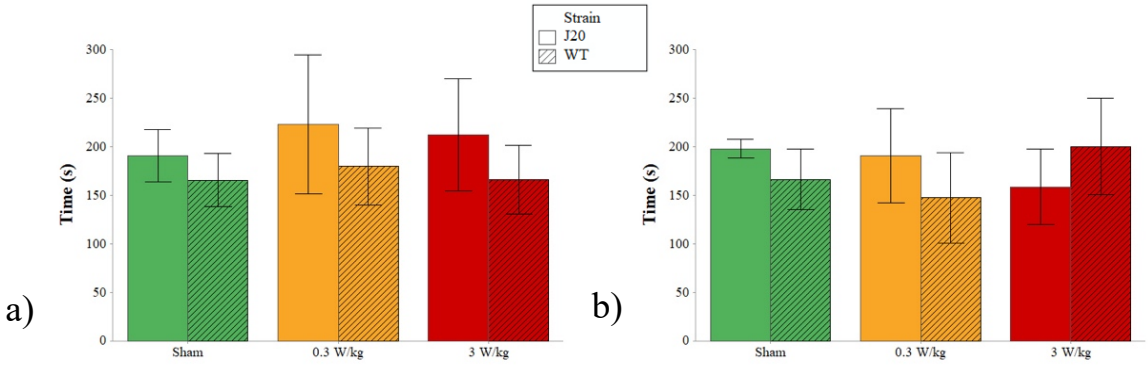


Figure 16: Exposure does not impact locomotor abilities. *The animals were exposed to either 3 W/kg RF or 0.3 W/kg or a sham exposure.* ***a)*** *There were no differences in the time to fall between groups in 6-month-old animals (for J20 animals, n= 5 for 3 W/kg and 0.3 W/kg, n= 8 for sham; for WT animals, n= 11 for 3 W/kg, n= 12 for 0.3 W/kg and n= 13 for sham);* ***b)*** *There were no significant differences in the time to fall between groups in 12-month-old mice (for J20 mice, n= 6 for 3 W/kg, n= 7 for 0.3 W/kg, n= 5 for sham; for WT mice, n= 7 for 3 W/kg and sham, n= 6 for 0.3 W/kg).*

5.3.1.2. O-Maze

5.3.1.2.1. Time spent inside compartments

At 6 months, there was a significant difference (ANOVA, p= 0.001) in the time spent inside the compartments between J20 and WT mice, with J20 mice staying for longer **outside** than their WT counterparts. There was a significant difference between exposure groups (ANOVA, p= 0.006), but no interaction between groups (ANOVA, p=0.135) as shown in figure 16a. 0.3 W/kg-exposed group show a statistically (ANOVA, p= 0.006) significant increase in the time spent **inside** when compared to 3 W/kg-exposed group (Tuckey post hoc test, 0.3 W/kg vs Sham, p= 0.208; 3 W/kg vs Sham, p= 0.203; 3 W/kg vs 0.3 W/kg, p= 0.004), as shown in figure 17a.

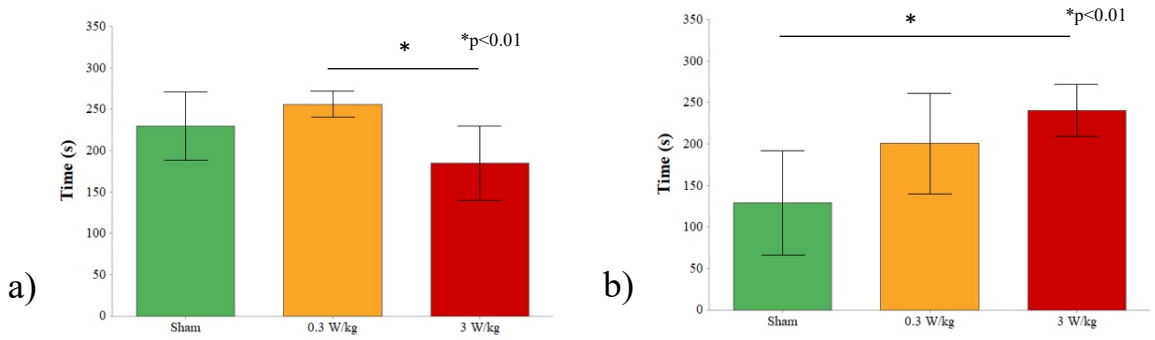


Figure 17: Exposure increases anxiety in O-maze test*. The animals were exposed to either 3 W/kg RF or 0.3W/kg or a sham exposure.* ***a)*** *At 6 months, there was a significant difference (ANOVA, p< 0.01) in the time spent within the enclosed compartments between 0.3 W/kg and 3 W/kg exposure groups, the 0.3 W/kg exposure group spending significantly more time in the compartments than the 3 W/kg-exposed (post hoc, p<0.01) (for J20 animals, n= 7 for 3 W/kg, n= 6 for 0.3 W/kg and sham; for WT animals, n= 8 for 3 W/kg, n= 7 for 0.3 W/kg and n= 10 for sham);* ***b)*** *At 12 months, there was a significant difference (ANOVA, p< 0.01) in the time spent within the enclosed compartments between 3W/kg and sham exposure groups, the time spent within the compartments for the sham-exposed group being significantly higher than the 3 W/kg exposure group (post hoc, p< 0.01) (for J20 animals, n= 8 for 3 W/kg, n= 7 for 0.3 W/kg and sham; for WT animals, n= 9 for 3 W/kg, n= 8 for 0.3 W/kg and sham).*

At 12-months old, there was no significant difference (ANOVA, p= 0.718) in the time spent inside the compartments between the J20 and the WT mice. There was a significant difference between exposure groups (ANOVA, p= 0.008) without any significant interaction (ANOVA, p= 0.408), as shown in figure 17b. 3 W/kg-exposed group show a statistically (ANOVA, p= 0.004) significant increase in the time spent inside when compared to sham-exposed group (Tuckey post hoc test, 0.3 W/kg vs Sham, p= 0.105; 3 W/kg vs Sham, p= 0.006; 3 W/kg vs 0.3 W/kg, p= 0.510), as shown in figure 18b.

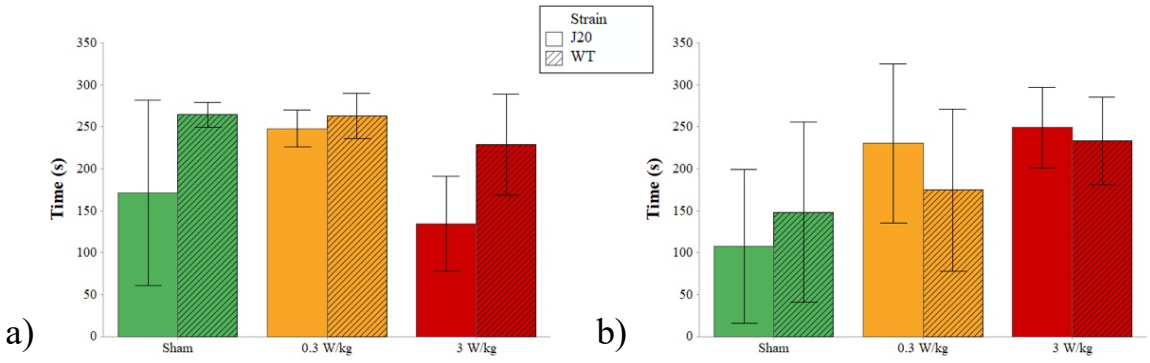


Figure 18: Exposure has an effect on anxiety in O-maze test*. The animals were exposed to either 3 W/kg RF or 0.3W/kg or a sham exposure.* ***a)*** *There were no significant differences in the time spent within the enclosed compartments between groups in 6-month-old mice (for J20 animals, n= 7 for 3 W/kg, n= 6 for 0.3 W/kg and sham; for WT animals, n= 8 for 3 W/kg, n= 7 for 0.3 W/kg and n= 10 for sham);* ***b)*** *There were no significant differences in the time spent within the enclosed compartments between groups in 12-month-old mice (for J20 animals, n= 8 for 3 W/kg, n= 7 for 0.3 W/kg and sham; for WT animals, n= 9 for 3 W/kg, n= 8 for 0.3 W/kg and sham).*

5.3.1.2.2. Latency to exit compartments

At 6-months old, there was no significant difference (ANOVA, p= 0.532) in the latency between the start of the trial and the first outing from the compartments between J20 and WT mice. There was no significant difference between exposure groups (ANOVA, p= 0.196), as shown in figure 19a. There was a significant interaction between exposure groups (ANOVA, p= 0.043) between the J20 group exposed to 3W/kg when compared to sham-exposed J20 (p= 0.013), thought the Tuckey post hoc test did not confirm this (adjusted p-value, p= 0.109), as shown in in figure 20a.

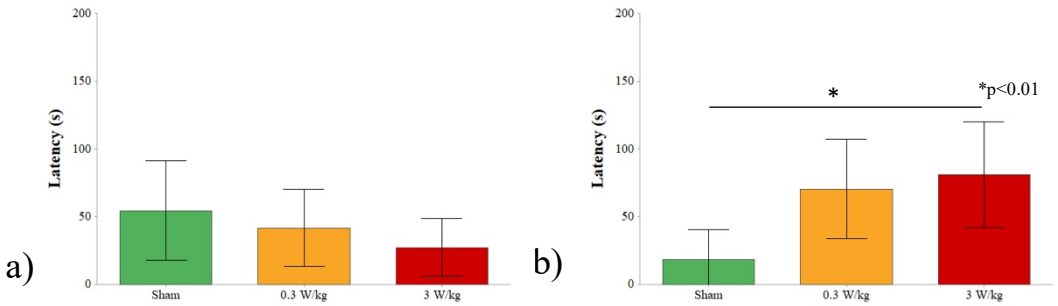


Figure 19: Exposure increases anxiety in O-maze test*. The animals were exposed to either 3 W/kg RF or 0.3W/kg or a sham exposure.* ***a)*** *There were no significant differences in the time to exit the enclosed compartments between groups in 6-month-old mice (for J20 animals, n= 7 for 3 W/kg, n= 6 for 0.3 W/kg and sham; for WT animals, n= 8 for 3 W/kg, n= 7 for 0.3 W/kg and n= 10 for sham);* ***b)*** *At 12 months, there was a significant difference (ANOVA, p< 0.01) in the latency to first exit the compartments between 3W/kg and sham exposure groups, the time to exit the compartments for the 3 W/kg-exposed group being significantly higher than the sham-exposed group (post hoc, p< 0.02) (for J20 animals, n= 8 for 3 W/kg, n= 7 for 0.3 W/kg and sham; for WT animals, n= 9 for 3 W/kg, n= 8 for 0.3 W/kg and sham).*

At 12 months, there were no significant differences (ANOVA, p= 0.492) in the latency between the start of the trial and the first outing from the compartments between J20 and WT mice. There was a significant difference between exposure groups (ANOVA, p= 0.015), though without any interaction between groups (ANOVA, p= 0.172) as shown in figure 19b. 3 W/kg-exposed group show a statistically (ANOVA, p= 0.004) significant increase in the latency to exit the compartments when compared to sham-exposed group (Tuckey post hoc test, 0.3 W/kg vs Sham, p= 0.055; 3 W/kg vs Sham, p= 0.018; 3 W/kg vs 0.3 W/kg, p= 0.920), as shown in in figure 20b.

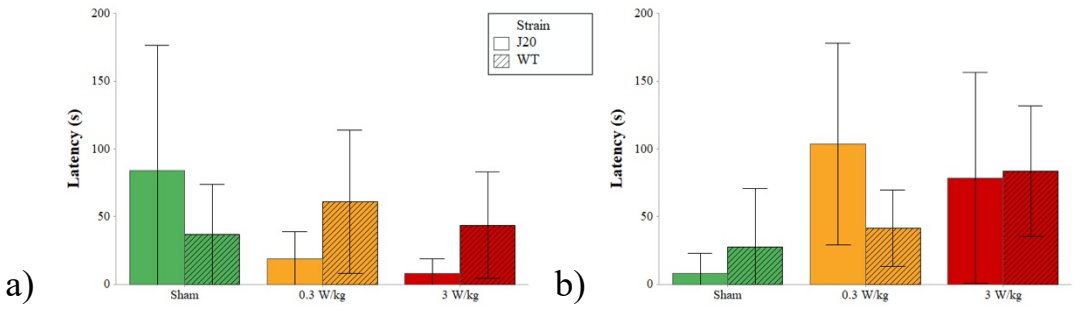


Figure 20: Exposure has an effect on anxiety in O-maze test*. The animals were exposed to either 3 W/kg RF or 0.3W/kg or a sham exposure.* ***a)*** *There were no significant differences in the time spent within the enclosed compartments between groups in 6-month-old mice (for J20 animals, n= 7 for 3 W/kg, n= 6 for 0.3 W/kg and sham; for WT animals, n= 8 for 3 W/kg, n= 7 for 0.3 W/kg and n= 10 for sham);* ***b)*** *There were no significant differences in the time spent within the enclosed compartments between groups in 12-month-old mice (for J20 animals, n= 8 for 3 W/kg, n= 7 for 0.3 W/kg and sham; for WT animals, n= 9 for 3 W/kg, n= 8 for 0.3 W/kg and sham).*

5.3.1.3. Morris Water Maze

5.3.1.3.1. Acquisition

5.3.1.3.1.1. Trial 2

####### a. Velocity

At 6 months of age, there were no significant differences in velocity (ANOVA, p= 0.87) between J20 and WT. There were no significant differences between exposure groups (ANOVA, p= 0.055) and no significant interaction between strain and exposure groups either (ANOVA, p=0.336), as shown in figure 21.

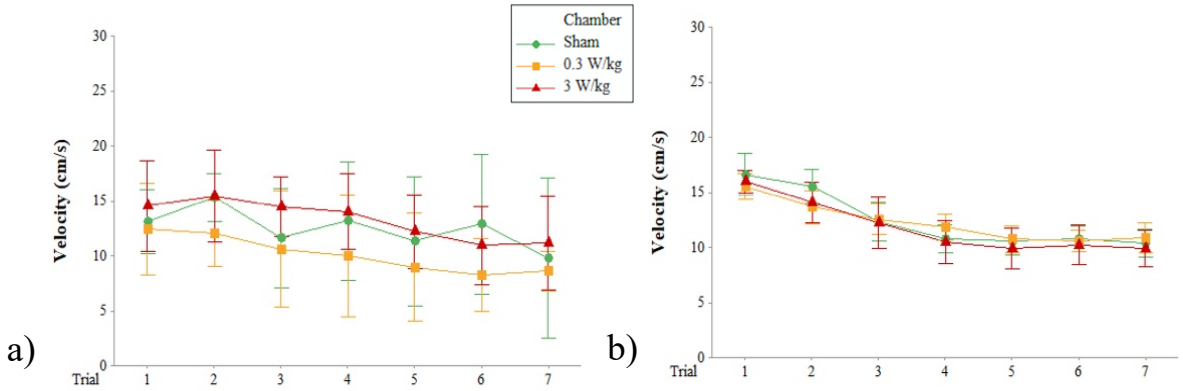


Figure 21: At 6 months, exposure has no effect on locomotion in MWM learning. *The animals were exposed to either 3 W/kg RF or 0.3W/kg or a sham exposure.* ***a)****, 0.3 W/kg-exposed J20 were significantly slower ($p<0.05$) than 3 W/kg-exposed J20 (n= 5 for 3 W/kg and for 0.3 W/kg, n = 4 for sham);* ***b)*** *There were no significant differences in velocity between groups in 6-month-old WT (n= 13 for 3 W/kg, n= 12 for 0.3 W/kg and n= 9 for sham).*

At 12 months of age, there were no significant differences in velocity (ANOVA, p= 0.377) between J20 and WT. There were no significant differences between exposure groups (ANOVA, p= 0.67) and no significant interaction between strain and exposure groups either (ANOVA, p=0.944), as shown in figure 22.

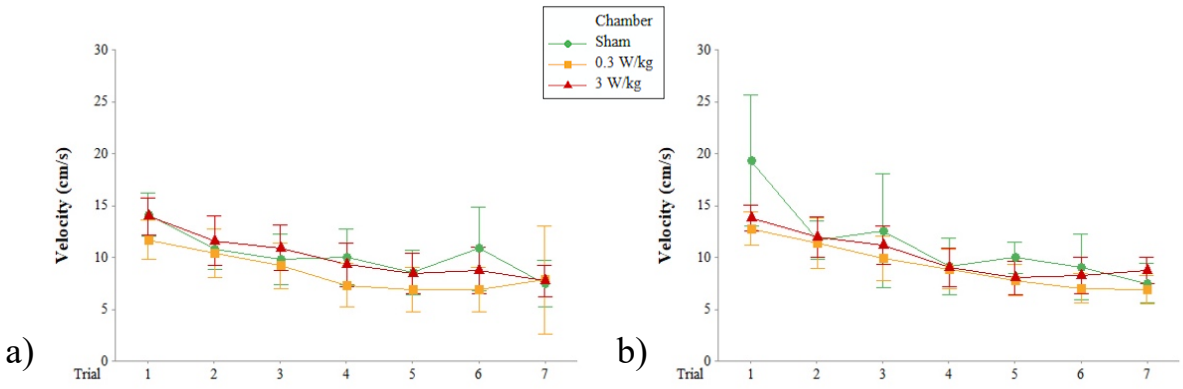


Figure 22: At 12 months, exposure has no effect on locomotion during learning. *The animals were exposed to either 3 W/kg RF or 0.3W/kg or a sham exposure.* ***a)*** *There were no significant differences in velocity between groups in 12-month-old J20 (n= 10 for 3 W/kg, n= 12 for 0.3 W/kg and n= 10 for sham);* ***b)*** *There were no significant differences in velocity between groups in 12-month-old WT (n= 12 for 3 W/kg, n= 14 for 0.3 W/kg and n= 11 for sham).*

b. Latency to reach the target area

At 6 months of age, there was a significant difference in the latency to first reach the platform area (ANOVA, $p < 0.01$) between J20 and WT, with J20 taking longer to reach the platform area than the WT mice. There were no significant differences between exposure groups (ANOVA, $p = 0.292$) but a significant interaction between strain and exposure groups (ANOVA, $p=0.006$), as shown in figure 23.

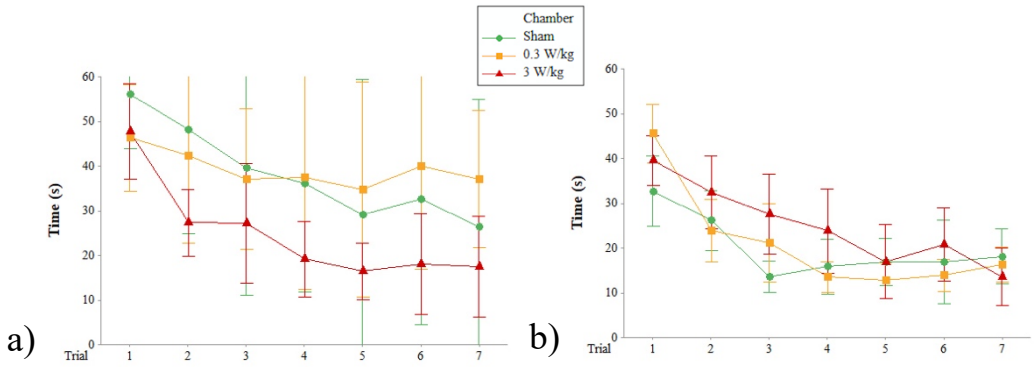


Figure 23: At 6 months, exposure has no effect on learning. *The animals were exposed to either 3 W/kg RF or 0.3W/kg or a sham exposure.* ***a)*** *There were no significant differences in the latency to reach the target area between groups in 6-month-old J20 (n= 5 for 3 W/kg and for 0.3 W/kg, n = 4 for sham);* ***b)*** *There were no significant differences in in the latency to reach the target area between groups in 6-month-old WT (n= 13 for 3 W/kg, n= 12 for 0.3 W/kg and n= 9 for sham).*

At 12 months of age, there was a significant difference in the latency to first reach the platform area (ANOVA, $p < 0.001$) between J20 and WT, with J20 taking longer to reach the platform area than the WT mice. There were no significant differences between exposure groups (ANOVA, $p = 0.72$) and no significant interaction between strain and exposure groups either (ANOVA, $p=0.487$), as shown in figure 24.

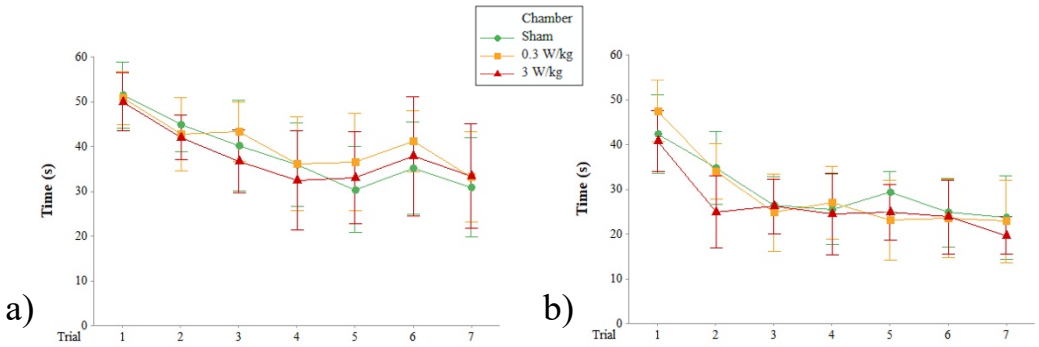


Figure 24: At 12 months, exposure has no effect on learning. *The animals were exposed to either 3 W/kg RF or 0.3W/kg or a sham exposure.* ***a)*** *There were no significant differences in the latency to reach the target area between groups in 12-month-old J20 (n= 10 for 3 W/kg, n= 12 for 0.3 W/kg and n= 10 for sham);* ***b)*** *There were no significant differences in the latency to reach the target area between groups in 12-month-old WT (n= 12 for 3 W/kg, n= 14 for 0.3 W/kg and n= 11 for sham).*

5.3.1.3.1.2. Trial 3

a. Velocity

At 6 months of age, there were no significant differences in velocity (ANOVA, p= 0.881) between J20 and WT. There were no significant differences between exposure groups (ANOVA, p= 0.264) and no significant interaction between strain and exposure groups either (ANOVA, p=0.164), as shown in figure 21.

At 12 months of age, there were no significant differences in velocity (ANOVA, p= 0.263) between J20 and WT. There were no significant differences between exposure groups (ANOVA, p= 0.382) and no significant interaction between strain and exposure groups either (ANOVA, p=0.613), as shown in figure 22.

b. Latency to reach the target area

At 6 months of age, there was a significant difference in the latency to first reach the platform area (ANOVA, p< 0.001) between J20 and WT, with J20 taking longer to reach the

platform area than the WT mice. There were no significant differences between exposure groups (ANOVA, p= 0.881) and no significant interaction between strain and exposure groups either (ANOVA, p=0.35), as shown in figure 23.

At 12 months of age, there was a significant difference in the latency to first reach the platform area (ANOVA, p< 0.001) between J20 and WT, with J20 taking longer to reach the platform area than the WT mice. There were no significant differences between exposure groups (ANOVA, p= 0.143) and no significant interaction between strain and exposure groups either (ANOVA, p=0.396), as shown in figure 24.

5.3.1.3.2. Memory

5.3.1.3.2.1. Pre-trial

a. Velocity

At 6 months of age, there was a significant difference in velocity (ANOVA, p<0.001) between J20 and WT mice, with the J20 mice being significantly slower than their WT counterparts. There was a significant difference between exposure groups (ANOVA, p= 0.032). 0.3 W/kg-exposed group had a statistically (ANOVA, p= 0.05) significant decrease in the average speed when compared to 3 W/kg-exposed group (Tuckey post hoc test, 0.3 W/kg vs Sham, p= 0.741; 3 W/kg vs Sham, p= 0.197; 3 W/kg vs 0.3 W/kg, p= 0.029). The interaction between strain and exposure groups was also significant (ANOVA, p= 0.033), with the 0.3 W/kg exposed J20 groups being significantly lower (Tuckey post hoc test, J20 0.3 W/kg vs WT 0.3 W/kg p= 0.003; J20 3 W/kg vs J20 0.3 W/kg, p= 0.036; J20 0.3 W/kg vs WT sham, p= 0.003).

At 12 months of age, there were no significant differences in velocity (ANOVA, p= 0.155) between J20 and WT mice. There were no significant differences between exposure groups (ANOVA, p= 0.189) and no significant interaction between strain and exposure groups either (ANOVA, p= 0.568).

b. Latency to reach the target area

At 6 months of age, there were no significant differences in the latency to reach the target area (ANOVA, p= 0.458) between J20 and WT mice. There were no significant differences between exposure groups (ANOVA, p= 0.554) and no significant interaction between strain and exposure groups either (ANOVA, p= 0.568)

At 12 months of age, there were no significant differences in the latency to reach the target area (ANOVA, p= 0.325) between J20 and WT mice. There were no significant differences between exposure groups (ANOVA, p= 0.084) and no significant interaction between strain and exposure groups either (ANOVA, p= 0.469).

c. Distance

At 6 months of age, there was a significant difference in the total distance swum by the mice (ANOVA, p<0.001) between J20 and WT mice, with the J20 mice swim less than their WT counterparts. There was a significant difference between exposure groups (ANOVA, p= 0.032). 0.3 W/kg-exposed group had a statistically (ANOVA, p= 0.05) significant decrease in the total distance swum when compared to 3 W/kg-exposed group (Tuckey post hoc test, 0.3 W/kg vs Sham, p= 0.730; 3 W/kg vs Sham, p= 0.199; 3 W/kg vs 0.3 W/kg, p= 0.028; J20 0.3 W/kg vs WT 3 W/kg p= 0.002). The interaction between strain and exposure groups was also

significant (ANOVA, p= 0.032), with the 0.3 W/kg-exposed J20 groups swimming significantly less (Tuckey post hoc test, J20 0.3 W/kg vs WT 0.3 W/kg p= 0.003; J20 3 W/kg vs J20 0.3 W/kg, p= 0.036; J20 0.3 W/kg vs WT sham, p= 0.003; J20 0.3 W/kg vs WT 3 W/kg p= 0.002).

At 12 months of age, there were no significant differences in the total distance swum by the mice (ANOVA, p= 0.149) between J20 and WT mice. There were no significant differences between exposure groups (ANOVA, p= 0.172) and no significant interaction between strain and exposure groups either (ANOVA, p= 0.607)

d. Immobility

At 6 months of age, there was a significant difference in the total time spent floating (ANOVA, p<0.001) between J20 and WT mice, with the J20 mice floating more than their WT counterparts. There was a significant difference between exposure groups (ANOVA, p= 0.041). 0.3 W/kg-exposed group had a statistically (ANOVA, p= 0.021) significant increase in the total time spent floating when compared to 3 W/kg-exposed group (Tuckey post hoc test, 0.3 W/kg vs Sham, p= 0.285; 3 W/kg vs Sham, p= 0.645; 3 W/kg vs 0.3 W/kg, p= 0.033). There was no significant interaction between strain and exposure groups (ANOVA, p=0.069).

At 12 months of age, there were no significant differences in the total time spent floating (ANOVA, p= 0.134) between J20 and WT mice. There were no significant differences between exposure groups (ANOVA, p= 0.542) and no significant interaction between strain and exposure groups either (ANOVA, p= 0.729)

5.3.1.3.2.2. Probe-trial

a. Velocity

At 6 months of age, there were no significant differences in velocity (ANOVA, p= 0.068) between J20 and WT mice. There were no significant differences between exposure groups (ANOVA, p= 0.288). The interaction between strain and exposure groups was significant (ANOVA, p= 0.04), with the 0.3 W/kg-exposed J20 group being significantly lower (p=0.029) when compared to the 3 W/kg-exposed J20 group (Tuckey post hoc test, J20 0.3 W/kg vs J20 0.3 W/kg p= 0.047), as shown in figure 25a.

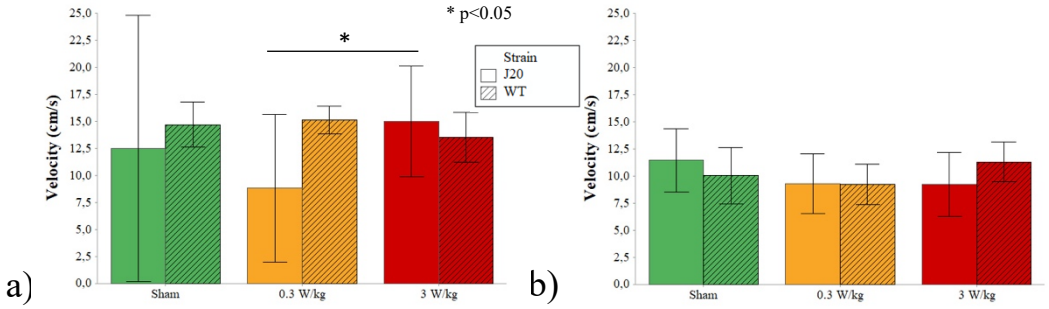


Figure 25: Exposure has no effect on locomotion in MWM probe-trial. *The animals were exposed to either 3 W/kg RF or 0.3W/kg or a sham exposure.* ***a)*** *At 6-month-old animals, 0.3 W/kg-exposed J20 were significantly slower (p<0.05) than 3 W/kg-exposed J20 (for J20 animals, n= 5 for 3 W/kg and for 0.3 W/kg, n = 4 for sham; for WT animals, n= 13 for 3 W/kg, n= 12 for 0.3 W/kg and n= 9 for sham);* ***b)*** *There were no significant differences in velocity between groups in 12-month-old animals (for J20 animals, n= 10 for 3 W/kg, n= 12 for 0.3 W/kg and n= 10 for sham; for WT animals, n= 12 for 3 W/kg, n= 14 for 0.3 W/kg and n= 11 for sham).*

At 12 months of age, there were no significant differences in velocity (ANOVA, p= 0.838) between J20 and WT mice. There were no significant differences between exposure groups (ANOVA, p= 0.385) and no significant interaction between strain and exposure groups either (ANOVA, p= 0.392), as shown in figure 25b.

b. Latency to reach the target area

At 6 months of age, there was a significant difference in the latency to reach the target area (ANOVA, $p< 0.001$) between J20 and WT mice, with WT mice being faster to first reach the platform area. There were no significant differences between exposure groups (ANOVA, $p= 0.641$) and no significant interaction between strain and exposure groups either (ANOVA, $p= 0.149$), as shown in figure 26a.

At 12 months of age, there was a significant difference in the latency to reach the target area (ANOVA, $p= 0.003$) between J20 and WT mice, with WT mice being faster to first reach the platform area. There were no significant differences between exposure groups (ANOVA, $p= 0.495$) and no significant interaction between strain and exposure groups either (ANOVA, $p= 0.647$), as shown in figure 26b.

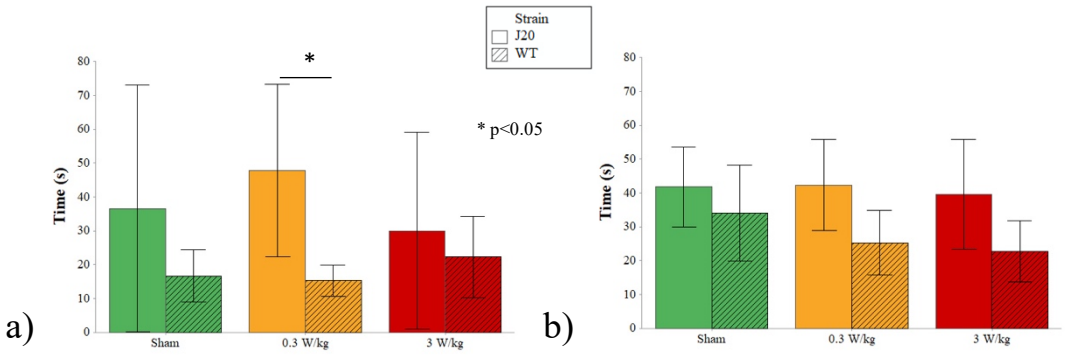


Figure 26: Exposure has no effect on memory in MWM probe-trial. *The animals were exposed to either 3 W/kg RF or 0.3W/kg or a sham exposure.* ***a)*** *There were no significant differences in the latency to reach the target area between groups in 6-month-old animals (for J20 animals, n= 5 for 3 W/kg and for 0.3 W/kg, n = 4 for sham; for WT animals, n= 13 for 3 W/kg, n= 12 for 0.3 W/kg and n= 9 for sham);* ***b)*** *There were no significant differences in the latency to reach the target area between groups in 12-month-old animals (for J20 animals, n= 10 for 3 W/kg, n= 12 for 0.3 W/kg and n= 10 for sham; for WT animals, n= 12 for 3 W/kg, n= 14 for 0.3 W/kg and n= 11 for sham).*

c. Distance

At 6 months of age, there were no significant differences in the total distance swum by the mice (ANOVA, p= 0.063) between J20 and WT mice. There were no significant differences between exposure groups (ANOVA, p= 0.295). The interaction between strain and exposure groups was significant (ANOVA, p= 0.042), with the 0.3 W/kg-exposed J20 group being significantly lower (p=0.03) when compared to the 0.3 W/kg-exposed WT group (Tuckey post hoc test, J20 0.3 W/kg vs WT 0.3 W/kg p= 0.046), as shown in figure 27a.

At 12 months of age, there were no significant differences in the total distance swum by the mice (ANOVA, p= 0.867) between J20 and WT mice. There were no significant differences between exposure groups (ANOVA, p= 0.392) and no significant interaction between strain and exposure groups either (ANOVA, p= 0.343), as shown in figure 27b.

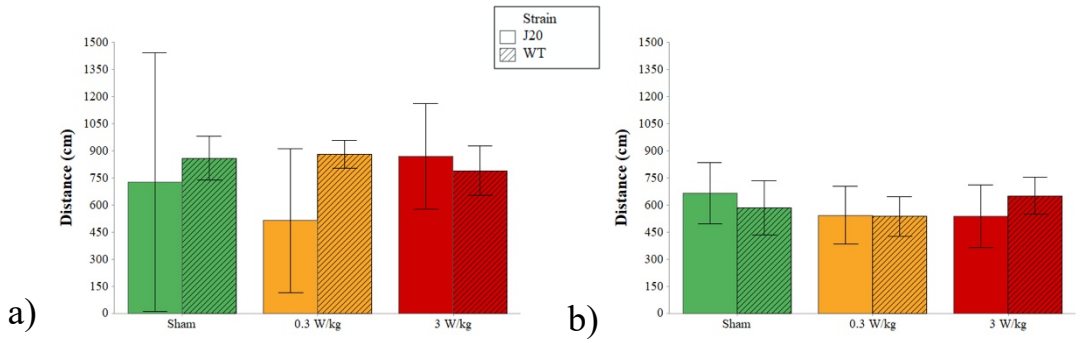


Figure 27: Exposure has no effect on locomotion in MWM probe-trial. *The animals were exposed to either 3 W/kg RF or 0.3W/kg or a sham exposure.* ***a)*** *At 6-month-old animals, 0.3 W/kg-exposed J20 were swimming significantly less (p<0.05) than 0.3 W/kg-exposed WT (for J20 animals, n= 5 for 3 W/kg and for 0.3 W/kg, n = 4 for sham; for WT animals, n= 13 for 3 W/kg, n= 12 for 0.3 W/kg and n= 9 for sham);* ***b)*** *There were no significant differences in the total distance swum between groups in 12-month-old animals (for J20 animals, n= 10 for 3 W/kg, n= 12 for 0.3 W/kg and n= 10 for sham; for WT animals, n= 12 for 3 W/kg, n= 14 for 0.3 W/kg and n= 11 for sham).*

d. Total time spent floating

At 6 months of age, there were no significant differences in the total time spent floating (ANOVA, p= 0.06) between J20 and WT mice. There were no significant differences between exposure groups (ANOVA, p= 0.392). The interaction between strain and exposure groups was significant (ANOVA, p= 0.031), with the 0.3 W/kg-exposed J20 group being significantly lower (p=0.014) when compared to the 0.3 W/kg-exposed WT group (Tuckey post hoc test, J20 0.3 W/kg vs WT 0.3 W/kg p= 0.023), as shown in figure 28a.

At 12 months of age, there were no significant differences in the total time spent floating (ANOVA, p= 0.711) between J20 and WT mice. There were no significant differences between exposure groups (ANOVA, p= 0.33) and no significant interaction between strain and exposure groups either (ANOVA, p= 0.107), as shown in figure 28b.

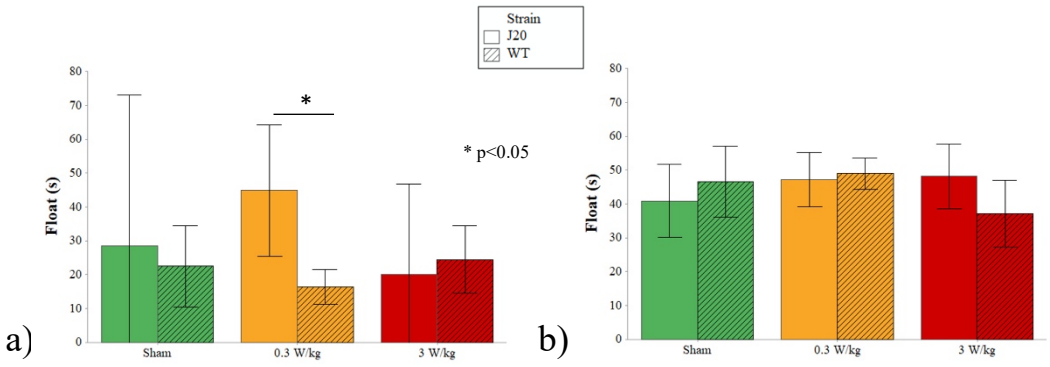


Figure 28: Exposure has an effect on floating behaviour in MWM probe-trial. *The animals were exposed to either 3 W/kg RF or 0.3W/kg or a sham exposure.* ***a)*** *At 6-month-old animals, 0.3 W/kg-exposed J20 were floating significantly more (p<0.05) than 0.3 W/kg-exposed WT (for J20 animals, n= 5 for 3 W/kg and for 0.3 W/kg, n = 4 for sham; for WT animals, n= 13 for 3 W/kg, n= 12 for 0.3 W/kg and n= 9 for sham);* ***b)*** *There were no significant differences in the total time spent floating between groups in 12-month-old animals (for J20 animals, n= 10 for 3 W/kg, n= 12 for 0.3 W/kg and n= 10 for sham; for WT animals, n= 12 for 3 W/kg, n= 14 for 0.3 W/kg and n= 11 for sham).*

5.3.2. Histological endpoints

5.3.2.1. Synaptophysin

5.3.2.1.1. CA1

At 6 months of age, there were no significant differences (ANOVA, p= 0.054) between J20 and WT mice. There was a significant difference in synaptic density between exposure groups (ANOVA, p< 0.01) as shown in figure 29a (Tuckey post hoc test, sham vs 0.3 W/kg, p= 0.781; 0.3 W/kg vs 3 W/kg, p< 0.01; 3 W/kg vs sham, p< 0.01). There were no significant interactions between groups (ANOVA, p=0.081), as shown in figure 30a.

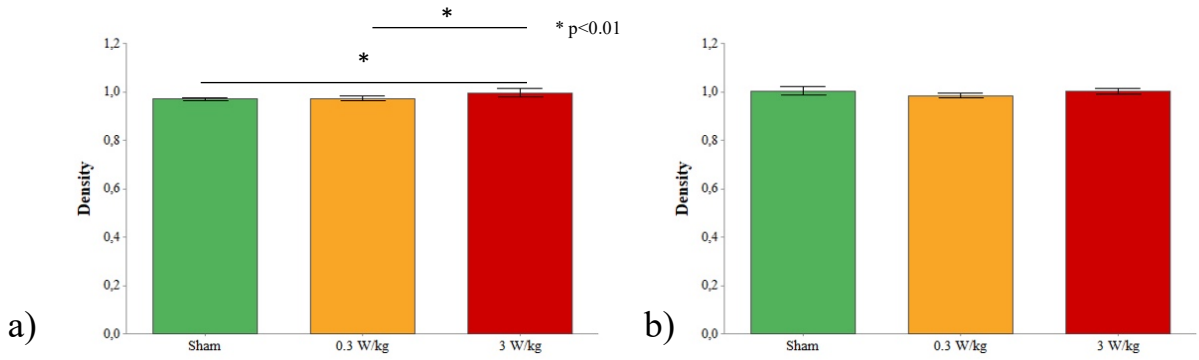


Figure 29: Exposure increases synaptic density in CA1 in 6-month mice. *The animals were exposed to either 3 W/kg RF or 0.3W/kg or a sham exposure.* ***a)*** *At 6 months, 3 W/kg exposure increased synaptic density in CA1 when compared to 0.3 W/kg (p< 0.01) and sham exposure (p< 0.01) (for J20 animals, n= 4 for 3 W/kg, n= 5 for 0.3 W/kg and n= 7 for sham; for WT animals, n= 14 for 3 W/kg, n= 12 for 0.3 W/kg and n= 11 for sham);* ***b)*** *At 12 months, there were no significant differences in synaptic density in CA1 (for J20 animals, n= 18 for 3 W/kg, n= 17 for 0.3 W/kg and sham; for WT animals, n= 18 for 3 W/kg).*

At 12 months of age, there were no significant differences (ANOVA, p= 0.938) between J20 and WT mice. There were no significant differences in synaptic density between exposure groups (ANOVA, p= 0.098) as shown in figure 29b. There were no significant interactions between groups (ANOVA, p=0.437), as shown in figure 30b.

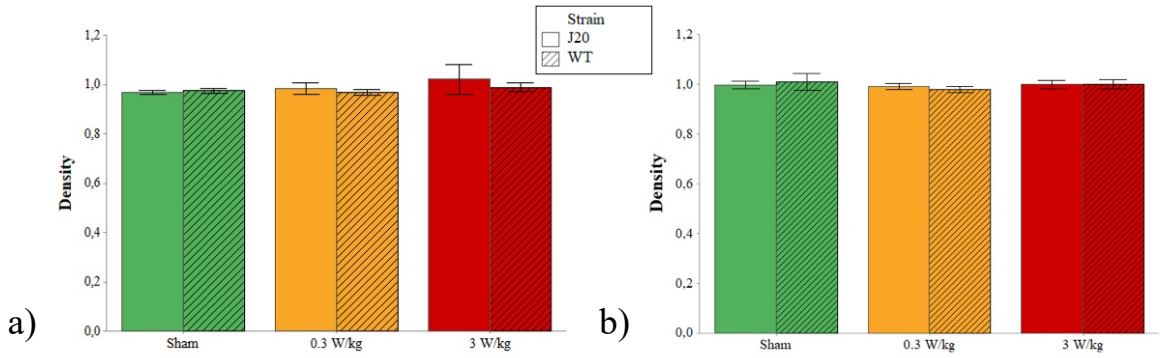


Figure 30: J20 mice do not show a difference in synaptic density in CA1 when compared to WT. *The animals were exposed to either 3 W/kg RF or 0.3W/kg or a sham exposure.* ***a)*** *At 6 months, J20 mice showed no significant differences in synaptic density in CA1 (for J20 animals, n= 4 for 3 W/kg, n= 5 for 0.3 W/kg and n= 7 for sham; for WT animals, n= 14 for 3 W/kg, n= 12 for 0.3 W/kg and n= 11 for sham);* ***b)*** *At 12 months, there were no significant differences in synaptic density in CA1 (for J20 animals, n= 18 for 3 W/kg, n= 17 for 0.3 W/kg and sham; for WT animals, n= 18 for 3 W/kg).*

5.3.2.1.2. CA3

At 6 months of age, there was a significant difference (ANOVA, p= 0.036) between J20 and WT mice. There was a significant difference in synaptic density between exposure groups (ANOVA, p< 0.01) as shown in figure 30a (Tuckey post hoc test, sham vs 0.3 W/kg, p= 0.985; 0.3 W/kg vs 3 W/kg, p< 0.01; 3 W/kg vs sham, p< 0.01). There were no significant interactions between groups (ANOVA, p=0.599) as shown in figure 31a.

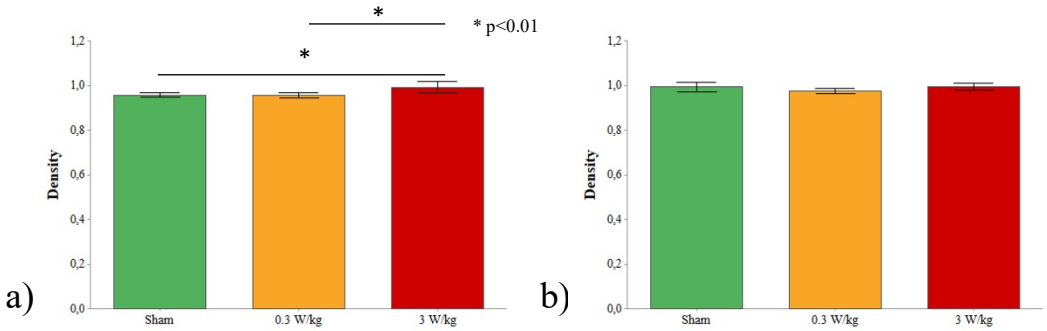


Figure 30: Exposure increases synaptic density in CA3. *The animals were exposed to either 3 W/kg RF or 0.3W/kg or a sham exposure.* ***a)*** *At 6 months, 3 W/kg exposure increased synaptic density in CA3 when compared to 0.3 W/kg (p< 0.01) and sham exposure (p< 0.01) (for J20 animals, n= 4 for 3 W/kg, n= 5 for 0.3 W/kg and n= 7 for sham; for WT animals, n= 14 for 3 W/kg, n= 12 for 0.3 W/kg and n= 11 for sham);* ***b)*** *At 12 months, there were no significant differences in synaptic density in CA3 (for J20 animals, n= 18 for 3 W/kg, n= 17 for 0.3 W/kg and sham; for WT animals, n= 18 for 3 W/kg).*

At 12 months of age, there were no significant differences (ANOVA, p= 0.173) between J20 and WT mice. There were no significant differences in synaptic density between exposure groups (ANOVA, p= 0.149), as shown in figure 30b. There were no significant interactions between groups (ANOVA, p=0.713), as shown in figure 31b.

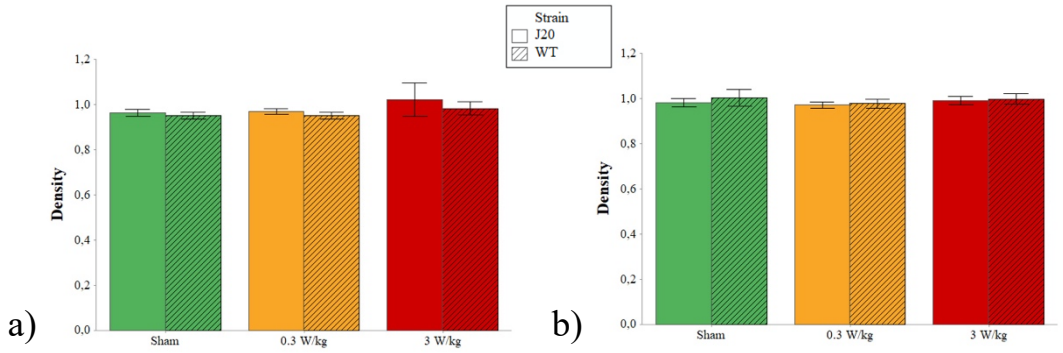


Figure 31: 6-month J20 mice show a difference in synaptic density in CA3 when compared to WT. *The animals were exposed to either 3 W/kg RF or 0.3W/kg or a sham exposure.* ***a)*** *At 6 months, At 6 months, J20 mice showed a significant difference (p< 0.01) in synaptic density in CA3 (for J20 animals, n= 4 for 3 W/kg, n= 5 for 0.3 W/kg and n= 7 for sham; for WT animals, n= 14 for 3 W/kg, n= 12 for 0.3 W/kg and n= 11 for sham);* ***b)*** *At 12 months, there were no significant differences in synaptic density in CA3 (for J20 animals, n= 18 for 3 W/kg, n= 17 for 0.3 W/kg and sham; for WT animals, n= 18 for 3 W/kg).*

5.3.2.1.3. Dentate Gyrus

At 6 months of age, there were no significant differences (ANOVA, p= 0.465) between J20 and WT mice. There were no significant differences in synaptic density between exposure groups (ANOVA, p= 0.67), as shown in figure 32a. There were no significant interactions between groups (ANOVA, p=0.187), as shown in figure 33a.

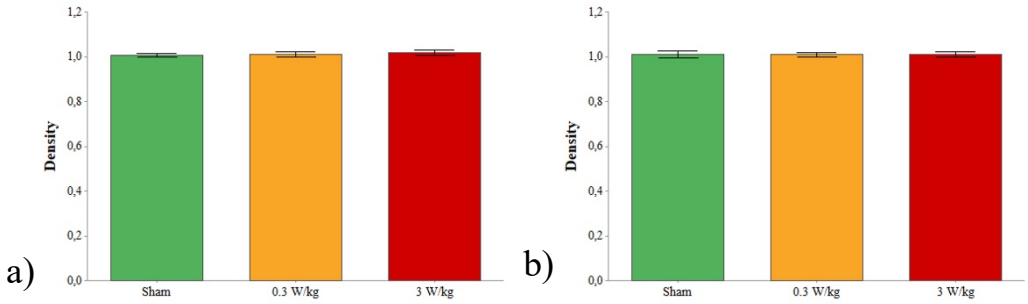


Figure 32: Exposure does not increase synaptic density in DG. *The animals were exposed to either 3 W/kg RF or 0.3W/kg or a sham exposure.* ***a)*** *At 6 months, there were no significant differences in synaptic density between exposure groups (for J20 animals, n= 4 for 3 W/kg, n= 5 for 0.3 W/kg and n= 7 for sham; for WT animals, n= 14 for 3 W/kg, n= 12 for 0.3 W/kg and n= 11 for sham);* ***b)*** *At 12 months, there were no significant differences in synaptic density in CA3 between exposure groups (for J20 animals, n= 18 for 3 W/kg, n= 17 for 0.3 W/kg and sham; for WT animals, n= 18 for 3 W/kg).*

At 12 months of age, there were no significant differences (ANOVA, p= 0.386) between J20 and WT mice. There were no significant differences in synaptic density between exposure groups (ANOVA, p= 0.977), as shown in figure 32b. There were no significant interactions between groups (ANOVA, p=0.826), as shown in figure 33b.

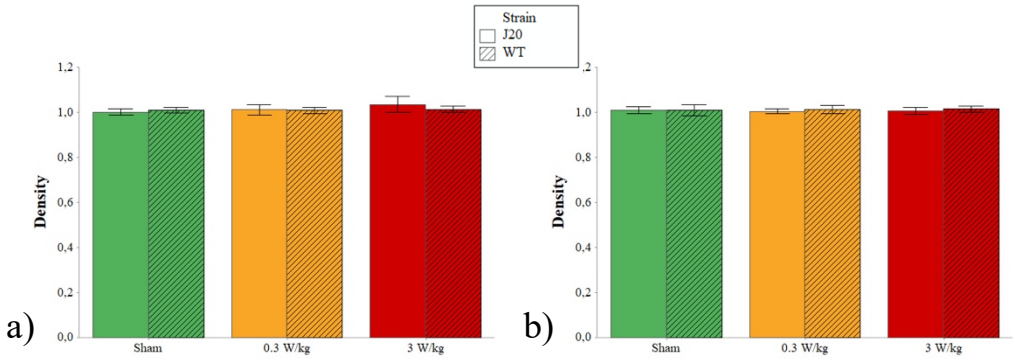


Figure 33: J20 mice do not show a difference in synaptic density in DG when compared to WT. *The animals were exposed to either 3 W/kg RF or 0.3W/kg or a sham exposure.* ***a)*** *At 6 months of age, there were no differences in synaptic density in DG between strains (for J20 animals, n= 4 for 3 W/kg, n= 5 for 0.3 W/kg and n= 7 for sham; for WT animals, n= 14 for 3 W/kg, n= 12 for 0.3 W/kg and n= 11 for sham);* ***b)*** *At 12 months, there were no significant differences in synaptic density in DG between strains (for J20 animals, n= 18 for 3 W/kg, n= 17 for 0.3 W/kg and sham; for WT animals, n= 18 for 3 W/kg, n= 17 for 0.3 W/kg and sham).*

5.3.2.2. Iba1

At 6 months, there was a significant increase (ANOVA, $p < 0.01$) in J20 Iba1-positive cell count when compared to WT mice, and there were no significant differences in Iba1 cell count between exposure groups (ANOVA, $p = 0.822$) or any significant interaction between groups (ANOVA, $p = 0.969$), as shown in figure 34a.

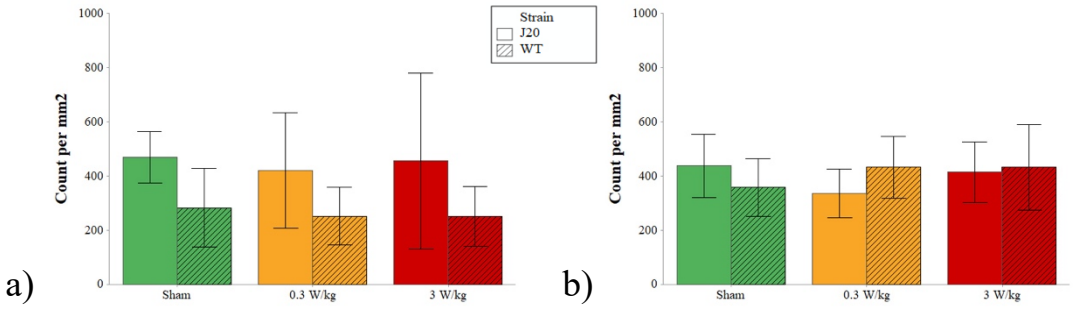


Figure 34: Exposure has no effect on microglia*. The animals were exposed to either 3 W/kg RF or 0.3W/kg or a sham exposure.* ***a)*** *At 6 months of age, there were no differences in the number of IbA1-positive cells in the hippocampus between groups (for J20 animals, n= 4 for 3 W/kg, n= 5 for 0.3 W/kg and n= 7 for sham; for WT animals, n= 13 for 3 W/kg, n= 12 for 0.3 W/kg and n= 11 for sham);* ***b)*** *At 12 months of age, there were no significant differences in the number of IbA1-positive cells in the hippocampus between groups (for J20 animals, n= 18 for 3 W/kg, n= 17 for 0.3 W/kg and sham; for WT animals, n= 10 for 3 W/kg, n= 16 for 0.3 W/kg and sham).*

At 12 months, there were no significant differences (ANOVA, p=0.776) between J20 and WT mice, and there were no significant differences in Iba1 cell count between exposure groups (ANOVA, p= 0.803) or any significant interaction between groups (ANOVA, p= 0.322), as shown in figure 34b.

5.3.2.3. ß-amyloid

At 6 months of age, there was a significant increase (ANOVA, p< 0.001) in the percentage of Aβ-stained areas in the hippocampus in J20 mice when compared to WT mice, as shown in figure 35a (Tuckey post hoc test, sham WT vs sham J20, p< 0.01; 0.3 W/kg WT vs 0.3 W/kg J20, p=0.369; 3 W/kg WT vs 3 W/kg J20, p=0.255). There were no significant (ANOVA, p= 0.063) differences between exposure groups and no significant interactions (ANOVA, p=0.098).

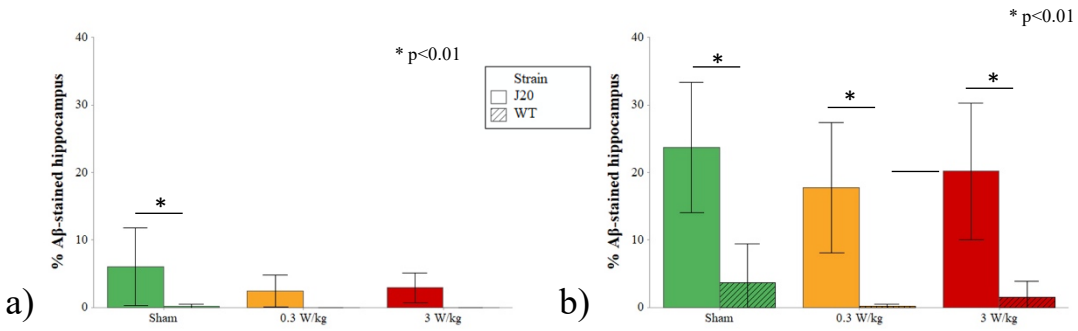


Figure 35: Exposure has no effect on the percentage of Aß -stained areas in the hippocampus. *The animals were exposed to either 3 W/kg RF or 0.3W/kg or a sham exposure.* ***a)*** *At 6 months of age, there were significant differences in the percentage of Aß-stained areas in the hippocampus between WT and J20 (p<0.01) for the sham-exposed group (post hoc: sham WT vs sham J20, p< 0.01) (for J20 animals, n= 4 for 3 W/kg, n= 5 for 0.3 W/kg and n= 7 for sham; for WT animals, n= 13 for 3 W/kg, n= 12 for 0.3 W/kg and n= 10 for sham);* ***b)*** *At 12 months of age, there were significant differences in the percentage of Aß-stained areas in the hippocampus between WT and J20 (p<0.01) for all exposure groups. J20 had a significantly higher area of Aß plaques Sham WT vs sham J20, p< 0.01; 0.3 W/kg WT vs 0.3 W/kg J20, p< 0.01; 3 W/kg WT vs 3 W/kg J20, p< 0.01) (for J20 animals, n= 18 for 3 W/kg, n= 17 for 0.3 W/kg and sham; for WT animals, n= 17 for 3 W/kg and 0.3 W/kg and n= 15 for sham).*

At 12 months of age, there was a significant increase (ANOVA, $p< 0.001$) in the percentage of Aβ-stained areas in the hippocampus in J20 mice when compared to WT mice, as shown in figure 35b (Tuckey post hoc test, sham WT vs sham J20, $p< 0.01$; 0.3 W/kg WT vs 0.3 W/kg J20, $p< 0.01$; 3 W/kg WT vs 3 W/kg J20, $p< 0.01$). There were no significant (ANOVA, $p= 0.480$) differences between exposure groups, and no significant interactions (ANOVA, $p= 0.945$).

5.4. Discussion

In this chapter, I examined the effect of EMF on learning and memory, locomotion, and anxiety in J20 mice. The most significant findings were that EMF seems to have an effect on motivation and activity, and that this effect lessens after the end of EMF exposure.

5.4.1. Behavioural endpoints

The rotarod revealed that there was no loss of locomotor abilities due to age between 6 and 12 months in the J20 AD model or the WT controls. The results of the test, while negative, were important because they confirmed that the animals would not be motor impaired in the MWM test. Others have examined locomotion in different mouse models of AD and found that motor function can be impaired. For example, the APPSwe Knock-In model displays significant impairment in locomotion (Olesen et al., 2016), while an APP/PSI Knock-In model showed no differences in locomotor abilities (Webster et al., 2013). A study of TgCRND8 mouse model showed an increased locomotion for all ages (Walker et al., 2011).

At 6 months the J20 mice showed an increase in locomotor abilities when compared to WT controls. We can emit three hypotheses: it could be random, it could be related to the APP mutation that has encouraged more mobility, or it could be an unrelated effect that has strain difference. Exposure had no impact on locomotion, and it seems unlikely that exposure would

have direct effects on motor function, but this outcome might have been the result of the EMF changing motivation or reducing anxiety. No one has described a positive effect of EMF exposure on motor function, but motor performance can be improved by environmental enrichment in WT animals (Song et al., 2018).

To assess anxiety, we considered two parameters in the elevated zero-maze: the time spent in the enclosed area of the maze, and the latency to the first exist outside of the compartment. While there was no difference between 6- and 12-month mice, at 6 months J20 mice showed an increase in the time spent outside, with the higher time spent outside of the enclosed area typically linked to lower anxiety (Sheperd, 1994), which is conflicting with the report that J20 mice are usually considered more anxious than their WT counterparts (Beauquis et al., 2014). This could be an artefact linked to the automatic detection, or it could be a sign of an increased activity and a potential undetected sex effect. WT females showed for example a higher time spent outside the enclosed area, linked to an increased activity in EZM as it has been shown before (Tucker et al., 2016).

At 6 months, 0.3 W/kg EMF exposure increased the time spent inside compartments when compared to 3 W/kg exposure, which might be due to an increase in anxiety, particularly as the 12-month-old group exposed to 3 W/kg also showed significantly later outings as well as a longer time spent inside, but the lack of significant differences in the latency to the first exit and the time spent outside the compartments when compared to sham animals would point that it might be more a case of decreased anxiety for the 3 W/kg-exposed group – or a case of bias, particularly as the 0.3W/kg exposure group showed significant differences in other behavioural tests.

At 12 months, mice exposed to 3 W/kg showed an increase in the time spent inside the compartments, as well as in the latency to first exit, when compared to sham, which might show an increase in anxiety or, if we consider all data, a decrease in motivation and activity.

In the MWM test, learning was assessed using the latency to first escape to the platform during the acquisition phase. 6-month-old mice were faster to escape to the platform than 12-month-old mice, which is consistent data for both J20 (Mucke et al., 2000) and WT (Frick et al., 2000). At 6 months of age, WT mice performed better than J20, showing an early deficit that has been described for this model (Mucke et al., 2000). When looking at the velocity and the time spent immobile during the trials, as together they can be used as a good indication of locomotor abilities as well as motivation, we can see that they were impacted by EMF exposure, which would mean that though learning might be affected by EMF exposure, cognition might not the only parameter involved.

However, there could also be several reasons for this: first, it could be a random occurrence; it could indeed be an impact of EMF exposure on cognition, as it has been described by Arendash (Arendash et al., 2010); it could also be a side effect of the impact of EMF exposure on other parameters such as locomotor abilities, activity or motivation. While the O-Maze and histology did show some impact, particularly for the 0.3 W/kg and 3 W/kg J20 exposure group, meaning that we cannot exclude an effect of EMF exposure on cognition, the variations in the effects observed, the inconsistency in the exposure groups affected and a lack of clear significance when compared to the sham groups means that we cannot exclude a bias linked to this particular group.

At 12 months of age, once again WT mice performed better than J20. There was no impact of EMF exposure on learning, which is confirmed by the lack of difference in the distance covered by the mice during trials. Velocity was likewise not impacted, and neither was the time spent immobile.

To assess memory, we looked at the number of visits to the platform area once we removed it.

First though, at the beginning of the MWM test, mice went through a pre-trial swim, where they were left to swim for a minute without a platform. All parameters were similar, meaning that we could consider probe-trial analysis, after the learning was done, to be representative of cognitive abilities, with the exception of J20 mice exposed to 0.3 W/kg. This group already showed deficits that manifested as a lower velocity, covering less distance when swimming during trial and an increased in floating behaviour, which will have to be considered in following interpretation.

At 6 months, 0.3 W/kg EMF exposure seems to decrease the distance covered during the probe trial and increase floating behaviour for J20 mice when compared to the 0.3 W/kg-exposed WT group at the same age. A lack of differences in the distance covered and the average velocity confirms that those results were not due to a sudden inability of the mice to swim, or any issues with their locomotor abilities. Immobility might be the key to understand those results: most of the groups show floating times that last for more than half the time of the probe trial, going up to nearly the entire trial for 12-month-old animals. While some demonstrated that there was a memory deficit for J20 in MWM for both 6-month-old (Palop et al., 2003) or 12-month-old (Murakami 2011, Galvan 2006) animals, several studies are now

considering that MWM, due to reluctance to swim and floating behaviour (Galvan et al., 2008; Karl et al., 2012b) might not be the best way to assess memory for mice.

As a conclusion for the MWM test, we can say that while it did not completely eliminate a potential EMF exposure effect on spatial learning and memory, it may highlight other potential impacts on motivation and activity, but those will have to be verified and completed by other tests. While some argue that EMF has an negative impact on spatial learning and memory (Sienkiewicz et al., 1998; Fragopoulou et al., 2010), more argue that high-frequency EMF has no impact (Sienkiewicz and Blackwell, 2000; Salunke et al., 2015). Any susceptibility to the positive effects of EMF in the 6-month-old animals appears to disappear when the animals get to 12 months. This might reflect a loss of plasticity potential, or that the effects are short-lived.

We also need to consider the fact that EMF exposure had no effect, strengthening the possibility that any EMF effect might stay transient and exposure-related, which is confirmed by other studies (Salunke et al., 2015) .

5.4.2. Histological endpoints

Synaptophysin is a protein localised in the presynaptic vesicles of neurons and indicates whether the neuron is functional and can transmit. Synaptophysin staining was assess in three parts of the hippocampus involved in memory formation, LTP and memory retrieval. Our results showed that 12 months mice showed an increase in synaptic density when compared to 6-month mice for CA1 and CA3. Unlike stated in several publications, at 12 months J20 did not show any differences in synaptic density when compared to their WT controls, meaning that the difference in cognition between the two strains is not related to synaptic densities.

Interestingly, at 6-months there was a significant increase in synaptic density in 3 W/kg exposure group when compared to 0.3 W/kg and sham exposure groups in CA1 and CA3, but not in DG. Interestingly, it has not been linked to better or worse cognitive performances during the behavioural testing, and this effect disappears at 12 months.

Exposure at 12 months had no effect on synaptic density.

There are variations, but overall, data show that a 3W/kg EMF exposure increases synaptic density in 6-months animals. The results are more fluctuant for WT mice, possibly due to the fact that they are not showing disease-related damages and have limited age-related modification. What was not possible to determine is whether EMF exposure acts by increasing neuronal growth or by decreasing neuronal death.

Microglia are brain immune cells that can be involved in brain inflammatory response. When activated, they express IbA1 (Ionised calcium binding Adapter 1) as a mediator for signalling. Our results show that there was an increase in microglia activation between 12-months and 6-months mice, which is coherent with ageing pathology. (Sandhir 2008)

At 6 months, there was an increase in microglia activation levels in the hippocampus in J20 when compared to WT mice, signalling an increase in neuronal inflammation. Exposure had no effect on brain microglia activation in J20 or WT.

At 12 months, there were no differences in microglia activation between J20 and WT mice. Exposure had no effect on brain microglia activation in WT. The lack of significant difference between J20 and WT animal at 12 months, but not at 6 months, with J20 showing an increased microglial activation is interesting. We can hypothesis that at 6 months, J20 animals

have started to develop brain inflammation linked to AD, and that at 12 months, ageing has raised the levels of WT mice to AD levels. It might be interesting to later study the morphology of cells in 12 months J20 and 12 months WT mice, since microglia in AD show loss of functionality and shape. (Boche 2012; Paasila 2019).

Aβ-plaques are the hallmark of AD. Our results show that age increased the percentage of Aß-stained areas in the hippocampus in 12-months mice when compared to 6-months mice. At 12 months, AD mice did develop Aβ plaques, as J20 mice had a significant increase of when compared to WT mice. Exposure had no effect on the percentage of Aβ-stained areas. At 6 months, AD mice had already started to develop Aß plaques, as J20 mice had a significant increase when compared to WT mice. Exposure had no effect on the percentage of Aß-stained areas.

On a key phenotype of AD, EMF exposure had no impact.

5.4.3. Conclusion on the effect of exposure on J20 model

Experiments show some exposure effects, with significant values and general trends that fail to be significant but occur frequently enough to be taken note of. Overall, EMF exposure seems to be more involved in motivation and activity than in a betterment of cognitive functions during exposure and differences disappeared after a period of non-exposure to EMF.

Generally, WT did not show significant differences with EMF exposure, meaning that EMF effect is very small and visible only in models that show deficits. Nevertheless, those issues could also come from specificities and experimental issues. For example, due to space constraints, females J20 had to be housed together after exposure while it was impossible to do so for males due to in-cage fighting after the first exposure, and it has been shown that

environment (Pietropaolo et al., 2014), housing (Burman et al., 2014) or social interaction can have an impact on cognition and behaviour. This might also be part of an explanation as to the high variability observed in tests such as the OM.

Finally, while the use of the MWM test had its place in this general study, allowing us to screen a wide range of diverse parameters, the fact remains that it is not the most adapted test, particularly for the J20 model and more generally mice (Karl et al., 2012a) who tend to display an hypoactivity and floating behavior that tend to make analysis more complicated.

In parallel, there were no significant histological differences visible in the hippocampus at 12 months, but there were some at 6 months, meaning that changes appeared as a result of exposure, and had since then been repaired, so that there were no lasting effects of EMF on brain structure. EMF exposure has been thought to have an impact on histological parameters in the rodent brain (Zymantiene 2020; Bas 2009), though the SAR was well above the levels we used and induced thermic effect, and the type of exposure were different, making it complicated to draw conclusion. A study by Zhang (Zhang, 2014), did not highlight any histological and behavioural changes using ELF-EMF, while Hao (Hao 2013), using a similar exposure protocol, highlighted that after a time, rats were adapted to EMF exposure, and that the cognitive deficits observed at one point were transient.

In conclusion, it might be more interesting for now to investigate the effect of EMF exposure on activity and motivation in mice, as those parameters seem to be more sensitive to EMF and have a strong impact on any further testing. An in-depth histological study, with a focus on morphology and the impact on blood-brain barrier, which has been thought to be a potential target of EMF exposure (Tang 2015), might be interesting as well.

6. SAM model

6.1. General background

6.1.1. Experimental approach

To assess whether RF exposure had a long-term impact on learning and memory in ageing populations following an early exposure, an ageing mouse model, Senescence-accelerated prone mouse model (SAMP8) and its control, senescence-accelerated resistant mouse model (SAMR1) were subjected to long-term, chronic exposure to 1800 MHz pulsed fields. The whole-body SARs were chosen to reflect the values currently in use in international guidelines for limiting the exposure of workers and the general population (ICNIRP, 1998). These values are well below the exposures required for whole body heating, as an investigation of overt thermal effects was not the subject of this work.

6.1.2. Mouse model

The senescence-accelerated mouse model SAM originated from inbreeding between AKR/J mice showing early signs of ageing (Takeda et al., 1981). SAMP8 mice are a line derived from the original SAMP2 line and supposed to show learning and memory deficits at as early as 2 months of age (Miyamoto et al., 1986). Compared to the senescence-resistant line issued from the same progenitors (SAMR1), SAMP8 demonstrated a prolonged latency to escape in MWM at 2 and 8 months of age as well as memory deficits in avoidance tasks. Later studies started to question the retention deficits in SAMP8 but confirmed an early-onset acquisition deficit when compared to SAMR1 (Yagi et al., 1988; Flood and Morley, 1992). SAMP8 showed also an increased in activity with an age-related decrease later in on, with reduced anxiety-like behaviour. Finally, this model did not show visual impairments that could impact its performance in spatial learning tasks such as MWM but did show age-related declines in

locomotor abilities that could complicated detection of cognitive impairment (Markowska et al., 1998a).

6.2. Experimental protocol

SAMP8 and SAMR1 mice were randomly distributed into three groups and were then exposed to 1800 MHz pulsed fields, at three different SARs: 3 W/kg, 0.3 W/kg and 0 W/kg (sham-exposed controls). To assess the effect of early exposures to RF in aged adults, mice were exposed at 8 weeks of age.

6.3. Results

6.3.1. Behavioural endpoints

6.3.1.1. Rotarod

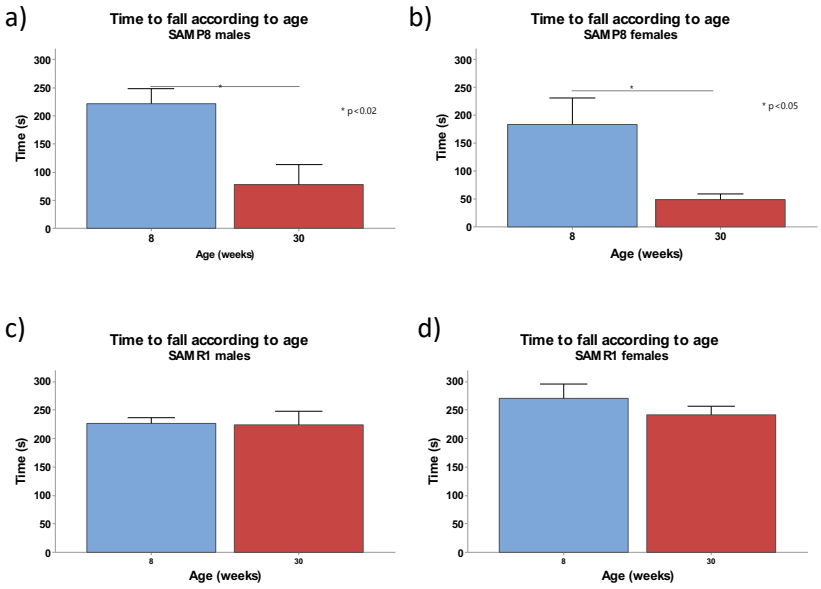


Figure 36: 30 weeks SAMP8 mice show a significant deficit in locomotion in the rotarod test. a) *There was significant difference in the time to fall off between the 8 weeks (n=6) and the 30 weeks (n=5) groups during the Rotarod test (ANOVA, p<0.02) in males SAMP8;* ***b)*** *There was significant difference in the time to fall off between the 8 weeks (n=3) and the 30 weeks (n=4) groups during the Rotarod test (ANOVA, p<0.05) in females SAMP8;* ***c)*** *There was no significant difference in the time to fall off between the 8 weeks (n=5) and the 30 weeks (n=8) groups during the Rotarod test (ANOVA, p<0.02) in males SAMR1;* ***d)*** *There was no significant difference in the time to fall off between the 8 weeks (n=4) and the 30 weeks (n=14) groups during the Rotarod test (ANOVA, p<0.02) in females SAMR1.*

6.3.1.2. Watermaze

6.3.1.2.1. Memory

6.3.1.2.1.1. Pre-trial

a. Velocity

At 8 weeks of age, there were no significant differences in velocity (ANOVA, p= 0.568) between SAMP8 and SAMR1. There were no significant differences between exposure groups (ANOVA, p= 0.104) and no interactions between strain and exposure groups (ANOVA, p= 0.3).

At 30 weeks of age, there was a significant difference in velocity (ANOVA, p< 0.001) between SAMP8 and SAMR1, with SAMP8 being slower than the SAMR1 mice. There were no significant differences between exposure groups (ANOVA, p= 0.217) and no significant interaction between strain and exposure groups either (ANOVA, p= 0.091).

b. Latency to reach the target area

At 8 weeks of age, there was a significant difference in the latency to first reach the platform area (ANOVA, p< 0.01) between SAMP8 and SAMR1, with SAMP8 taking more time to reach the platform than the SAMR1 mice. There were no significant differences between exposure groups (ANOVA, p= 0.231) and no significant interaction between strain and exposure groups either (ANOVA, p= 0.838).

At 30 weeks of age, there was a significant difference in the latency to first reach the platform area (ANOVA, p= 0.028) between SAMP8 and SAMR1, with SAMP8 taking longer to reach the platform area than the SAMR1 mice. There were no significant differences between

exposure groups (ANOVA, p= 0.678) and no significant interaction between strain and exposure groups either (ANOVA, p= 0.447).

c. Distance

At 8 weeks of age, there were no significant differences in the total distance moved (ANOVA, p= 0.871) between SAMP8 and SAMR1. There were no significant differences between exposure groups (ANOVA, p= 0.440) and no interactions between strain and exposure groups (ANOVA, p= 0.923).

At 30 weeks of age, there was a significant difference in the total distance swum (ANOVA, p< 0.001) between SAMP8 and SAMR1, with SAMP8 swimming less than the SAMR1 mice. There were no significant differences between exposure groups (ANOVA, p= 0.221) and no significant interaction between strain and exposure groups either (ANOVA, p= 0.097).

d. Immobility

At 8 weeks of age, there was a significant difference in the time spent floating during the trial (ANOVA, p= 0.015) between SAMP8 and SAMR1, with SAMP8 exhibiting more floating behaviour than the SAMR1 mice. There were no significant differences between exposure groups (ANOVA, p= 0.146) and no significant interaction between strain and exposure groups either (ANOVA, p= 0.06).

At 30 weeks of age, there was a significant difference in the time spent floating during the trial (ANOVA, p= 0.008) between SAMP8 and SAMR1, with SAMP8 exhibiting more

floating behaviour than the SAMR1 mice. There were no significant differences between exposure groups (ANOVA, p= 0.868) and no significant interaction between strain and exposure groups either (ANOVA, p= 0.456).

6.3.1.2.1.2. Probe-trial

a. Velocity

At 8 weeks of age, there was a significant difference in velocity (ANOVA, p= 0.045) between SAMP8 and SAMR1, with SAMP8 being slower than the SAMR1 mice. There were no significant differences between exposure groups (ANOVA, p= 0.09) and no significant interaction between strain and exposure groups either (ANOVA, p= 0.061), as shown in figure 37a.

At 30 weeks of age, there was a significant difference in velocity (ANOVA, p< 0.001) between SAMP8 and SAMR1, with SAMP8 being slower than the SAMR1 mice. There were no significant differences between exposure groups (ANOVA, p= 0.669) and no significant interaction between strain and exposure groups either (ANOVA, p= 0.108), as shown in figure 37b.

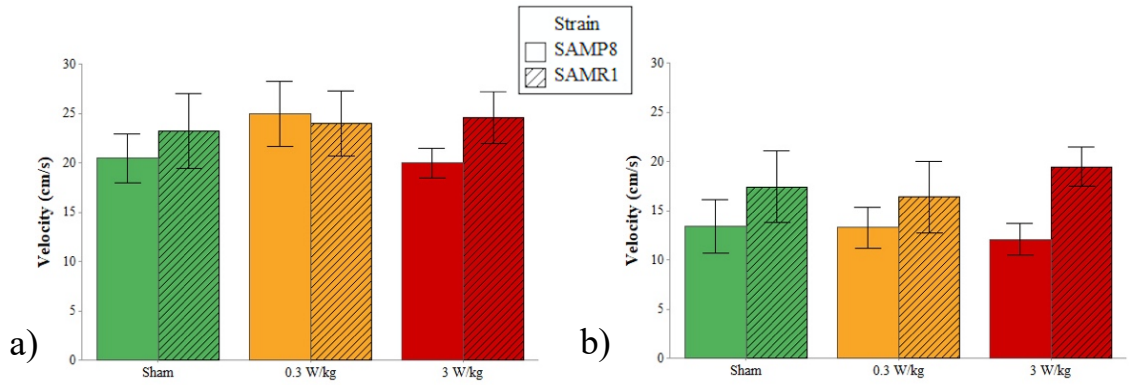


Figure 37: Exposure has no effect on locomotion in MWM probe-trial. *The animals were exposed to either 3 W/kg RF or 0.3W/kg or a sham exposure.* ***a)*** *At 8 weeks, there were no significant differences in velocity between exposure groups (for SAMP8 mice, n= 16 for 3 W/kg, n= 12 for 0.3 W/kg, n = 11 for sham; for SAMR1 mice, n= 12 for 3 W/kg, n= 11 for 0.3 W/kg and n= 7 for sham);* ***b)*** *There were no significant differences in velocity between groups in 30-weeks-old animals (for SAMP8 mice, n= 15 for 3 W/kg, n= 12 for 0.3 W/kg, n = 11 for sham; for SAMR1 mice, n= 12 for 3 W/kg, n= 10 for 0.3 W/kg and n= 6 for sham).*

b. Latency to reach the target area

At 8 weeks of age, there was a significant difference in the latency to reach the target area (ANOVA, p= 0.02) between SAMP8 and SAMR1, with SAMP8 taking more time to reach the platform than the SAMR1 mice. There were no significant differences between exposure groups (ANOVA, p= 0.322) and no significant interaction between strain and exposure groups either (ANOVA, p= 0.899), as shown in figure 38a.

At 30 weeks of age, there was a significant difference in the latency to reach the target area (ANOVA, p= 0.025) between SAMP8 and SAMR1, with SAMP8 taking more time to reach the platform than the SAMR1 mice. There were no significant differences between exposure groups (ANOVA, p= 0.798) and no significant interaction between strain and exposure groups either (ANOVA, p= 0.335), as shown in figure 38b.

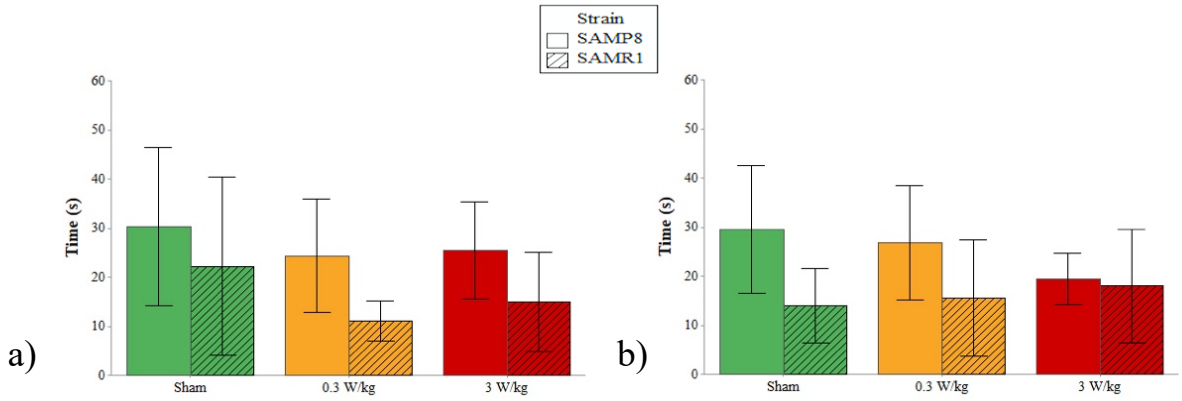


Figure 38: Exposure has no effect on memory in MWM probe-trial. *The animals were exposed to either 3 W/kg RF or 0.3W/kg or a sham exposure.* ***a)*** *At 8 weeks, there were no significant differences in the latency to first reach the target area between exposure groups (for SAMP8 mice, n= 16 for 3 W/kg, n= 12 for 0.3 W/kg, n = 11 for sham; for SAMR1 mice, n= 12 for 3 W/kg, n= 11 for 0.3 W/kg and n= 7 for sham);* ***b)*** *There were no significant differences in the latency to first reach the target area between groups in 30-weeks-old animals (for SAMP8 mice, n= 15 for 3 W/kg, n= 12 for 0.3 W/kg, n = 11 for sham; for SAMR1 mice, n= 12 for 3 W/kg, n= 10 for 0.3 W/kg and n= 6 for sham).*

c. Distance

At 8 weeks of age, there was a significant difference in the total distance moved (ANOVA, p= 0.001) between SAMP8 and SAMR1 with SAMP8 swimming less than the SAMR1 mice. There were no significant differences between exposure groups (ANOVA, p= 0.760) and no interactions between strain and exposure groups (ANOVA, p= 0.332), as shown in figure 39a.

At 30 weeks of age, there was a significant difference in the total distance swum (ANOVA, p< 0.001) between SAMP8 and SAMR1, with SAMP8 swimming less than the SAMR1 mice. There were no significant differences between exposure groups (ANOVA, p= 0.679) and no significant interaction between strain and exposure groups either (ANOVA, p= 0.104 as shown in figure 39b.

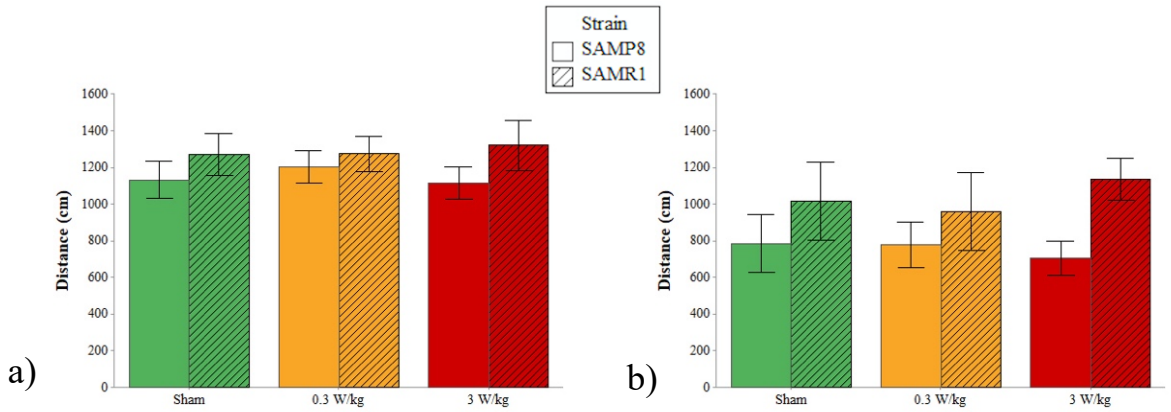


Figure 39: Exposure has no effect on locomotion in MWM probe-trial. *The animals were exposed to either 3 W/kg RF or 0.3W/kg or a sham exposure.* ***a)*** *At 8 weeks, there were no significant differences in the total distance swum between exposure groups (for SAMP8 mice, n= 16 for 3 W/kg, n= 12 for 0.3 W/kg, n = 11 for sham; for SAMR1 mice, n= 12 for 3 W/kg, n= 11 for 0.3 W/kg and n= 7 for sham);* ***b)*** *There were no significant differences in the total distance swum between groups in 30-weeks-old animals (for SAMP8 mice, n= 15 for 3 W/kg, n= 12 for 0.3 W/kg, n = 11 for sham; for SAMR1 mice, n= 12 for 3 W/kg, n= 10 for 0.3 W/kg and n= 6 for sham).*

d. Total time spent floating

At 8 weeks of age, there were no significant differences in the time spent floating during the trial (ANOVA, p= 0.207) between SAMP8 and SAMR1. There were no significant differences between exposure groups (ANOVA, p= 0.582) and no significant interaction between strain and exposure groups either (ANOVA, p= 0.373), as shown in figure 40a.

At 30 weeks of age, there was a significant difference in the time spent floating during the trial (ANOVA, p< 0.01) between SAMP8 and SAMR1, with SAMP8 exhibiting more floating behaviour than the SAMR1 mice. There were no significant differences between exposure groups (ANOVA, p= 0.906) and no significant interaction between strain and exposure groups either (ANOVA, p= 0.479), as shown in figure 40b.

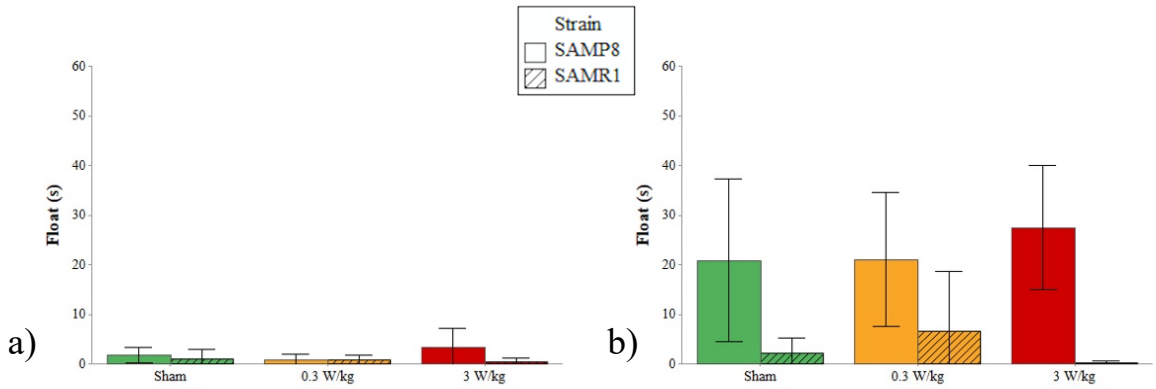


Figure 40: Exposure has no effect on floating behaviour in MWM probe-trial. *The animals were exposed to either 3 W/kg RF or 0.3W/kg or a sham exposure.* ***a)*** *At 8 weeks, there were no significant differences in floating behaviour between exposure groups (for SAMP8 mice, n= 16 for 3 W/kg, n= 12 for 0.3 W/kg, n = 11 for sham; for SAMR1 mice, n= 12 for 3 W/kg, n= 11 for 0.3 W/kg and n= 7 for sham);* ***b)*** *There were no significant differences in floating behaviour between groups in 30-weeks-old animals (for SAMP8 mice, n= 15 for 3 W/kg, n= 12 for 0.3 W/kg, n = 11 for sham; for SAMR1 mice, n= 12 for 3 W/kg, n= 10 for 0.3 W/kg and n= 6 for sham).*

6.3.1.2.2. Acquisition

6.3.1.2.2.1. Trials 2

a) Velocity

At 8 weeks of age, there was a significant difference in velocity (ANOVA, $p< 0.001$) between SAMP8 and SAMR1, with SAMP8 being slower than the SAMR1 mice. There was a significant difference between exposure groups (ANOVA, $p< 0.01$) and significant interactions between strain and exposure groups either (ANOVA, $p= 0.017$) (Tuckey post hoc, for the SAMP8, 0.3 W/kg-exposed vs sham, $p< 0.01$; 0.3 W/kg-exposed vs 3 W/kg-exposed, $p<0.01$). 0.3 W/kg-exposed animals were significantly faster than 3 W/kg-exposed and sham animals (Tuckey post hoc, 0.3 W/kg-exposed vs sham, $p= 0.045$; 0.3 W/kg-exposed vs 3 W/kg-exposed, $p<0.01$), as shown in figure 41.

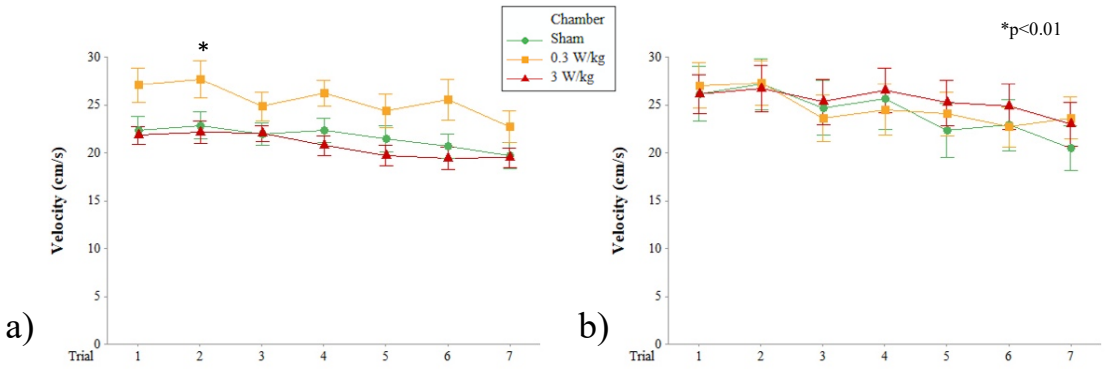


Figure 41: At 8 weeks, 0.3 W/kg exposure increase locomotion in MWM learning. *The animals were exposed to either 3 W/kg RF or 0.3W/kg or a sham exposure.* ***a)*** *At 8 weeks, 0.3 W/kg-exposed SAMP8 were faster than the rest of the SAMP8 exposure groups (post hoc 0.01) (n= 16 for 3 W/kg, n= 12 for 0.3 W/kg, n = 11 for sham;);* ***b)*** *There were no significant differences in the latency to first reach the target area between SAMR1 groups (n= 12 for 3 W/kg, n= 11 for 0.3 W/kg and n= 7 for sham).*

At 30 weeks of age, there was a significant difference in velocity (ANOVA, $p< 0.001$) between SAMP8 and SAMR1, with SAMP8 being slower than the SAMR1 mice. There was a significant difference between exposure groups (ANOVA, $p= 0.015$) and significant interactions between strain and exposure groups either (ANOVA, $p= 0.013$) (Tuckey post hoc, for the SAMR1, 0.3 W/kg-exposed vs sham, $p< 0.01$; 0.3 W/kg-exposed vs 3 W/kg-exposed, $p<0.01$). 0.3 W/kg-exposed animals were significantly faster (ANOVA, $p= 0.031$) than 3 W/kg-exposed (Tuckey post hoc, 0.3 W/kg-exposed vs 3 W/kg-exposed, $p= 0.011$), as shown in figure 42.

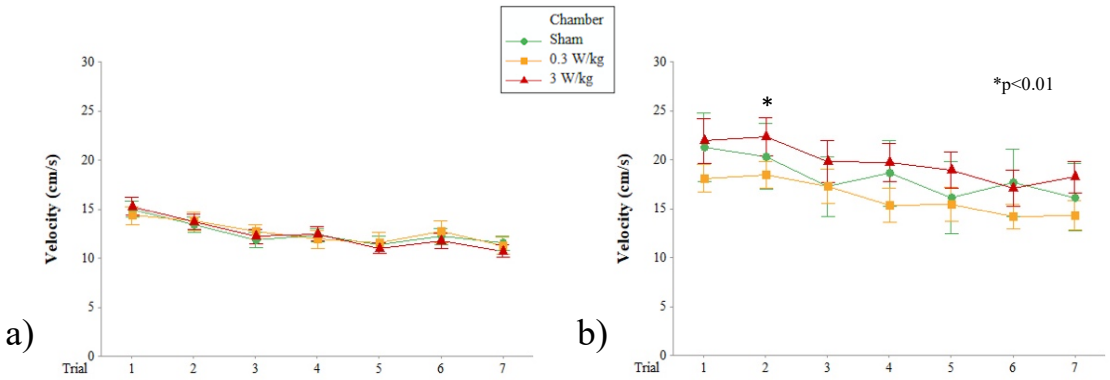


Figure 42: At 30 weeks, 0.3 W/kg exposure decreases locomotion in MWM learning. *The animals were exposed to either 3 W/kg RF or 0.3W/kg or a sham exposure.* ***a)****, At 30 weeks, in T2 and T3 there were no significant differences in velocity between SAMP8 exposure groups (n= 15 for 3 W/kg, n= 12 for 0.3 W/kg, n = 11 for sham);* ***b)*** *For T2 and T3, the 0.3 W/kg exposure group was significantly (post hoc p< 0.01) slower than the others in 30-weeks-old SAMR1 (n= 12 for 3 W/kg, n= 10 for 0.3 W/kg and n= 6 for sham).*

b) Latency to reach the target area

At 8 weeks of age, there was a significant difference in the latency to first reach the platform area (ANOVA, p= 0.028) between SAMP8 and SAMR1, with SAMP8 taking longer to reach the platform area than the SAMR1 mice. There were no significant differences between exposure groups (ANOVA, p= 0.678) and no significant interaction between strain and exposure groups either (ANOVA, p= 0.447), as shown in figure 43.

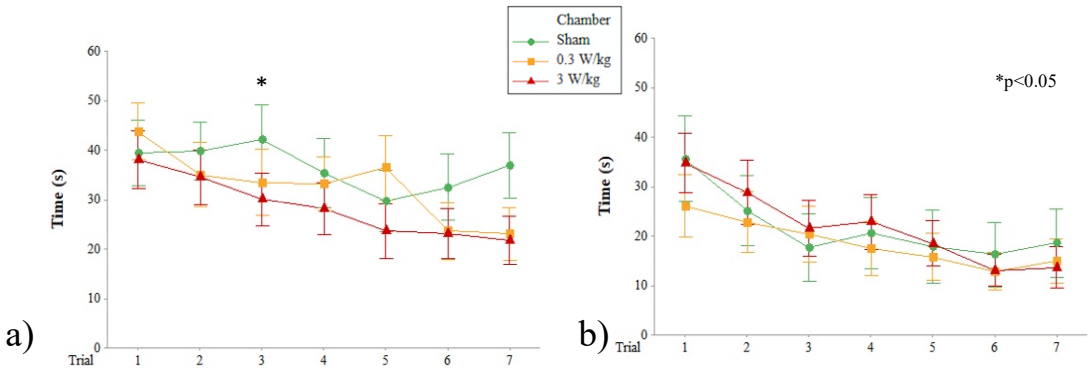


Figure 43: At 8 weeks, exposure has no effect on spatial learning. *The animals were exposed to either 3 W/kg RF or 0.3W/kg or a sham exposure.* ***a)*** *At 8 weeks, there were no significant differences in the latency to first reach the target area between SAMP8 exposure groups (n= 16 for 3 W/kg, n= 12 for 0.3 W/kg, n = 11 for sham;);* ***b)*** *There were no significant differences in the latency to first reach the target area between SAMR1 groups (n= 12 for 3 W/kg, n= 11 for 0.3 W/kg and n= 7 for sham).*

At 30 weeks of age, there was a significant difference in the latency to first reach the platform area (ANOVA, p< 0.01) between SAMP8 and SAMR1, with SAMP8 taking longer to reach the platform area than the SAMR1 mice. There were no significant differences between exposure groups (ANOVA, p= 0.234) and no significant interaction between strain and exposure groups either (ANOVA, p= 1), as shown in figure 44.

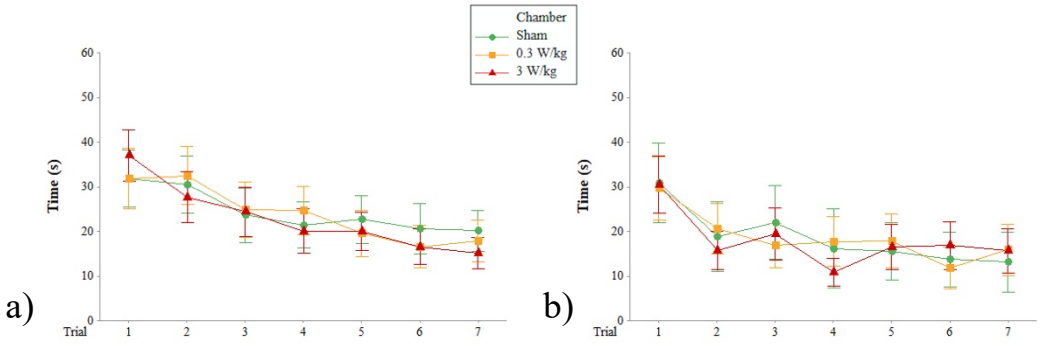


Figure 44: At 30 weeks, exposure has no effect on spatial learning. *The animals were exposed to either 3 W/kg RF or 0.3W/kg or a sham exposure.* ***a)****, At 30 weeks, there were no significant differences in the latency to first reach the target area between SAMP8 exposure groups (n= 15 for 3 W/kg, n= 12 for 0.3 W/kg, n = 11 for sham);* ***b)*** *There were no significant differences in the latency to first reach the target area between groups in 30-weeks-old SAMR1 (n= 12 for 3 W/kg, n= 10 for 0.3 W/kg and n= 6 for sham).*

6.3.1.2.2.2. Trials 3

a) Velocity

At 8 weeks of age, there was a significant difference in velocity (ANOVA, p= 0.033) between SAMP8 and SAMR1, with SAMP8 being slower than the SAMR1 mice. There were no significant differences between exposure groups (ANOVA, p= 0.639) but significant interactions between strain and exposure groups either (ANOVA, p= 0.021), though the Tuckey post hoc test was not significant, as shown in figure 41.

At 30 weeks of age, there was a significant difference in velocity (ANOVA, p< 0.001) between SAMP8 and SAMR1, with SAMP8 being slower than the SAMR1 mice. There were no significant differences between exposure groups (ANOVA, p= 0.130) and no significant interaction between strain and exposure groups either (ANOVA, p= 0.079), as shown in figure 42.

b) Latency to reach the target area

At 8 weeks of age, there was a significant difference in the latency to first reach the platform area (ANOVA, p< 0.001) between SAMP8 and SAMR1, with SAMP8 taking longer to reach the platform area than the SAMR1 mice. There were no significant differences between exposure groups (ANOVA, p= 0.503) and no significant interaction between strain and exposure groups either (ANOVA, p=0.332), as shown in figure 43.

At 30 weeks of age, there was a significant difference in the latency to first reach the platform area (ANOVA, p= 0.05) between SAMP8 and SAMR1, with SAMP8 taking longer to reach the platform area than the SAMR1 mice. There were no significant differences between exposure groups (ANOVA, p= 0.835) and no significant interaction between strain and exposure groups either (ANOVA, p=0.625), as shown in figure 44.

6.3.2. Histology

6.3.2.1. GFAP

6.3.2.1.1. CA1

At 30 weeks of age, there were no significant differences (ANOVA, p= 0.171) in astrogliosis between SAMP8 and SAMR1 mice. There were no significant differences in

astrogliosis between exposure groups (ANOVA, p= 0.466). There were no significant interactions between groups (ANOVA, p=0.589), as shown in figure 45.

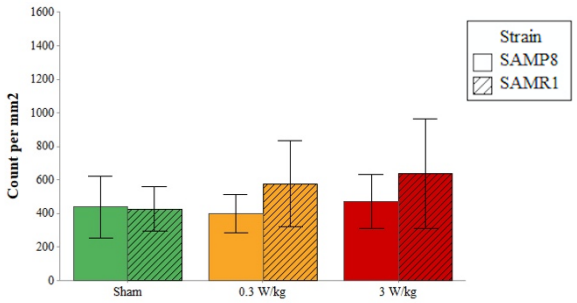


Figure 45: Exposure does not increase astrogliosis in CA1. *The animals were exposed to either 3 W/kg RF or 0.3W/kg or a sham exposure. At 12 months of age, there were no significant differences in astrogliosis in the CA1 area between groups (for SAMP8 mice, n= 12 for 3 W/kg, n= 12 for 0.3 W/kg, n = 11 for sham; for SAMR1 mice, n= 11 for 3 W/kg, n= 8 for 0.3 W/kg and n= 6 for sham).*

6.3.2.1.2. CA3

At 30 weeks of age, there were no significant differences (ANOVA, p= 0.332) between SAMP8 and SAMR1 mice. There were no significant differences in astrogliosis between exposure groups (ANOVA, p= 0.331). There were no significant interactions between groups (ANOVA, p=0.46), as shown in figure 46.

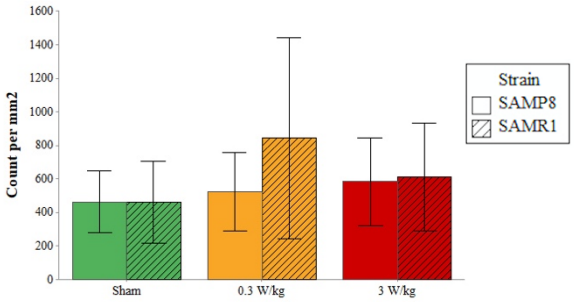


Figure 46: Exposure does not increase astrogliosis in CA3. *The animals were exposed to either 3 W/kg RF or 0.3W/kg or a sham exposure. At 12 months of age, , there were no significant differences in astrogliosis in the CA3 area between groups (for SAMP8 mice, n= 12 for 3 W/kg, n= 12 for 0.3 W/kg, n = 11 for sham; for SAMR1 mice, n= 11 for 3 W/kg, n= 8 for 0.3 W/kg and n= 6 for sham).*

6.3.2.1.3. Dentate Gyrus

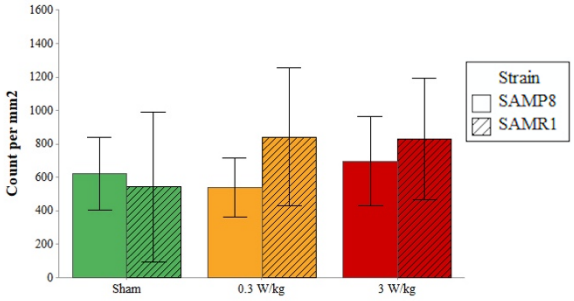


Figure 47: Exposure does not increase astrogliosis in DG. *The animals were exposed to either 3 W/kg RF or 0.3W/kg or a sham exposure. At 12 months of age, , there were no significant differences in astrogliosis in the DG area between groups (for SAMP8 mice, n= 12 for 3 W/kg, n= 12 for 0.3 W/kg, n = 11 for sham; for SAMR1 mice, n= 11 for 3 W/kg, n= 8 for 0.3 W/kg and n= 6 for sham).*

At 30 weeks of age, there were no significant differences (ANOVA, p= 0.288) in astrogliosis between SAMP8 and SAMR1 mice. There were no significant differences in astrogliosis between exposure groups (ANOVA, p= 0.427). There were no significant interactions between groups (ANOVA, p=0.415), as shown in figure 47.

6.3.2.2. SYP

6.3.2.2.1. CA1

At 30 weeks of age, there were no significant differences in synaptic density in CA1 (ANOVA, p=0.859) between SAMP8 and SAMR1 mice. There were no significant differences in synaptic density between exposure groups (ANOVA, p= 0.279) or any significant interaction between groups (ANOVA, p= 0.905), as shown in figure 48.

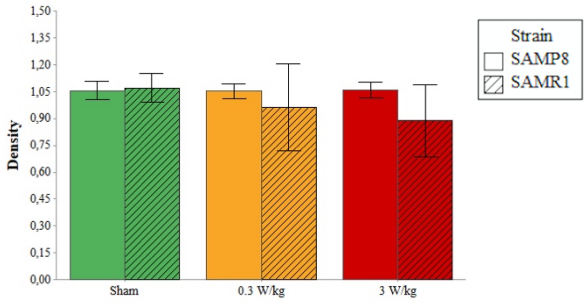


Figure 48: Exposure does not increase synaptic density in CA1. *The animals were exposed to either 3 W/kg RF or 0.3W/kg or a sham exposure.**)** At 30 weeks, there were no significant differences in synaptic density in CA1 (for SAMP8 mice, n= 13 for 3 W/kg, n= 12 for 0.3 W/kg, n = 11 for sham; for SAMR1 mice, n= 12 for 3 W/kg, n= 9 for 0.3 W/kg and n= 6 for sham).*

6.3.2.2.2. CA3

At 30 weeks of age, there were no significant differences in synaptic density in CA3 (ANOVA, p=0.516) between SAMP8 and SAMR1 mice. There were no significant differences in synaptic density between exposure groups (ANOVA, p= 0.264) or any significant interaction between groups (ANOVA, p= 0.925), as shown in figure 49.

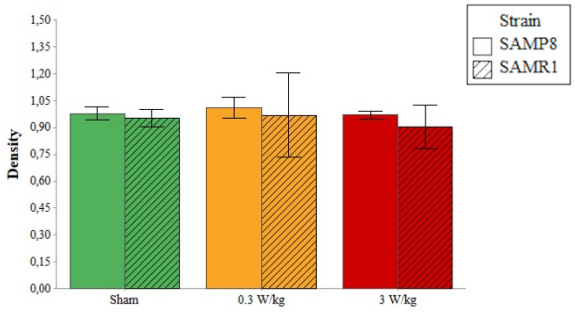


Figure 49: Exposure does not increase synaptic density in CA3. *The animals were exposed to either 3 W/kg RF or 0.3W/kg or a sham exposure. At 30 weeks, there were no significant differences in synaptic density in CA3 (for SAMP8 mice, n= 13 for 3 W/kg, n= 12 for 0.3 W/kg, n = 11 for sham; for SAMR1 mice, n= 12 for 3 W/kg, n= 9 for 0.3 W/kg and n= 6 for sham).*

6.3.2.2.3. Dentate Gyrus

At 30 weeks of age, there were no significant differences in synaptic density in DG (ANOVA, p=0.368) between SAMP8 and SAMR1 mice. There were no significant differences in synaptic density between exposure groups (ANOVA, p= 0.106) or any significant interaction between groups (ANOVA, p= 0.329), as shown in figure 50.

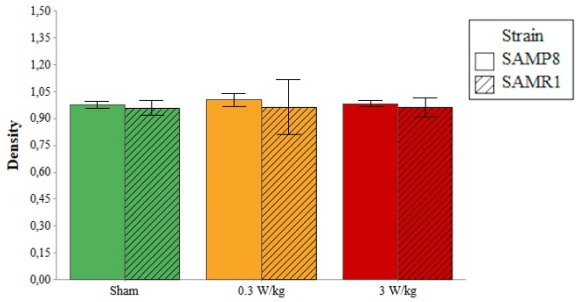


Figure 50: Exposure does not increase synaptic density in DG. *The animals were exposed to either 3 W/kg RF or 0.3W/kg or a sham exposure. At 30 weeks, there were no significant differences in synaptic density in DG (for SAMP8 mice, n= 13 for 3 W/kg, n= 12 for 0.3 W/kg, n = 11 for sham; for SAMR1 mice, n= 12 for 3 W/kg, n= 9 for 0.3 W/kg and n= 6 for sham).*

6.3.2.3. IbA1

At 30 weeks of age, there were no significant differences (ANOVA, p=0.903) between SAMP8 and SAMR1 mice, and there were no significant differences in Iba1 cell count between exposure groups (ANOVA, p= 0.079) or any significant interaction between groups (ANOVA, p= 0.801), as shown in figure 51.

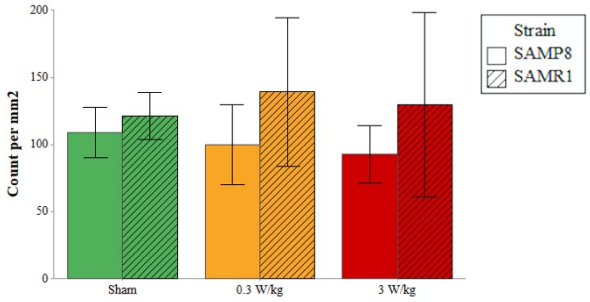


***Figure 51: Exposure has no effect on microglia**. The animals were exposed to either 3 W/kg RF or 0.3W/kg or a sham exposure. At 12 months of age, there were no significant differences in the number of IbA1-positive cells in the hippocampus between groups (for SAMP8 mice, n= 13 for 3 W/kg, n= 13 for 0.3 W/kg, n = 11 for sham; for SAMR1 mice, n= 12 for 3 W/kg, n= 8 for 0.3 W/kg and n= 5 for sham).*

6.3.2.4. NeuN

6.3.2.4.1. CA1

At 30 weeks of age, there was a significant difference in neurogenesis in CA1 (ANOVA, p=0.002) between SAMP8 and SAMR1 mice, with SAMR1 showing an increased number of NeuN-positive cells. There were no significant differences in neurogenesis between exposure groups (ANOVA, p= 0.514) or any significant interaction between groups (ANOVA, p= 0.919), as shown in figure 52.

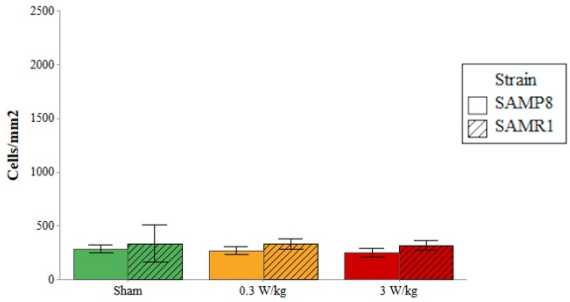


Figure 52: Exposure does not increase neurogenesis in CA1. *The animals were exposed to either 3 W/kg RF or 0.3W/kg or a sham exposure. At 12 months, there were no significant differences in neurogenesis in CA1 (for SAMP8 mice, n= 13 for 3 W/kg, n= 8 for 0.3 W/kg and n=10 for sham; for SAMR1 mice, n= 6 for 3 W/kg, n= 8 for 0.3 W/kg and n=3 for sham).*

6.3.2.4.2. CA3

At 30 weeks of age, there were no significant differences in neurogenesis in CA3 (ANOVA, p=0.492) between SAMP8 and SAMR1 mice, and there were no significant differences in neurogenesis between exposure groups (ANOVA, p= 0.363) or any significant interaction between groups (ANOVA, p= 0.137), as shown in figure 53.

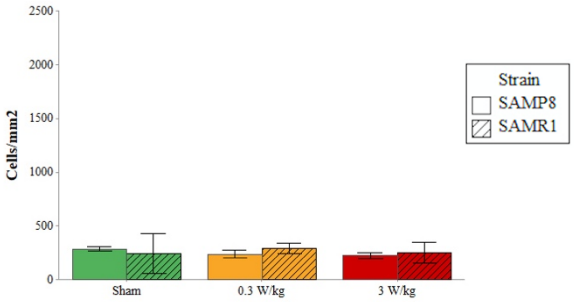


Figure 53: Exposure does not increase neurogenesis in CA3. *The animals were exposed to either 3 W/kg RF or 0.3W/kg or a sham exposure. At 12 months, there were no significant differences in neurogenesis in CA3 (for SAMP8 mice, n= 13 for 3 W/kg, n= 8 for 0.3 W/kg and n=10 for sham; for SAMR1 mice, n= 6 for 3 W/kg, n= 8 for 0.3 W/kg and n=3 for sham).*

6.3.2.4.3. Dentate Gyrus

At 30 weeks of age, there were no significant differences in neurogenesis in the DG (ANOVA, p=0.13) between SAMP8 and SAMR1 mice, and there were no significant differences in neurogenesis between exposure groups (ANOVA, p= 0.362) or any significant interaction between groups (ANOVA, p= 0.272), as shown in figure 54.

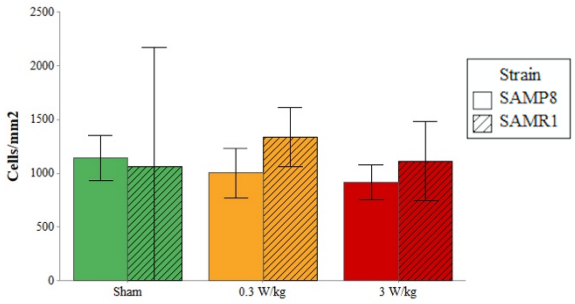


Figure 54: Exposure does not increase neurogenesis in DG. *The animals were exposed to either 3 W/kg RF or 0.3W/kg or a sham exposure. At 12 months, there were no significant differences in neurogenesis in DG (for SAMP8 mice, n= 13 for 3 W/kg, n= 8 for 0.3 W/kg and n=10 for sham; for SAMR1 mice, n= 6 for 3 W/kg, n= 8 for 0.3 W/kg and n=3 for sham).*

6.3.2.5. β-amyloid

No β-amyloid plaques were visible in any of the groups.

6.4. Discussion

6.4.1. General considerations

Analysis of data needed to account for differences in locomotion- SAMP8 were significantly slower and more prone to floating, which might bias the other parameters that are linked to speed (time first and foremost).

Rotarod tests confirmed that ageing SAMP8 showed increased locomotion deficits in line with their phenotypes and that they could not be compared to SAMR1 in the MWM. However, since exposure had no impact in velocity between chambers, MWM could be used to investigate memory and acquisition between exposures groups.

6.4.2. Discussion

An analysis of the pre-trial, meaning the first introduction of the mice to the MWM, left to swim for 60 seconds without a platform, showed that already, at 8 weeks, SAMP8 presented significant differences when compared to SAMR1 controls. They showed an increase in the latency to first reach the platform area, and an increased time floating, hinting at a possible inadaptability to the MWM test. Nevertheless, the lack of significant difference in velocity and total distance swum during the trial seems to confirm a lack of locomotive issues at this age.
The probe-trial at 8 weeks, done after 7 training trials with a platform, and consisting, like in the pre-trial, of a 60 seconds swim with the platform removed, shows that SAMP8 mice already present a significant decrease in velocity. This seems to particularly affect the group exposed to 3 W/kg EMF while the group exposed 0.3 W/kg fared much better. The latency to first reach to the platform as well as the total distance swum were significantly decreased as well. These findings lead to three possible conclusions: (i) the SAMP8 are already physically impacted and

cannot handle the rigorous MWM training; (ii) the SAMP8 present an increased lack of motivation or depression-like behaviour; (iii) both issues are correct. Studies done in the MWM (Miyamoto et al., 1986; Miyamoto, 1997) have reported that SAMP8 mice in MWM swam slowly and showed a delay in starting to look for the platform. SAMP8 have not been known to exhibit signs of depression in the tail suspension test, showing responses similar to SAMR1 (Miyamoto, 1997), but a more recent study, done on 4-month-old SAMP8, suggested that SAMP8 showed increased anxiety-like behaviours as well as increased depression-like behaviour in the forced-swim test (Yanai and Endo, 2016), which would be coherent with the previously mentioned lack of motivation in MWM.

At 30 weeks, the pre-trial analysis showed significant differences between SAMP8 and SAMR1. SAMP8 were slower, swam less, exhibited more refractory behaviour and showed already significant differences in their latency to reach the platform area. However, the animals had already been introduced to the MWM at 8 weeks, so there might be a bias here. The probe-trial also did not show any effect of exposure on ageing, the issues present in the pre-trial making any further conclusions difficult.

Studies mention that memory and learning deficits were highlighted as early as 2 months of age in passive and active avoidance tasks (Miyamoto et al., 1986; Yagi et al., 1988). However, other studies (Frick et al., 1995; Markowska et al., 1998b) discuss that while there seems to be apparent cognitive deficits, those deficits may not be solely linked to cognitive abilities and may be overshadowed by the apparition of locomotion deficits as well as deficit of motivation. In tasks that do not require such an input of locomotor abilities, the cognitive differences between SAMP8 and SAMR1 are not so pronounced (Frick et al., 1995).

Histologically, there were no significant differences visible in the hippocampus, though there should have been an increased astrogliosis in SAMP8 when compared to SAMR1 (Okuma and Nomura, 1998; Akiguchi et al., 2017), though those changes have been reported around 9 or 12 months. As thirty weeks is equivalent to roughly 6 and a half months, it might be that the study was too short to properly assess histological changes. Del Valle shows a decrease of synaptophysin in SAMP8 when compared to SAMR1 starting 6 months, but that it worsened around 9 months (del Valle et al., 2012). It has been reported that the apparition of AB deposits in SAMP8 hippocampus start around 6 months (Del Valle et al., 2010; Manich et al., 2011), but we were not able to show the presence of any deposits, despite the positive results we obtained using this method for the staining of an AD transgenic model. The increased neurogenesis in SAMR1 CA1 when compared to SAMP8 CA1 was reported in literature (Gang et al., 2011; Manich et al., 2011). While the lack of differences in brain structure stays consistent with the lack of exposure impact in behavioural testing and would imply that there was no effect of EMF on brain structure, due to the inadaptation of the mouse model to the behavioural test and the long period before the final behavioural testing, we cannot exclude the hypothesis that some changes appeared during acute phase (i.e during exposure) and had since then been repaired.

In conclusion, the SAMP8 model seems to be attractive- a spontaneous occurrence of accelerated ageing, with cognitive deficits that seemed to mimic AD without requiring the construction of a transgenic model is an interesting notion for a complex mechanism that is only partially understood. It is a favoured model to test a number of substances (Ueda et al., 2011; Cristòfol et al., 2012). Studies describing this model have focused mainly on the cognitive deficits, but so far few have properly investigated the locomotion deficits of this strain, which might account for part of the cognitive deficits of this model.

However, despite those shortcomings, we were able to conclude that, within the conditions of this experiments, EMF had no impact on the phenotype and behaviour of SAMP8 and SAMR1 mice, whether after a one-week, acute exposure or after a chronic, 8-week long exposure. Still, the long interval of time between the end of exposure at 16 weeks old and the final behavioural testing might have impacted the results. We cannot conclude whether changes did appear during the long exposure and had since then been repaired, or there was no effect of EMF on learning, memory and brain structure.

7. Conclusion

The studies however had some design flaws. The way the experiment was conducted, with ongoing inclusions in the study made it sometimes difficult to get even groups, though it did help in making sure that there was a homogeneity by including animals from different litters. Nevertheless, the ongoing inclusion with rather long timepoints (6 and 12 months) also made it hard to correct ongoing tests and protocols, and when it was done with the addition of several behavioural and locomotor test when preliminary results came in, meaning a loss of power in some tests.

The breeding requirements of the J20 was made it difficult to get even groups, due to having to both keep transgenic males for breeding and replace transgenic animals that died of seizure within the first 6 months of life. As we tried to fill in the 12-month group first, the 6-month transgenic group particularly suffered.

While the MWM is a reference test for learning and memory and particularly used in both AD and EMF studies, in retrospect this test may not have been the best suited to the particular mouse models we were using- the SAMP8 due to a strong loss of locomotor abilities that have

overshadowed any potential cognitive deficit linked to age, and the J20 due to floating behaviour that masked cognitive deficits as well.

Another issue that might have impacted results are the housing, which due to space constraint in the animal house could not be keep consistent for all animals. It might be coming from the differences in housing conditions, where females were housed together, while males had to be separated after their first exposure due to in-cage fighting. It is known that for social animals such as mice, isolation could be a factor of psychological and neurological decline that might influence brain composition, and it has been shown that changes in environment (Pietropaolo et al., 2014), housing (Burman et al., 2014) or social interaction can have an impact on cognitive abilities.

Regarding the exposure, it might be argued that the exposure pattern (30min/day, 2 or 3 days a week) might not be intense enough when compared to current cell phone use. While the material constraint due to the number of exposures to realise forced us to adopt this scheme, it might have been better to have daily, longer exposure.

Keeping in mind those limitations, it was not possible to show clear evidence of the effect of EMF exposure on ageing and AD, but some behavioural and histological tests showed the possibility of EMF effect on cognition and activity.

Those effects could be linked to physiological changes that might be reversible: they are either reversible and will disappear some point after the end of exposure, or they are not reversible and will end up impacting ageing and AD pathology.

More in-depth histological studies at different time-points will be required to help explain behavioural results. A more focused approach targeting the influence of EMF with a few selected parameters and with a full cohort of animals to begin with, might help to get more

powerful studies. It is also important to investigate both sexes, the power needed to properly investigate such differences was difficult to attain. According to Broestl (Broestl et al., 2018), J20 females showed an increased in cognitive behaviour dysfunction, possibly linked to altered patterns of ovarian cycles, and that Estrogen could worsen their cognitive deficit (Broestl et al., 2018).

Also, while adult changes seem to be reversible, question of foetal and childhood exposure- can those be reversed, when affecting a non-mature organism? Several studies showed an impact of young and in utero exposure for rodents (Bas et al., 2009; İkinci et al., 2016; Odacı et al., 2016).

Finally, on a human health level further epidemiological studies will be needed. Regarding the multifactorial aspect of AD, EMF seems unlikely to have an impact that would overshadow proven risks factors for AD, such as a sedentary lifestyle and other lifestyle choices (Anstey et al., 2014; Edwards et al., 2019), particularly in a mature brain. It would however been interesting -though difficult- to ascertain if EMF exposure could work with or against those factors.

It should also be noted that common practices regarding the use of mobile phones (and now mainly smartphones) are constantly evolving. The phones are now being used less and less for traditional phone calls, with the phone keep next to the ear and so the head for long periods of time, but they are kept consistently in a close perimeter- in front of the face for video calls, in the pocket during the entire day, on the nightstand while sleeping… As the dose received decrease by the distance squared, the doses are strongly decreased but the longer of duration increases, it might be interesting to reassess the effective dosimetry received, particularly by

the youngest population who are now more and more exposed at a younger age and in utero. There will be a necessity though to try and find a way to assess EMF effect independently of the effect of screen time, which has been pointed as a factor for issues in brain development.(Madigan et al., 2019)

Finally, another recent technological development with the apparition of 5G technology will raise other questions on the safety and whether the studies done with different exposure protocols can be applied.

Bibliography

Aguzzi, A., Barres, B.A., and Bennett, M.L. (2013). Microglia: Scapegoat, saboteur, or something else? Science (80-.). *339*: 156–161.

Akiguchi, I., Pallàs, M., Budka, H., Akiyama, H., Ueno, M., Han, J., et al. (2017). SAMP8 mice as a neuropathological model of accelerated brain aging and dementia: Toshio Takeda's legacy and future directions. Neuropathology *37*: 293–305.

Akiyama, H., Arai, T., Kondo, H., Tanno, E., Haga, C., and Ikeda, K. (2000). Cell mediators of inflammation in the Alzheimer disease brain. Alzheimer Dis. Assoc. Disord. *14 Suppl 1*: S47-53.

Allaman, I., Gavillet, M., Bélanger, M., Laroche, T., Viertl, D., Lashuel, H.A., et al. (2010). Amyloid-β aggregates cause alterations of astrocytic metabolic phenotype: Impact on neuronal viability. J. Neurosci. *30*: 3326–3338.

Allen, B. (2002). Multimodal behavior management for people with dementia. Am. J. Alzheimers. Dis. Other Demen. *17*: 89–91.

Anstey, K.J., Kingston, A., Kiely, K.M., Luszcz, M.A., Mitchell, P., and Jagger, C. (2014). The influence of smoking, sedentary lifestyle and obesity on cognitive impairment-free life expectancy. Int. J. Epidemiol. *43*: 1874–1883.

Arendash, G.W., Mori, T., Dorsey, M., Gonzalez, R., Tajiri, N., and Borlongan, C. (2012). Electromagnetic treatment to old Alzheimer's mice reverses β-amyloid deposition, modifies cerebral blood flow, and provides selected cognitive benefit. PLoS One *7*: e35751.

Arendash, G.W., Sanchez-Ramos, J., Mori, T., Mamcarz, M., Lin, X., Runfeldt, M., et al. (2010). Electromagnetic field treatment protects against and reverses cognitive impairment in Alzheimer's disease mice. J. Alzheimers. Dis. *19*: 191–210.

Arnold, S.E., Hyman, B.T., Flory, J., Damasio, A.R., and Hoesen, G.W. Van (1991). The

topographical and neuroanatomical distribution of neurofibrillary tangles and neuritic plaques in the cerebral cortex of patients with alzheimer's disease. Cereb. Cortex *1*: 103–116.

Barron, M., Gartlon, J., Dawson, L.A., Atkinson, P.J., and Pardon, M.C. (2017). A state of delirium: Deciphering the effect of inflammation on tau pathology in Alzheimer's disease. Exp. Gerontol. *94*: 103–107.

Bas, O., Odaci, E., Mollaoglu, H., Ucok, K., and Kaplan, S. (2009). Chronic prenatal exposure to the 900 megahertz electromagnetic field induces pyramidal cell loss in the hippocampus of newborn rats. Toxicol. Ind. Health *25*: 377–384.

Beauquis, J., Vinuesa, A., Pomilio, C., Pavía, P., Galván, V., and Saravia, F. (2014). Neuronal and glial alterations, increased anxiety, and cognitive impairment before hippocampal amyloid deposition in PDAPP mice, model of Alzheimer's disease. Hippocampus *24*: 257–69.

Bonda, D.J., Mailankot, M., Stone, J.G., Garrett, M.R., Staniszewska, M., Castellani, R.J., et al. (2010). Indoleamine 2,3-dioxygenase and 3-hydroxykynurenine modifications are found in the neuropathology of Alzheimer's disease. Redox Rep. *15*: 161–168.

Braak, H., and Braak, E. (1991). Neuropathological stageing of Alzheimer-related changes. Acta Neuropathol. *82*: 239–259.

Braak, H., and Braak, E. (1995). Staging of Alzheimer's disease-related neurofibrillary changes. Neurobiol. Aging *16*: 271–8; discussion 278-84.

Broestl, L., Worden, K., Moreno, A.J., Davis, E.J., Wang, D., Garay, B., et al. (2018). Ovarian Cycle Stages Modulate Alzheimer-Related Cognitive and Brain Network Alterations in Female Mice. Eneuro *5*: ENEURO.0132-17.2018.

Burke, S.N., and Barnes, C.A. (2006). Neural plasticity in the ageing brain. Nat. Rev. Neurosci. *7*: 30–40.

Burman, O., Buccarello, L., Redaelli, V., and Cervo, L. (2014). The effect of two different

Individually Ventilated Cage systems on anxiety-related behaviour and welfare in two strains of laboratory mouse. Physiol. Behav. *124*: 92–99.

Calhoun, M.E., Kurth, D., Phinney, A.L., Long, J.M., Hengemihle, J., Mouton, P.R., et al. (1998). Hippocampal neuron and synaptophysin-positive bouton number in aging C57BL/6 mice. Neurobiol. Aging *19*: 599–606.

Campbell, B.M., Charych, E., Lee, A.W., and Möller, T. (2014). Kynurenines in CNS disease: Regulation by inflammatory cytokines. Front. Neurosci. *8*:.

Charan, J., and Kantharia, N. (2013). How to calculate sample size in animal studies? J. Pharmacol. Pharmacother. *4*: 303–306.

Cheng, I.H., Scearce-Levie, K., Legleiter, J., Palop, J.J., Gerstein, H., Bien-Ly, N., et al. (2007). Accelerating amyloid-β fibrillization reduces oligomer levels and functional deficits in Alzheimer disease mouse models. J. Biol. Chem. *282*: 23818–23828.

Chishti, M.A., Yang, D.S., Janus, C., Phinney, A.L., Horne, P., Pearson, J., et al. (2001). Early-onset Amyloid Deposition and Cognitive Deficits in Transgenic Mice Expressing a Double Mutant Form of Amyloid Precursor Protein 695. J. Biol. Chem. *276*: 21562–21570.

Cristòfol, R., Porquet, D., Corpas, R., Coto-Montes, A., Serret, J., Camins, A., et al. (2012). Neurons from senescence-accelerated SAMP8 mice are protected against frailty by the sirtuin 1 promoting agents melatonin and resveratrol. J. Pineal Res. *52*: 271–281.

Davies, P., and Maloney, A.J.F. (1976). Selective Loss of Central Cholinergic Neurons in Alzheimer'S Disease. Lancet *308*: 1403.

Duff, K., Eckman, C., Zehr, C., Yu, X., Prada, C.M., Perez-Tur, J., et al. (1996). Increased amyloid-β42(43) in brains of mice expressing mutant presenilin 1. Nature *383*: 710–713.

Edwards, G.A., Gamez, N., Escobedo, G., Calderon, O., and Moreno-Gonzalez, I. (2019). Modifiable risk factors for Alzheimer's disease. Front. Aging Neurosci. *11*: 146.

Erickson, C.A., and Barnes, C.A. (2003). The neurobiology of memory changes in normal

aging. In Experimental Gerontology, (Exp Gerontol), pp 61–69.

Faul, F., Erdfelder, E., Lang, A.G., and Buchner, A. (2007). G*Power 3: A flexible statistical power analysis program for the social, behavioral, and biomedical sciences. Behav. Res. Methods *39*: 175–191.

Flood, J.F., and Morley, J.E. (1992). Early onset of age-related impairment of aversive and appetitive learning in the SAM-P/8 mouse. Journals Gerontol. *47*:.

Flood, J.F., and Morley, J.E. (1993). Age-related changes in footshock avoidance acquisition and retention in senescence accelerated mouse (SAM). Neurobiol. Aging *14*: 153–157.

Fragopoulou, A.F., Miltiadous, P., Stamatakis, A., Stylianopoulou, F., Koussoulakos, S.L., and Margaritis, L.H. (2010). Whole body exposure with GSM 900MHz affects spatial memory in mice. Pathophysiology *17*: 179–187.

Frick, K.M., Baxter, M.G., Markowska, A.L., Olton, D.S., and Price, D.L. (1995). Age-related spatial reference and working memory deficits assessed in the water maze. Neurobiol. Aging *16*: 149–160.

Frick, K.M., Burlingame, L.A., Arters, J.A., and Berger-Sweeney, J. (2000). Reference memory, anxiety and estrous cyclicity in C57BL/6NIA mice are affected by age and sex. Neuroscience *95*: 293–307.

Galvan, V., Zhang, J., Gorostiza, O.F., Banwait, S., Huang, W., Ataie, M., et al. (2008). Long-term prevention of Alzheimer's disease-like behavioral deficits in PDAPP mice carrying a mutation in Asp664. Behav. Brain Res. *191*: 246–255.

Games, D., Adams, D., Alessandrini, R., Barbour, R., Borthelette, P., Blackwell, C., et al. (1995). Alzheimer-type neuropathology in transgenic mice overexpressing V717F β-amyloid precursor protein. Nature *373*: 523–527.

Gang, B., Yue, C., Han, N., Xue, H., Li, B., Sun, L., et al. (2011). Limited hippocampal neurogenesis in SAMP8 mouse model of Alzheimer's disease. Brain Res. *1389*: 183–93.

Geula, C., Nagykery, N., and Wu, C.K. (2002). Amyloid-β deposits in the cerebral cortex of the aged common marmoset (Callithrix jacchus): Incidence and chemical composition. Acta Neuropathol. *103*: 48–58.

Ginhoux, F., Greter, M., Leboeuf, M., Nandi, S., See, P., Gokhan, S., et al. (2010). Fate mapping analysis reveals that adult microglia derive from primitive macrophages. Science (80-.). *330*: 841–845.

Gomez-Arboledas, A., Davila, J.C., Sanchez-Mejias, E., Navarro, V., Nuñez-Diaz, C., Sanchez-Varo, R., et al. (2018). Phagocytic clearance of presynaptic dystrophies by reactive astrocytes in Alzheimer's disease. Glia *66*: 637–653.

Guillemin, G.J., Brew, B.J., Noonan, C.E., Takikawa, O., and Cullen, K.M. (2005). Indoleamine 2,3 dioxygenase and quinolinic acid Immunoreactivity in Alzheimer's disease hippocampus. Neuropathol. Appl. Neurobiol. *31*: 395–404.

Hardy, J., and Selkoe, D.J. (2002). The amyloid hypothesis of Alzheimer's disease: Progress and problems on the road to therapeutics. Science (80-.). *297*: 353–356.

Health Protection Agency (2012). Health Effects from Radiofrequency Electromagnetic Fields.

Hedden, T., and Gabrieli, J.D.E. (2004). Insights into the ageing mind: A view from cognitive neuroscience. Nat. Rev. Neurosci. *5*: 87–96.

Henríquez, J.P., Cross, D., Vial, C., and Maccioni, R.B. (1995). Subpopulations of tau interact with microtubules and actin filaments in various cell types. Cell Biochem. Funct. *13*: 239–50.

Holcomb, L., Gordon, M.N., McGowan, E., Yu, X., Benkovic, S., Jantzen, P., et al. (1998). Accelerated Alzheimer-type phenotype in transgenic mice carrying both mutant amyloid precursor protein and presenilin 1 transgenes. Nat. Med. *4*: 97–100.

Hong, S., Beja-Glasser, V.F., Nfonoyim, B.M., Frouin, A., Li, S., Ramakrishnan, S., et al. (2016). Complement and microglia mediate early synapse loss in Alzheimer mouse models.

Science *352*: 712–716.

Hsiao, K., Chapman, P., Nilsen, S., Eckman, C., Harigaya, Y., Younkin, S., et al. (1996). Correlative memory deficits, Aβ elevation, and amyloid plaques in transgenic mice. Science (80-.). *274*: 99–102.

IARC (2013). Radiofrequency electromagnetic fields. IARC Monogr. Eval. Carcinog. … *102*:.

ICNIRP (1998). Guidelines for limiting exposure to time-varying electric, magnetic, and electromagnetic fields (up to 300 GHz). Health Phys. *74*:.

İkinci, A., Mercantepe, T., Unal, D., Erol, H.S., Şahin, A., Aslan, A., et al. (2016). Morphological and antioxidant impairments in the spinal cord of male offspring rats following exposure to a continuous 900 MHz electromagnetic field during early and mid-adolescence. J. Chem. Neuroanat. *75*: 99–104.

Irizarry, M.C., McNamara, M., Fedorchak, K., Hsiao, K., and Hyman, B.T. (1997a). APP(Sw) transgenic mice develop age-related Aβ deposits and neuropil abnormalities, but no neuronal loss in CA1. J. Neuropathol. Exp. Neurol. *56*: 965–973.

Irizarry, M.C., Soriano, F., McNamara, M., Page, K.J., Schenk, D., Games, D., et al. (1997b). Abeta deposition is associated with neuropil changes, but not with overt neuronal loss in the human amyloid precursor protein V717F (PDAPP) transgenic mouse. J. Neurosci. *17*: 7053–9.

Jankowsky, J.L., and Zheng, H. (2017). Practical considerations for choosing a mouse model of Alzheimer's disease. Mol. Neurodegener. *12*: 89.

Karl, T., Bhatia, S., Cheng, D., Kim, W.S., and Garner, B. (2012a). Cognitive phenotyping of amyloid precursor protein transgenic J20 mice. Behav. Brain Res. *228*: 392–7.

Karl, T., Bhatia, S., Cheng, D., Kim, W.S., and Garner, B. (2012b). Cognitive phenotyping of amyloid precursor protein transgenic J20 mice. Behav. Brain Res. *228*: 392–397.

Kitado, H., Higuchi, K., and Takeda, T. (1994). Molecular genetic characterization of the senescence-acceler. J Gerontol. *49*: 247–254.

Kitazawa, M., Medeiros, R., Laferla, F.M., and Disorders, N. (2015). Better Model as a Tool for Therapeutic Interventions. *18*: 1131–1147.

Kowall, N.W., and Kosik, K.S. (1987). Axonal disruption and aberrant localization of tau protein characterize the neuropil pathology of Alzheimer's disease. Ann. Neurol. *22*: 639–643.

Kuchibhotla, K. V., Lattarulo, C.R., Hyman, B.T., and Bacskai, B.J. (2009). Synchronous hyperactivity and intercellular calcium waves in astrocytes in Alzheimer mice. Science (80-.). *323*: 1211–1215.

Kulkarni, S.K., Singh, K., and Bishnoi, M. (2007). Elevated zero maze: A paradigm to evaluate antianxiety effects of drugs. Methods Find. Exp. Clin. Pharmacol. *29*: 343–348.

Kumar-Singh, S., Theuns, J., Broeck, B. Van, Pirici, D., Vennekens, K., Corsmit, E., et al. (2006). Mean age-of-onset of familial alzheimer disease caused by presenilin mutations correlates with both increased Abeta42 and decreased Abeta40. Hum. Mutat. *27*: 686–95.

Lecomte, A., Abdelmelek, H., Seze, R. De, Sakly, M., Gamez, C., and Ammari, M. (2010). GFAP expression in the rat brain following sub-chronic exposure to a 900 MHz electromagnetic field signal. Int. J. Radiat. Biol. *86*: 367–375.

Lewis, J., Dickson, D.W., Lin, W.L., Chisholm, L., Corral, A., Jones, G., et al. (2001). Enhanced neurofibrillary degeneration in transgenic mice expressing mutant tau and APP. Science (80-.). *293*: 1487–1491.

Lewis, J., McGowan, E., Rockwood, J., Melrose, H., Nacharaju, P., Slegtenhorst, M. Van, et al. (2000). Neurofibrillary tangles, amyotrophy and progressive motor disturbance in mice expressing mutant (P301L)tau protein. Nat. Genet. *25*: 402–405.

Li, Q., and Barres, B.A. (2018). Microglia and macrophages in brain homeostasis and disease.

Nat. Rev. Immunol. *18*: 225–242.

Madigan, S., Browne, D., Racine, N., Mori, C., and Tough, S. (2019). Association between Screen Time and Children's Performance on a Developmental Screening Test. JAMA Pediatr. *173*: 244–250.

Manich, G., Mercader, C., Valle, J. del, Duran-Vilaregut, J., Camins, A., Pallàs, M., et al. (2011). Characterization of amyloid-β granules in the hippocampus of SAMP8 mice. J. Alzheimers. Dis. *25*: 535–46.

Markowska, A.L., Spangler, E.L., and Ingram, D.K. (1998a). Behavioral assessment of the senescence-accelerated mouse (SAM P8 and R1). Physiol. Behav. *64*: 15–26.

Markowska, A.L., Spangler, E.L., and Ingram, D.K. (1998b). Behavioral Assessment of the Senescence-accelerated Mouse (SAM P8 and R1). Physiol. Behav. *64*: 15–26.

McGowan, E., Eriksen, J., and Hutton, M. (2006). A decade of modeling Alzheimer's disease in transgenic mice. Trends Genet. *22*: 281–289.

Miyamoto, M. (1994). [Experimental techniques for developing new drugs acting on dementia (8)--Characteristics of behavioral disorders in senescence-accelerated mouse (SAMP8): possible animal model for dementia]. Nihon Shinkei Seishin Yakurigaku Zasshi *14*: 323–35.

Miyamoto, M. (1997). Characteristics of age-related behavioral changes in senescence-accelerated mouse SAMP8 and SAMP10. Exp. Gerontol. *32*: 139–148.

Miyamoto, M., Kiyota, Y., Yamazaki, N., Nagaoka, A., Matsuo, T., Nagawa, Y., et al. (1986). Age-related changes in learning and memory in the senescence-accelerated mouse (SAM). Physiol. Behav. *38*: 399–406.

Mohler, E., Frei, P., Fröhlich, J., Braun-Fahrländer, C., Röösli, M., and QUALIFEX-team, the (2012). Exposure to Radiofrequency Electromagnetic Fields and Sleep Quality: A Prospective Cohort Study. PLoS One *7*:.

Morris, J.C., and Price, J.L. (2001). Pathologic correlates of nondemented aging, mild cognitive impairment, and early-stage Alzheimer's disease. J. Mol. Neurosci. *17*: 101–118.

Morris, R. (1984). Developments of a water-maze procedure for studying spatial learning in the rat. J. Neurosci. Methods *11*: 47–60.

Morrison, J.H., and Hof, P.R. (1997). Life and death of neurons in the aging brain. Science (80-.). *278*: 412–419.

Mucke, L., Masliah, E., and Yu, G. (2000). High-Level Neuronal Expression of AB 1–42 in Wild-Type Human Amyloid Protein Precursor Transgenic Mice : Synaptotoxicity without Plaque Formation. J. … *20*: 4050–4058.

Mudher, A., and Lovestone, S. (2002). Alzheimer's disease-do tauists and baptists finally shake hands? Trends Neurosci. *25*: 22–6.

Musiek, E.S., and Holtzman, D.M. (2015). Three dimensions of the amyloid hypothesis: Time, space and 'wingmen'. Nat. Neurosci. *18*: 800–806.

Ng, T.P., Lim, M.L., Niti, M., and Collinson, S. (2012). Long-term digital mobile phone use and cognitive decline in the elderly. Bioelectromagnetics *33*: 176–185.

O'Farrell, K., and Harkin, A. (2017). Stress-related regulation of the kynurenine pathway: Relevance to neuropsychiatric and degenerative disorders. Neuropharmacology *112*: 307–323.

Odacı, E., Hancı, H., İkinci, A., Sönmez, O.F., Aslan, A., Şahin, A., et al. (2016). Maternal exposure to a continuous 900-MHz electromagnetic field provokes neuronal loss and pathological changes in cerebellum of 32-day-old female rat offspring. J. Chem. Neuroanat. *75*: 105–110.

Okuma, Y., and Nomura, Y. (1998). Senescence-accelerated mouse (SAM) as an animal model of senile dementia: Pharmacological, neurochemical and molecular biological approach. Jpn. J. Pharmacol. *78*: 399–404.

Olesen, L.Ø., Bouzinova, E. V., Severino, M., Sivasaravanaparan, M., Hasselstrøm, J.B., Finsen, B., et al. (2016). Behavioural phenotyping of APPswe/PS1δE9 mice: Age-rrelated changes and effect of long-term paroxetine treatment. PLoS One *11*: e0165144.

Palop, J.J., Jones, B., Kekonius, L., Chin, J., Yu, G.-Q., Raber, J., et al. (2003). Neuronal depletion of calcium-dependent proteins in the dentate gyrus is tightly linked to Alzheimer's disease-related cognitive deficits. Proc. Natl. Acad. Sci. U. S. A. *100*: 9572–7.

Pannese, E. (2011). Morphological changes in nerve cells during normal aging. Brain Struct. Funct. *216*: 85–89.

Pavlov, P.F., Petersen, C.H., Glaser, E., and Ankarcrona, M. (2009). Mitochondrial accumulation of APP and Aβ: Significance for Alzheimer disease pathogenesis. J. Cell. Mol. Med. *13*: 4137–4145.

Perez-Nievas, B.G., and Serrano-Pozo, A. (2018). Deciphering the astrocyte reaction in Alzheimer's disease. Front. Aging Neurosci. *10*: 114.

Pietropaolo, S., Feldon, J., and Yee, B.K. (2014). Environmental enrichment eliminates the anxiety phenotypes in a triple transgenic mouse model of Alzheimer's disease. Cogn. Affect. Behav. Neurosci. *14*: 996–1008.

Price, J.L., and Morris, J.C. (1999). Tangles and plaques in nondemented aging and 'preclinical' Alzheimer's disease. Ann. Neurol. *45*: 358–68.

Rahman, A., Ting, K., Cullen, K.M., Braidy, N., Brew, B.J., and Guillemin, G.J. (2009). The excitotoxin quinolinic acid induces tau phosphorylation in human neurons. PLoS One *4*:.

Reed, M.N., Liu, P., Kotilinek, L.A., and Ashe, K.H. (2010). Effect size of reference memory deficits in the Morris water maze in Tg2576 mice. Behav. Brain Res. *212*: 115–120.

Richards, J.G., Higgins, G.A., Ouagazzal, A.-M., Ozmen, L., Kew, J.N.C., Bohrmann, B., et al. (2003). PS2APP transgenic mice, coexpressing hPS2mut and hAPPswe, show age-related cognitive deficits associated with discrete brain amyloid deposition and inflammation. J.

Neurosci. *23*: 8989–9003.

Salunke, B.P., Umathe, S.N., and Chavan, J.G. (2015). Behavioral in-effectiveness of high frequency electromagnetic field in mice. Physiol. Behav. *140*: 32–37.

Santacruz, K., Lewis, J., Spires, T., Paulson, J., Kotilinek, L., Ingelsson, M., et al. (2005). Medicine: Tau suppression in a neurodegenerative mouse model improves memory function. Science (80-.). *309*: 476–481.

SCENIHR (2015). Potential health effects of exposure to electromagnetic fields (EMF).

Schöll, M., Lockhart, S.N., Schonhaut, D.R., O'Neil, J.P., Janabi, M., Ossenkoppele, R., et al. (2016). PET Imaging of Tau Deposition in the Aging Human Brain. Neuron *89*: 971–982.

Schüz, J., Waldemar, G., Olsen, J.H., and Johansen, C. (2009). Risks for Central Nervous System Diseases among Mobile Phone Subscribers: A Danish Retrospective Cohort Study. PLoS One *4*: e4389.

Selkoe, D. (2001). Alzheimer's Disease: Genes, Proteins, and Therapy. Physiol. Rev. *81*: 741–766.

Selkoe, D.J., Podlisny, M.B., Joachim, C.L., Vickers, E.A., Lee, G., Fritz, L.C., et al. (1988). Beta-amyloid precursor protein of Alzheimer disease occurs as 110- to 135-kilodalton membrane-associated proteins in neural and nonneural tissues. Proc. Natl. Acad. Sci. U. S. A. *85*: 7341–5.

Sheperd, J.K. (1994). Behavioural and pharmacological characterisation of the elevated "zero-maze" as an animal model of anxiety. Psychopharmacology (Berl). 56–64.

Sienkiewicz, Z., and Blackwell, R. (2000). Low-level exposure to pulsed 900 MHz microwave radiation does not cause deficits in the performance of a spatial learning task in mice. … *158*: 151–158.

Sienkiewicz, Z.J., Haylock, R.G., and Saunders, R.D. (1998). Deficits in spatial learning after exposure of mice to a 50 Hz magnetic field. Bioelectromagnetics *19*: 79–84.

Söllvander, S., Nikitidou, E., Brolin, R., Söderberg, L., Sehlin, D., Lannfelt, L., et al. (2016). Accumulation of amyloid-β by astrocytes result in enlarged endosomes and microvesicle-induced apoptosis of neurons. Mol. Neurodegener. *11*: 38.

Song, S.Y., Chae, M., Yu, J.H., Lee, M.Y., Pyo, S., Shin, Y.K., et al. (2018). Environmental enrichment upregulates striatal synaptic vesicle-associated proteins and improves motor function. Front. Neurol. *9*: 465.

Sturchler-Pierrat, C., Abramowski, D., Duke, M., Wiederhold, K.H., Mistl, C., Rothacher, S., et al. (1997). Two amyloid precursor protein transgenic mouse models with Alzheimer disease-like pathology. Proc. Natl. Acad. Sci. U. S. A. *94*: 13287–13292.

Takeda, T., Hosokawa, M., Takeshita, S., Irino, M., Higuchi, K., Matsushita, T., et al. (1981). A new murine model of accelerated senescence. Mech. Ageing Dev. *17*: 183–194.

Takeuchi, A., Irizarry, M.C., Duff, K., Saido, T.C., Ashe, K.H., Hasegawa, M., et al. (2000). Age-related amyloid β deposition in transgenic mice overexpressing both alzheimer mutant presenilin 1 and amyloid β precursor protein swedish mutant is not associated with global neuronal loss. Am. J. Pathol. *157*: 331–339.

Terry, R.D., Masliah, E., Salmon, D.P., Butters, N., DeTeresa, R., Hill, R., et al. (1991). Physical basis of cognitive alterations in alzheimer's disease: Synapse loss is the major correlate of cognitive impairment. Ann. Neurol. *30*: 572–580.

Tremblay, M.È., Lecours, C., Samson, L., Sánchez-Zafra, V., and Sierra, A. (2015). From the Cajal alumni Achúcarro and Río-Hortega to the rediscovery of never-resting microglia. Front. Neuroanat. *9*: 45.

Tucker, L.B., Fu, A.H., and McCabe, J.T. (2016). Performance of Male and Female C57BL/6J Mice on Motor and Cognitive Tasks Commonly Used in Pre-Clinical Traumatic Brain Injury Research. J. Neurotrauma *33*: 880–94.

Ueda, Y., Wang, M.F., Irei, A.V., Sarukura, N., Sakai, T., and Hsu, T.F. (2011). Effect of

dietary lipids on longevity and memory in the SAMP8 mice. J. Nutr. Sci. Vitaminol. (Tokyo). *57*: 36–41.

Valle, J. del, Bayod, S., Camins, A., Beas-Zárate, C., Velázquez-Zamora, D.A., González-Burgos, I., et al. (2012). Dendritic spine abnormalities in hippocampal CA1 pyramidal neurons underlying memory deficits in the SAMP8 mouse model of Alzheimer's disease. J. Alzheimers. Dis. *32*: 233–40.

Valle, J. Del, Duran-Vilaregut, J., Manich, G., Casadesús, G., Smith, M.A., Camins, A., et al. (2010). Early amyloid accumulation in the hippocampus of SAMP8 mice. J. Alzheimers. Dis. *19*: 1303–15.

Vécsei, L., Szalárdy, L., Fülöp, F., and Toldi, J. (2013). Kynurenines in the CNS: Recent advances and new questions. Nat. Rev. Drug Discov. *12*: 64–82.

Walker, J.M., Fowler, S.W., Miller, D.K., Sun, A.Y., Weisman, G.A., Wood, W.G., et al. (2011). Spatial learning and memory impairment and increased locomotion in a transgenic amyloid precursor protein mouse model of Alzheimer's disease. Behav. Brain Res. *222*: 169–175.

Wang, X., Wang, W., Li, L., Perry, G., Lee, H., and Zhu, X. (2014). Oxidative stress and mitochondrial dysfunction in Alzheimer's disease. Biochim. Biophys. Acta - Mol. Basis Dis. *1842*: 1240–1247.

Webster, S.J., Bachstetter, A.D., and Eldik, L.J. Van (2013). Comprehensive behavioral characterization of an APP/PS-1 double knock-in mouse model of Alzheimer's disease. Alzheimer's Res. Ther. *5*: 28.

Wengenack, T.M., Curran, G.L., and Poduslo, J.F. (2000a). Targeting Alzheimer amyloid plaques in vivo. Nat. Biotechnol. *18*: 868–872.

Wengenack, T.M., Whelan, S., Curran, G.L., Duff, K.E., and Poduslo, J.F. (2000b). Quantitative histological analysis of amyloid deposition in Alzheimer's double transgenic

mouse brain. Neuroscience *101*: 939–944.

West, M.J. (1993). Regionally specific loss of neurons in the aging human hippocampus. Neurobiol. Aging *14*: 287–293.

Wilcock, G.K., and Esiri, M.M. (1982). Plaques, tangles and dementia. A quantitative study. J. Neurol. Sci. *56*: 343–356.

Wimo, A., and Prince, M. (2010). World Alzheimer Report 2010; the global economic impact of dementia. Dementia 96.

Wright, A.L., Zinn, R., Hohensinn, B., Konen, L.M., Beynon, S.B., Tan, R.P., et al. (2013). Neuroinflammation and Neuronal Loss Precede Aβ Plaque Deposition in the hAPP-J20 Mouse Model of Alzheimer's Disease. PLoS One *8*: e59586.

Yagi, H., Katoh, S., Akiguchi, I., and Takeda, T. (1988). Age-related deterioration of ability of acquisition in memory and learning in senescence accelerated mouse: SAM-P/8 as an animal model of disturbances in recent memory. Brain Res. *474*: 86–93.

Yanai, S., and Endo, S. (2016). Early onset of behavioral alterations in senescence-accelerated mouse prone 8 (SAMP8). Behav. Brain Res. *308*: 187–195.

Zhou, Z., Chan, C.H., Ma, Q., Xu, X., Xiao, Z., and Tan, E.-K. (2011). The roles of amyloid precursor protein (APP) in neurogenesis. Cell Adh. Migr. *5*: 280–292.

Zwilling, D., Huang, S.Y., Sathyasaikumar, K. V., Notarangelo, F.M., Guidetti, P., Wu, H.Q., et al. (2011). Kynurenine 3-monooxygenase inhibition in blood ameliorates neurodegeneration. Cell *145*: 863–874.